Mitochondrial Epigenetics and its Role in Mitochondrial Biology

Thesis submitted to Jawaharlal Nehru University
for the partial fulfillment of the award of

DOCTOR OF PHILOSOPHY

Submitted by

Sunil Kumar Saini

School of Life Sciences
Jawaharlal Nehru University
New Delhi-67

School of Life Sciences
Jawaharlal Nehru University
New Delhi-110067
India

CERTIFICATE

This is to certify that this thesis entitled **"Mitochondrial Epigenetics and its Role in Mitochondrial Biology"** submitted to the Jawaharlal Nehru University, New Delhi, by **Mr. Sunil Kumar Saini** is based on the studies carried out in School of Life Sciences, Jawaharlal Nehru University, New Delhi. This work is original and has not been submitted so far, in part or in full, for any degree or diploma in this or any other university or institute.

Sunil

Sunil Kumar Saini
(Candidate)

R. Bamezai

Prof. R.N.K. Bamezai
(Supervisor)

23.2.17

Prof. S. K. Goswami
(Dean)

Dedicated to...

Mummy and Papa

"We must not forget that when radium was discovered no one knew that it would prove useful in hospitals. The work was one of pure science. And this is a proof that scientific work must not be considered from the point of view of the direct usefulness of it. It must be done for itself, for the beauty of science, and then there is always the chance that a scientific discovery may become like the radium a benefit for humanity. "

- Marie Curie, Lecture at Vassar College, 1921-

ACKNOWLEDGEMENT

This thesis does not represent my singular effort at the keyboard; it is a milestone of a journey travelled with the kind help, guidance and support of many people. Though it will not be enough to express my gratitude in words to all those people who helped me, I would still like to covey my many, many thanks.

First and foremost, I would like to extend my sincerest gratitude and respect to my supervisor, Prof. R, N.K. Bamezai, who not only gave me the opportunity to pursue my Ph.D. under his guidance, but did so most generously and wholeheartedly. I am especially grateful to him for his passion and devotion to my growth both as a researcher and as a person. He has been an incredible mentor who always gave me enough freedom to tease my naïve mind along with his expert guidance to introduce me to minute methodological approaches, which helped me with new insights and graver exploration of my research area. His everlasting smiling face with radiating positive vibes and innocent consent for all my demands has made me reach this stage. He made this experience not only enriching but also a joyful one. I hope I have imbibed enough to someday be as lively, enthusiastic, and energetic to command an audience as he can. I shall always remain indebted for his constant encouragement and affection towards me.

As this journey comes to an end, I cannot but reflect to the beginning, when I had just joined the lab. It is a great privilege to express my deep sense of gratitude to all the lab seniors, Dr. Shafat, Dr. Amit, Dr. Askander, Dr. Rajnish, Dr. Bhupendra, Dr. Siddhart, Dr. Kalai, Dr. Shazia, Dr. Mamta, Dr. Noor, Mr. Gopinath and Mr. Kailash, for creating a harmonious and congenial environment in lab that helped me work impeccably throughout my PhD. Special thanks to Mr. Gopinath and Mr. Kailash, who set high standards and great examples to follow and were my walking encyclopedia for any professional queries. They were always available when I got stuck in experiments and data solving, and lent me helping hand. I owe my special thanks to Rita Mam, Ghanshyam jee, and Late Kamta jee for creating a friendly and familiar environment in the laboratory throughout these years.

My heartfelt and sincere thanks to Prof. S.K. Goswami, Dean, School of Life Sciences and the former Deans Prof. B.C. Tripathi, Prof. B.N. Mallick and Prof. N.B. Sarin for providing me a platform to work in a scientifically rich environment. My deep gratitude to Prof. S.K. Abraham, Prof. Sher Ali, Prof. R.P. Singh and Dr. A.B. Tiku for evaluation of my annual research progress and providing me the critical appraisal and thoughts throughout the process to portray this work. I am also thankful to all faculty members of the School of Life Sciences, members of central instrument facility and advanced instrumentation research facility for their cooperative and friendly behavior. My sincere thanks to CIF

incharge Dr. Surya Prakash, Dr. Sarika, Mr. Mishra, Mrs. Tripti, Mr. Jugendra, Mr. Suresh, Mr. Amar Chand, Mr. Rajendra for their kind help and support. Special thanks to Administrative Officer Mr. Deepal Ayra, SLS office staff, Shiney ma'm, Kirti ma'm, Suneeta Ma'm, Mr. Ramkripal and particularly Meenu Ma'm for all their help which was always extended with a smile and kind words.

I was blessed with having wonderful caring seniors at School of Life Sciences: Dr. Dhanir, Dr. Praveen, Mr. Somesh, Dr. Anil, Dr. Rohit, Mr. Ravi, Dr. Mrigya, Dr. Neha, Dr. Nitesh, Mr. Vipin, Mr. Subash, who always helped me by providing technical details of the experiments and specially the reagents which I used to lend from them more frequently.

Ph.D. students often talk about loneliness during the course of their study but this is something I never experienced at SLS, a heartfelt thanks to my really supportive and active batch-mates: Arpit, Sandy, Ramraj, Kishore, Ritu, Archana, Atanu, Anshuman, Nimisha, Ashutosh, Rishi, Pooja, Sumit and others; you guys will always be remembered and cherished. The journey is more appreciated when we meet companions along life's road, and I was lucky to find some great friends; especially to mention my friends: Arpit, Sandy, Ramraj and Kishore, who were always there to help me with the resources that I procured indefinite number of times from you guys. We laughed at the dumbest jokes, put-up with each other's idiosyncrasies, went along with the craziest ideas, still our friendship stands rock solid like a mountain, unshakeable. I take pleasure in acknowledging my precious friends: Bajrang, Manoj, Govinda and Madan, who had made this journey a pleasant one by their sensible and personal advice at difficult times which kept my spirit high.

I gratefully acknowledge CSIR for the financial support during the course of my Ph.D.

I express my deepest gratitude to my family, whose silent encouragement and desire to see my success vented in this denouement. They have always believed in me and encouraged me to follow my dreams. The journey would not have been so beautiful had they not been with me. Their love, care and support are priceless.

Above all, I bow my head before the Almighty God, with whose grace and beatitude I moved through this venture. Thank you God for all your blessings to my family and me. For the strength you give me each day and for all the people around me who make life more meaningful. You were with me in my each passing phase. I know that I am not perfect, I know sometimes I forget to pray and question my faith but still you were the first I looked up to, I asked for, whenever I had some problem. You are the first and foremost who deserves my thanks and gratitude when I achieve something big, like this thesis. Thank You God for all your benediction and blessings on me and being with me always.

Sunil Kumar Saini

ABBREVIATIONS

3'UTR	3' Untranslated Region
5'UTR	5' Untranslated Region
ATP	Adenosine Tri Phosphate
ATP	Adenosine Tri Phosphate
Bp	Base pair
BSA	Bovine Serum Albumin
CGI	CpG Island
DMEM	Dulbecco's Minimal Essential Media
DMSO	Di methyl sulphoxide
DNA	Deoxyribonucleic acid
dNTPs	Deoxy nucleotide triphosphate
EtBr	Ethidium Bromide
FACS	Fluorescent activated cell sorter
FBS	Fetal Bovine Serum
GFP	Green Fluorescence Protein
Gm	Gram
HVR2	Hypervariable region 2
IMM	Inner mitochondrial membrane
Kb	Kilobase
LSO	L-Strand origin of replication
M	Molar
mA	Milliampere
MAS	Membrane attachment site
mtDNA	Mitochondrial DNA
Min	Minute
Ml	Milliliter
MLS	Mitochondrial Localization Signal Sequence
mM	Milli Molar
mRNA	Messenger RNA
mtROS	Mitochondrial reactive oxygen Species
NAD^+	Nicotinamide adenine dinucleotide (Oxidised)
NADH	Nicotinamide Adenine dinucleotide (Reduced)
ND	NADH Dehydrogenase
Ng	Nano gram
Nm	Nano meter
OMM	Outer mitochondrial membrane
PBS	Phosphate Buffer Saline
PCR	Polymerase Chain Reaction

PCR	Polymerase chain Reaction
RACE	Rapid Amplification of cDNA ends
ROS	Reactive oxygen Species
rRNA	ribosomal RNA
RT	Room Temperture
SAM	S-adenosyl Methionine
SS	Single Stranded
Taq	Thermus aquaticus
Tris	Tris [hydroxymethyl] amino methane
tRNA	transfer RNA
TTF	Transcription termination factor
µg	Micro gram
µl	Micro liter
µM	Micro Molar

List of contents

List of Figures

List of Tables

1. INTRODUCTION

INTRODUCTION

Mitochondria are crucial cell organelle, ubiquitously present in all multicellular eukaryotes. They are involved in diverse and essential key cellular functions, including TCA cycle, oxidative phosphorylation, fatty acid metabolism, amino acid metabolism, biosynthesis of hormones, heme, FeS clusters, apoptosis, ion homeostasis, innate immunity, etc. Abnormalities in the functioning of the organelle lead to a group of heterogeneous diseases and disorders, often characterized by morphological changes, a defective respiratory chain and variable symptoms (Durhuus et al., 2015; Giampazolias and Tait, 2016; Zong et al., 2016). These range from severe metabolic disorders with onset in early infancy or childhood to late onset adult myopathies. Mutations in mitochondrial DNA are the most recurrent cause of mitochondrial diseases in adults. Proteomic analysis has revealed the presence of thousands of proteins within mitochondria (Calvo et al., 2015), however, the mtDNA encodes for a subset of these proteins. The rest majority of proteins are coded by the nuclear genome (Gray, 2015). Hence, most of the mitochondrial disorders are caused by mutations in the nuclear encoded mitochondrial genes. The symptoms of these diseases vary depending on which mitochondrial functions are disturbed; and not all of them cause morphological changes in the mitochondria. In general terms, tissues and organs (retina, optic nerve, brain, heart, testis, muscle, etc.) that are heavily dependent upon oxidative phosphorylation bear the brunt of the pathology (Kim et al., 2016; Raza et al., 2015). It is also puzzling that many mitochondrial disorders affect multiple organ systems; whereas, others have a highly stereotyped and organ specific phenotype. A well-orchestrated interplay between nuclear and mitochondrial (mt) genomes is, therefore, essential for the proper functioning of both the organelles and the cell (Koch, 2016).

The organization of mitochondrial genome is quite simple in comparison to nuclear genome. Mitochondrial DNA, a 16569 bp long multicopy, double stranded circular molecule, codes for a total of 37 genes: 13 polypeptides, 2 rRNA and 22 tRNA (Anderson et al., 1981b). However, a 14th polypeptide, named as humanin, is discovered, which encodes from MT-RNR2 gene that usually codes for mitochondrial 16s rRNA (Guo et al., 2003; Hashimoto et al., 2001). Human mitochondria lack histone proteins and are thus devoid of the complex epigenetic regulation as observed in the nucleus. The nuclear

genome epigenetics is complex and widely studied which in general, includes three types of epigenetic modifications. First, cytosine methylation in DNA is a mark of transcription silencing at CpG dinucleotides. Second, various covalent and non-covalent modifications of several histone and non-histone proteins that differentially regulate gene expression and third, microRNA mediated post transcriptional gene silencing. Promoter regions of genes lacking methylation at CpG sites are generally in transcriptionally permeable configuration (Ramirez-Carrozzi et al., 2009). This is due to unstable nucleosomal assembly in CGI (CpG Island) region which are devoid of methylation. On methylation, MBD (Methyl CpG Binding Domain) proteins either recruit corepressor complex or directly inhibit transcription factor binding, ultimately leading to transcription repression (Bogdanovic and Veenstra, 2009), (Klose and Bird, 2006). One of the epigenetic modifications that could take place inside mitochondria is the methylation of this genome.

Epigenetic regulation generates phenotypic differences in different cell types, despite same genotype background. Mitochondria, as a cellular organelle participates in epigenetic communications with the nucleus in two different ways. One, initiated from the nucleus, the epigenetic mechanisms that modulate the expression of nuclear genome by regulating the expression of nuclear-encoded mitochondrial genes, affecting the function of mitochondria. And the other, initiated from the mitochondria, where the health and activity of mitochondria determine the methylation pattern of nuclear genes involved in various cellular pathways. The very first study conducted 40 years ago reported absence of mitochondrial DNA methylation in frogs and HeLa cells (Dawid, 1974). Thereafter, several studies suggested low levels of methylation in mitochondria in different species, including mouse and humans (Nass, 1973). But the extent and the process of methylation of this genome remained debatable for long; as both kinds of reports emerged in literature, one which showed an absence of methylation in mitochondria and the other which showed the presence of the same (Dawid, 1974; Hong et al., 2013; Infantino et al., 2011; Li et al., 2017; Mawlood et al., 2016b; Menga et al., 2017; Pirola et al., 2013). In support of the occurrence of methylation, Shock et al for the first time showed an existence of a DNA methyltrasferase (DNMT1) inside mitochondria (Shock et al., 2011). After this, a number of reports in favor of this epigenetic modification continued to increase; and found differential methylation at certain CpG regions of mitochondrial genome in association

with several pathophysiological conditions (Byun et al., 2013a) (Bellizzi et al., 2013) (Pirola et al., 2013) (Ghosh et al., 2014) (Janssen et al., 2015) (Baccarelli and Byun, 2015) (Gao et al., 2015) (Madeddu et al., 2016) (Li et al., 2017).

However, none of these studies provided an insight into the mechanistic details of the epigenetic process and its role in mitochondrial biology. In the background of our previous studies (Darvishi et al., 2007; Gochhait et al., 2008), related to mitochondrial genomics and ROS mediated retrograde signaling and epigenetic modulation of nuclear gene expression (Singh et al., 2014), we attempted to understand the process of mitochondrial epigenetic regulation. A direct approach of exogenous overexpression of specific isoforms of DNMT1 was used to find out if these localized in mitochondria and played a role in influencing its biology epigenetically.

Given the small genome of mitochondria and the fact that most of the mitochondrial proteins are encoded by nuclear genome, it was important to explore the possible role of miRNAs in mitochondrial biogenesis and function, at least bioinformatically. Pertinently to find out if the key nuclear encoded genes involved in mitochondrial biogenesis were targeted by miRNA, affecting its function. As is known, microRNAs (miRNAs) play a vital role in regulating gene expression post transcriptionally by repressing mRNA translation or promoting their degradation. MicroRNAs (miRNAs) constitute a class of non-coding RNAs that play an important role in epigenetic regulation of gene expression. These RNA molecules act at the post transcriptional level, and are known to fine–tune the expression of ~ 30% of all mammalian protein encoding genes (Sioud and Cekaite, 2010). Mature microRNAs are short, single stranded RNA molecules, approximately 22 nucleotides in length. MicroRNAs have been shown to be involved in a diverse range of biological processes, such as cell cycle control, apoptosis and several developmental and physiological processes including stem cell differentiation, hematopoiesis, hypoxia, cardiac and skeletal muscle development, neurogenesis, insulin secretion, cholesterol metabolism, aging, immune response and viral replication (Booton and Lindsay, 2014; Guay and Regazzi, 2015; Hayes and Chayama, 2016; Jiangpan et al., 2016; Maegdefessel, 2014; Paul et al., 2017). Since miRNAs are involved in diverse biological processes, they are considered as a key to explain the pathogenesis and probably cure multifactorial

diseases. Several studies have demonstrated the presence of miRNAs either within (Latronico and Condorelli, 2012) or associated with (Carrer et al., 2012; Sripada et al., 2012; Yamamoto et al., 2012) mitochondria isolated from various cell types and tissues, including the CNS (Wang and Springer, 2015). The present study on the basis of a detailed bioinformatics analysis suggests a possible role of a miRNA, has-miR-19b-2-5p, in regulating the mitochondrial biogenesis. Interestingly this miRNA targeted the five key mitochondrial biogenesis genes that were epigenetically upregulated on exogenous expression of DNMT1-isoform3. The pathway enrichment analysis suggested that this miRNA participated in several metabolic pathways which could be a key to the regulation of the mitochondrial gene expression and biogenesis.

2. REVIEW OF LITERATURE

REVIEW OF LITERATURE

2.1. Mitochondria: history, structure, function and dynamics

Historical account: Only a few years after the discovery of nucleus (Brown, 1833), evidences accumulated for the existence of mitochondria like organelle inside the cells (Henle, 1841). Nearly after five decades, it was Altman, who noticed their elementary nature and ubiquitous presence within many types of cells, performing vital functions (Altmann, 1894). He named these as Bioblast and hypothesized their symbiotic behavior within cells; which is now the best accepted model for origin of this organelle inside cells (Mereschcowsky, 1910). The name mitochondrion was coined by Carl Benda in 1898 (Benda, 1898). The first unexplained hint about the role of mitochondria in redox metabolism came from the observation in 1900s, when it was identified that the redox dye Janus Green B specifically binds to this organelle (Michaelis, 1900). This property remained an official portrait of the organelle for many years, till the first electron micrograph was published (Palade, 1952). By 1908, presence of lipid and protein were confirmed within mitochondria (Regaud, 1908). Meves et, al. described plant mitochondria in 1904 (Meves, 1908). In 1909, Regaud suggested that mitochondria could be a bearer of genes (Ragaud, 1909). In the following two decades, many researchers proposed the role of mitochondria in expression of reducing substances required for cellular respiration, mainly based on structural and direct visual observations. It was in 1934, when Bensley and Hoerr isolated globular and rod shaped structures from liver tissue of guinea-pig, corresponding to mitochondrial fraction; the way opened for research toward understanding the role of mitochondria in cell physiology, including cellular respiration (Bensley and Hoerr, 1934). In-between, mainly from the work of Battelli and Stern (Battelli and Stern, 1912) and Warburg (Warburg, 1913), the oxido-reductive enzymatic characteristics of mitochondria were attributed to the non-soluble particulate fraction of mitochondria. Identification of cytochrome paved the way for definition of respiratory chain as chain of dehydrogeneases (Keilin, 1925). Between fourth and fifth decade of 19^{th} century, great discoveries in mitochondrial physiology were achieved, where Krebs discovered citric acid cycle (Krebs and Johnson, 1937). Similarly, Kalckar presented observations which demonstrated aerobic phosphorylation (Kalckar, 1937, 1939). In 1939,

Belister and Tsybakova experimentally showed that at least 2 molecules of ATP were formed per atom of oxygen consumed (Belitser and Tsybakova, 1939). In 1941, Lipmann developed the concept of Phosphate-Bond-Energy as a general form of energy storage in cell metabolism (Lipmann, 1941) and in 1943, a direct link between glycolysis and mitochondrial energy metabolism was established. The latter was mainly from the work of Ochoa, where he showed that oxidation of pyruvate gave 3 moles of organically bound phosphate for each atom of oxygen consumed (Ochoa, 1943). Concluding evidences about respiratory chain linked phosphorylation came from the work of Friedkin and Lehninger where they used particulate fraction from rat liver as enzyme and hydroxybutyrate or NADH as substrate in their successful enzyme activity assays (Friedkin and Lehninger, 1948; Friedkin and Lehninger, 1949). Altogether, these findings and further improvement in techniques of mitochondrial isolation set a stage for direct biochemical approach for determining other mitochondrial functions. The Next decade (1950-60s) witnessed identification of several enzymes in addition to those involved in the citric acid cycle, fatty acid oxidation, respiration, and phosphorylation. Among these enzymes were, adenylate kinase (Kielley and Kielley, 1951), glutamate dehydrogenase (Hunter and Hixon, 1949), pyruvate carboxylase (Lardy and Adler, 1956) and nucleoside diphosphokinase (Herbert and Potter, 1956), as well as enzymes involved in the substrate-level phosphorylation linked to the oxidation of α-ketoglutarate (Hunter and Hixon, 1949), the synthesis of porphyrine and heme (Sano et al., 1959, 1960), citrulline (Siekevitz and Potter, 1953), and phospholipids (Kennedy and Weiss, 1956). Mitochondria were also found to contain a part of the cellular hexokinase (Crane and Sols, 1953). Isolated intact mitochondria also showed adenine nucleotides (Siekevitz and Potter, 1955) as well as a variety of inorganic ions including phosphate, Na^+, K^+, and Mg^{2+} (Bartley and Davies, 1954). Mitochondria were also demonstrated to take up and accumulate Ca^{2+} (Slater and Cleland, 1953) and Mn^+ (Maynard and Cotzias, 1955). These early observations foreshadowed the occurrence of active ion-transport across the mitochondrial membrane.

Structural overview: Mitochondria are present in all eukaryotic cells - including all *animal cells* and *plant cells*. They are believed to be the remnant of a prokaryotic organism that had become a vital symbiotic partner to the eukaryotic cell early in the evolution (Gray et al., 1999). The number of mitochondria in each cell varies considerably, from just one

mitochondrion up to 10,000 mitochondria in some specialized types of cells. A "typical" number of mitochondria per cell is around 200. Mitochondria are "oval-shaped" cell organelles surrounded by two phospholipid layers. The outer membrane defines the external shape of the mitochondrion and contains multiple copies of a transport protein porin, which forms aqueous channels allowing molecules with a maximal molecular weight of 5kD to penetrate the membrane. The inner membrane is evidently folded and forms a tubular or lamellar structure called cristae. Between the inner and outer membranes is the space, which is referred to as "inter membrane space". The volume enclosed inside the inner membrane is the "matrix". Mitochondrial matrix comprises of the enzymes of the TCA cycle, other structures and molecules, including ribosomes, matrix granules and mitochondrial DNA.

Functional account: For a long time mitochondria were known to perform the task of energy production via oxidative phosphorylation. However, in the last few decades, the understanding about their multiple functions has gained new insights. They are involved in many essential cellular functions, including TCA cycle, oxidative phosphorylation, fatty acid metabolism, amino acid metabolism, biosynthesis of hormones, heme, FeS clusters, apoptosis, ion homeostasis, innate immunity, etc. Mitochondrial proteins are encoded by two distinct genetic systems, mtDNA and nuclear DNA (nDNA). MtDNA, a small 16.6 kb circle of double stranded DNA, codes for 13 respiratory chain polypeptides of respiratory complexes I, III, IV, and V (only complex II is solely composed of proteins encoded by nuclear genes) and 24 nucleic acids necessary for intra-mitochondrial protein synthesis (Anderson et al., 1981). Mitochondria are intimately involved in cellular homeostasis. They nourish cells by converting energy from carbon sources into ATP (adenosine triphosphate). Additionally, they are important for thermogenesis, calcium and iron homeostasis, intracellular signaling and apoptosis, various metabolic intermediary pathways including metabolism of amino acids, lipids, cholesterol, steroids and nucleotides through oxidative phosphorylation (OXPHOS). Oxidative metabolism is fuelled by pyruvate generated from carbohydrates in glycolysis and fatty acids produced from triglycerides. These are selectively taken into the mitochondrial matrix and broken down into acetyl CoA by the pyruvate dehydrogenase complex or the β oxidation pathway. The acetyl group then is involved in the citric acid cycle, producing substrates for OXPHOS, like NADH and

FADH. Electrons generated from NADH are passed along a series of carrier molecules called the electron transport chain (ETC), the products of this process being water and ATP. In this process, protons are pumped from the matrix across the mitochondrial inner membrane through respiratory complexes: I, III, and IV. When protons return to the mitochondrial matrix down their electrochemical gradient, ATP is synthesized via complex V (ATP synthase). Thus the mitochondria convert energy derived from the OXPHOS process which is more efficient than anaerobic glycolysis. In the mitochondrion the metabolism of one molecule of glucose produces about 30 molecules of ATP, while only two molecules of ATP are produced by glycolysis in the cytoplasm. This means that organs with a high-energy demand are vulnerable to the depletion of mitochondrial energy production.

Dynamics: Mitochondria adopt variable shapes, depending on the cell type and the metabolic demands of the cell. Two predominant morphologies are reflected in the Greek name of the organelle– 'mitos' for thread and 'chondros' for grain. Mitochondrial movement and fission were first observed with light microscopy more than 100 years ago (Lewis and Lewis 1914). Later on electron microscopy provided their fine and detailed structure. Technological advances which made it easier to track mitochondria in live cells have contributed magnificently to our understanding of mitochondrial dynamics in the past few decades. Live cell microscopy of mammalian cells, using vital dyes and targeted fluorescent proteins, showed that mitochondria periodically divide and fuse with other mitochondria (Qian et al., 2012). Under normal physiological conditions, the fusion events are often rapidly followed by fission that helps in maintaining the number of mitochondria in a given cell. However, this sorting event could be asymmetric, giving rise to the daughter mitochondria with different membrane potentials. This is a quality control process that separates the healthy mitochondria from a mitochondria with a heavy load of defective components (Youle and Van Der Bliek, 2012). Mitochondria that cannot recover membrane potential because of these defects become targets for Pink1- and Parkin mediated degradation (Jin et al., 2010). Mitochondrial dynamics has an important role in combating and countering the cellular stress levels. Low levels of stress increase the process of fusion and/or decrease fission to partially restore the function of defective mitochondria by mixing the components as a form of complementation; whereas high

levels of stress conditions result in a decreased fusion and/or increased fission to separate the damaged mitochondria from the healthy ones. Low levels of stress are seen with starvation, during which mitochondrial fission is inhibited to protect cells from excessive autophagosomal degradation of mitochondria (Gomes et al., 2011; Rambold et al., 2011). Fission rates are drastically increased during apoptosis to eliminate the damaged mitochondria through mitophagy, which if accumulated could be detrimental to the cells. Several disease conditions in humans have been found associated with mutations in the pathways of fusion and fission process. These diseases are mainly related to the tissues where the proper function of mitochondria is of upmost requirement. These include; neurodegenerative (Parkinson's, CharcotMarie-Tooth, Dominant Optic Atrophy, and Alzheimer's), diabetes, ischemia reperfusion, and liver related (Chan, 2012; Liesa et al., 2009; Nunnari and Suomalainen, 2012a) diseases.

2.2. Mitochondrial Genome

2.2.1. Mitochondrial DNA: A brief history, replication and transcription

Historical account: In the known background of DNA as genetic material and advancement in electron microscopy, it was a great lead in mitochondrial genetics when Nass and Nass showed the presence of intra-mitochondrial fibers with characteristics of DNA inside mitochondria in electron micrographs (Nass and Nass, 1963a). These fibers were observed to be digested by DNase but not by RNase, which proved their DNA nature (Nass and Nass, 1963b). For the first time, DNA from mitochondria was isolated in 1965 from heart and liver tissues of chick embryo (Rabinowitz et al., 1965). In the very next year, the ubiquitous occurrence of mitochondrial DNA was reported, where their presence in yeast and several mammalian species was reported (Corneo et al., 1966). Mitochondrial DNA showed differential buoyant density when compared with nuclear DNA (Luck and Reich, 1964). In 1966, the circular nature and differential length of mitochondrial DNA within different species was reported. Eventually, breakthrough molecular techniques allowed scientists to clone, sequence and characterize mtDNA from a range of species (Gray, 1982).

In fact, the first non-viral genomes to be completely sequenced were the mouse and human mtDNAs in 1981 (Anderson et al., 1981a). Soon after, complete mtDNAs of bovine (Anderson et al., 1982) and other animals were deciphered (Clary and Wolstenholme,

1985). By early to mid-1990s, mitochondrial DNA from various animals, plants (Oda et al., 1992), algae (Vahrenholz et al., 1993), fungi (Cummings et al., 1990) and other protists (Kairo et al., 1994) were sequenced. After a few amendments in the mitochondrial DNA sequences of Anderson (1981), referred to as revised Cambridge Reference Sequence (rCRS), it was clear that mitochondrion encodes a total of 37 genes: 22 tRNAs, 2 rRNAs and 13 mRNAs. However in 2001, MT-RNR2 gene was discovered to code for humanin, the 14th biologically active mitochondrial encoded polypeptide, besides 16s rRNA. The mtDNA-encoded polypeptides are all subunits of enzyme complexes of the oxidative phosphorylation system, except for the humanin. The rest of the polypeptide subunits in the mitochondrial oxidative phosphorylation system and other mitochondrial proteins, including numerous enzymes, transport proteins, structural proteins etc., are encoded by the nuclear genome and are translated on cytoplasmic ribosomes before being imported into the mitochondria. On the basis of differential density of the two strands, due to more number of guanines in one strand, the two strands are known as the heavy (H) and the light (L) strand. The H strand harbours: 13 out of the 14 polypeptide-encoding, 14 of the 22 tRNA-encoding and both rRNA-encoding genes (Table 2.1). Mitochondrial DNA lacks introns and has small inter-genic spacers, where the reading frames overlap. mtDNA also contains the sequences vital for origin of mtDNA replication and transcription within the non-coding region called displacement loop (D-loop), a region of 1121 bp that possesses origin of replication for the H-strand (O_H), and the promoters of light (L) and H-strand transcription.

Table 2. 1: Mitochondrial genome encoded genes with their co-ordinates.

Gene belongs to	Gene Symbol	Coding strand	Position
NADH Ubiquinone Oxido-Reductase (Complex I)	ND1	Heavy	3307-4262
	ND2	Heavy	4470-5511
	ND3	Heavy	10059-10404
	ND4	Heavy	10760-12137
	ND4L	Heavy	10470-10766
	ND5	Heavy	12337-14148
	ND6	Light	14149-14673
Succinate Dehydrogenase (Complex II)	X	X	X
CoenzymeQ-Cytochrome reductase (Complex III)	CytB	Heavy	14747-15887

Cytochrome C-Oxidase (complex IV)	CO1	Heavy	5904-7445
	CO2	Heavy	7586-8269
	CO3	Heavy	9207-9990
ATP Synthase(complex V)	ATP6	Heavy	8527-9207
	ATP8	Heavy	8366-8572
rRNA	MT-RNR1(12S)	Heavy	648-1601
	MT-RNR2(16S)	Heavy	1671-3229
Humanin	MT-RNR2(16S)	Heavy	X
tRNA	MT-TA	Light	5587-5655
	MT-TC	Light	5761-5826
	MT-TD	Heavy	7518-7585
	MT-TE	Light	14674-14742
	MT-TF	Heavy	577-647
	MT-TG	Heavy	9991-10058
	MT-TH	Heavy	12138-12206
	MT-TI	Heavy	4263-4331
	MT-TK	Heavy	8295-8364
	MT-TL1	Heavy	3230-3304
	MT-TL2	Heavy	12266-12336
	MT-TM	Heavy	4402-4469
	MT-TN	Light	5657-5729
	MT-TP	Light	15956-16023
	MT-TQ	Light	4329-4400
	MT-TR	Heavy	10405-10469
	MT-TS1	Light	7446-7514
	MT-TS2	Heavy	12207-12265
	MT-TT	Heavy	15888-15953
	MT-TV	Heavy	1602-1670
	MT-TW	Heavy	5512-5579
tRNA	MT-TY	Light	5826-5891

Replication: of human mitochondrial DNA is independent of nuclear DNA (Attardi and Schatz, 1988). It is replicated by proof reading compromised DNA polymerase γ in a bidirectional but asynchronous manner, using largely separated strand-specific unidirectional origins of replication. The mtDNA replication initiates from O_H (H strand origin) and L-strand origin (O_L), in each of the two strands.

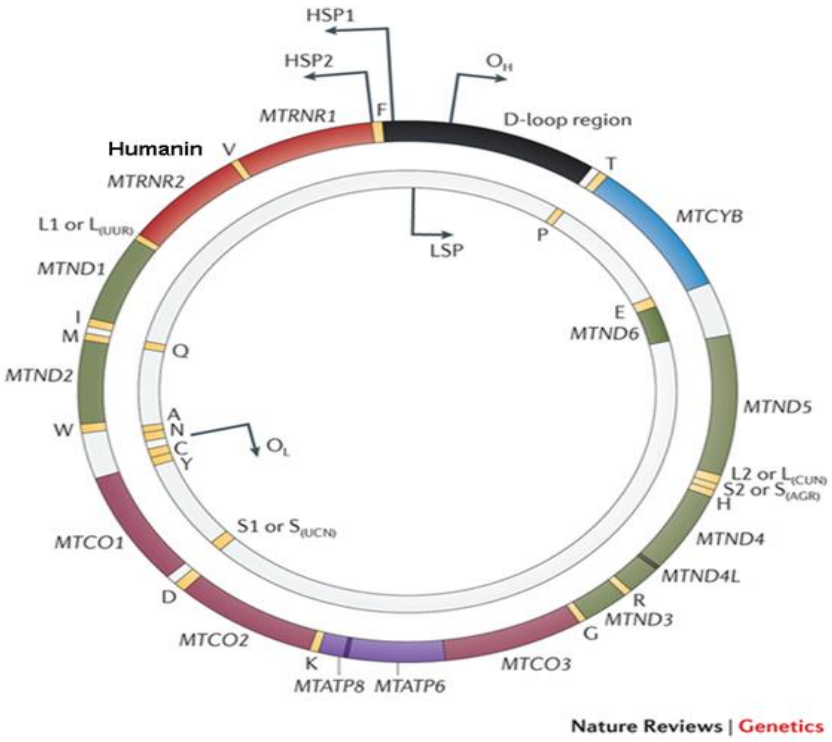

Figure 2. 1: Schematic presentation of mitochondrial genome (Source: Nature Reviews Genetics, 2015).

DNA replication initiated at O_H, as a leading strand, uses an RNA primer generated from the L-strand transcript. H-strand synthesis proceeds two-thirds around the mtDNA, displacing the parental H-strand until it reaches the L-strand origin (O_L), situated in a cluster of five tRNA genes. The origin of replication for the lagging strand (O_L) is then exposed and synthesis of the nascent L-strand proceeds in the opposite direction on the single-stranded template of the expanded D-loop. The consequence of strand-asymmetric synthesis results in a delay in completion of the daughter molecule with the new L-strand with respect to the other daughter molecule, and results in its segregation prior to completing replication. These molecules are termed gapped circles (GpC), since they contain a gap in newly synthesized L-strand DNA, leaving an H-strand template region that is still single-stranded.

Transcription: of mitochondrial DNA is unlike transcription of nuclear genes. Each nuclear gene is almost always transcribed separately using individual promoters. However, mtDNA transcription generates a polycistronic RNA, which is subsequently processed into individual mRNA, rRNA, and tRNA molecules by various RNases (Aloni and Attardi,

1971; Lightowlers et al., 1997). Transcription of human mtDNA is directed by a single-subunit RNA polymerase, POLRMT, which requires two primary transcription factors, TFB2M (transcription factor B2, mitochondrial) and TFAM (transcription factor A, mitochondrial), to achieve basal regulation of the system. Transcription initiates from the three promoters (Bestwick and Shadel, 2013), one L-strand promoter (LSP) and two H-strand promoters (HSP1 and HSP2). Transcripts from HSP1 are preferentially terminated in a tRNA gene immediately after the rRNA genes, and transcripts from LSP and HSP2 are complete upto full genome length (Montoya et al., 1983). These primary transcripts are subsequently processed into individual mRNA, rRNA, and tRNA molecules by various RNases.

Genetic code: of mitochondria which is used to encode 13 polypeptides are slightly different from the nuclear genetic code. As there are only 22 tRNAs, individual tRNA molecules are needed to interpret several different codons. For most organisms, UAA, UAG and UGA are recognized as stop codons, however, in vertebrate mitochondria UAA and UAG have similar function but UGA codes for Tryptophan instead. Most organisms use AUA code for isoleucine; but in vertebrate mitochondrial mRNA it codes for methionine. Similarly, the universal code AGA and AGG code for arginine in most organisms, but in vertebrate mitochondria these are recognized as stop codons or as serine by the translation machinery. AUG is the standard initiation codon for protein synthesis, however in human mitochondria AUA and AUU could also function as alternate initiation codons. The consideration of this deviation from the standard code is very important when using mitochondrial gene for experimental studies as there is a codon bias during translation when expressing in different species. To avoid this, codon optimization is required.

2.2.2. Mitochondrial DNA Sequencing: A perspective

Historical account: The foundation of mtDNA sequencing was laid in 1972 when Ray Wu attempted for DNA sequencing, using location specific primer extension method. Later, progress was made in 1974 by Jay Bambara and others using the approach of polymerase catalysis and nucleotide labeling to sequence mitochondrial DNA. In 1977, chain termination method for DNA sequencing designed by Sanger was key to sequence whole

genome of bacteriophage Φx 174 (Sanger et al., 1977). Few years later and just two years before the concept of PCR, a combined approach of molecular cloning and DNA sequencing made it possible for Anderson et.al, (1981) to sequence whole mitochondrial genome of humans, known as Cambridge reference sequence (CRS). Except for a few mistakes and skipped polymorphisms, this sequence signified more than 99% accuracy and was used as a reference sequence worldwide for further studies in mitochondrial genomics. Discovery of Taq polymerase from *Thermus aquaticus* provided a platform for *in-vitro* amplification of DNA through polymerase chain reaction designed by Karl Mullis in 1983. Progression in the field of DNA sequencing provided another addition to the field of molecular genetics, which gained momentum in the era of the automated DNA sequencing. The three step tedious process of mtDNA sequencing (mitochondrial DNA isolation, molecular cloning and manual sequencing) improved to a comparatively easier two-step process (direct amplification of mtDNA by PCR and automated sequencing). This advancement also made multiple sequencing reactions possible at the same time. Later studies found a few inaccuracies in the mtDNA sequence from Anderson at some of the positions. In the process of refinement, a revised version of mtDNA sequence was published in 1999 by Andrews et.al (1999) with a comprehensive information about polymorphisms. This sequence is now referred as revised Cambridge reference sequence (rCRS).

Present era: Next-generation sequencing methods have made it fast and convenient to sequence whole mitochondrial genome. Mitochondrial DNA sequence-database has established its highly polymorphic nature and the presence of several pathogenic mutations in general population (Elliott et al., 2008). These single nucleotide polymorphisms (SNPs) in mitochondrial DNA have been used for elucidation of evolutionary and migratory paths, providing information on differential susceptibility or protection towards various pathophysiological conditions as well. Late onset and complex disorders, ranging from mild myopathy to Alzheimer's, Parkinson's, aging and various cancers have been shown in association with mtDNA variations (Dhillon and Fenech, 2014; Kazuno et al., 2006; Nunnari and Suomalainen, 2012b; Wallace, 2013). Whole mitochondrial genome comparisons between tumor and adjacent normal tissues of prostate (Petros et al., 2005), head and neck (Zhou et al., 2007), bladder (Dasgupta et al., 2008), pancreas (Lam et al.,

2012), breast and esophagus (Gochhait et al., 2008) have identified a number of pathogenic mutations, providing a probable advantage in cancers for tumor growth. Similarly, case-control comparison studies in diverse cancers in different populations have also shown an association with both germline and somatic mitochondrial DNA SNPs with breast (Darvishi et al., 2007; Gochhait et al., 2008), esophagus (Gochhait et al., 2008; Li et al., 2011), prostate and renal (Booker et al., 2006), endometrial (Liu et al., 2003), and other cancers.

Implications: Mitochondrial DNA (mtDNA) sequence-database has documented the highly polymorphic nature and several pathogenic mutations prevalent in general population (Elliott et al., 2008). These single nucleotide polymorphisms (SNPs) in mitochondrial DNA have been used for elucidation of evolutionary and migratory paths; and also providing information on patho-physiological conditions. The usefulness of mtDNA sequences has emerged in studying mtDNA variants that are selectively neutral and avoid elimination by selection, thus becoming prevalent through genetic drift. Since mtDNA is strictly maternally inherited, it has evolved by sequential accumulation of base substitutions along radiating maternal lineages. Mitochondrial DNA sequences have revealed information of the polymorphisms that occurred tens of thousands of years ago and are population-specific, creating groups of related mtDNA haplotypes or haplogroups (Torroni and Wallace, 1994; Wallace et al., 1995). The information gained from the polymorphisms has been useful in analysing putatively pathogenic mutations, and for constructing mtDNA phylogenies (Finnila et al., 2000; Torroni and Wallace, 1994) for tracing population migrations (Wallace and Torroni, 1992; Watson et al., 1997).

2.3. Mitochondria in Signaling

Mitochondria have generally been viewed as bioenergetic and biosynthetic cell organelles that autonomously co-exist within a cell. However, the past two decades have provided enough evidence that mitochondria function as signaling organelles, continuously communicating with the cytosol to initiate biological events under various pathophysiological conditions. Signal transduction from mitochondria to the cytosol is stated as retrograde signaling and signal transduction from cytosol to mitochondria as anterograde signaling (Figure. 2.2).

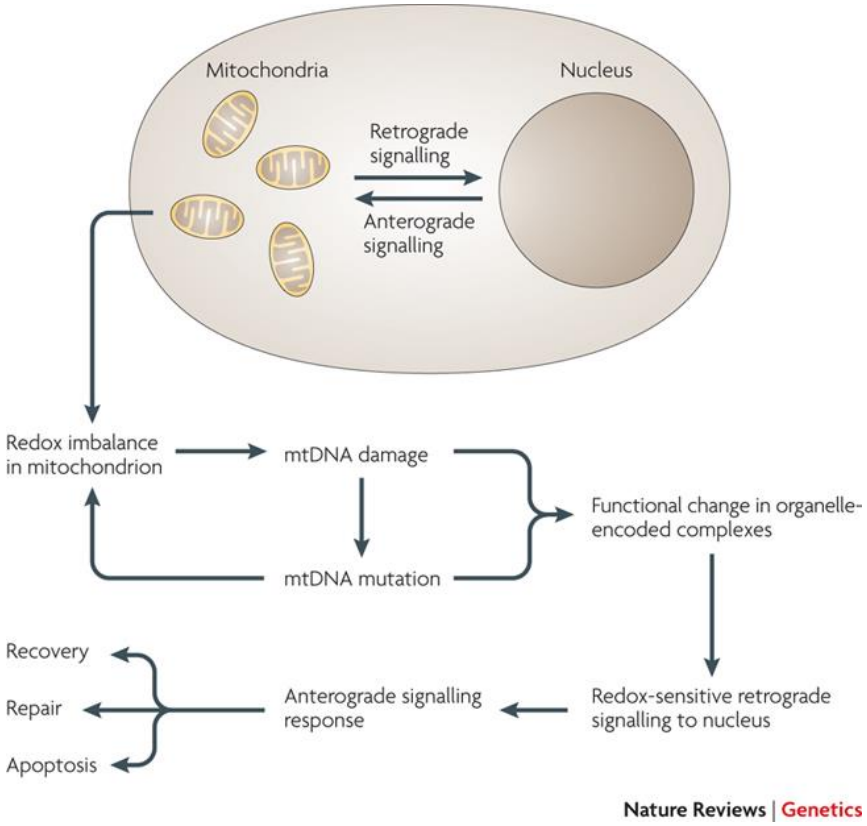

Figure 2. 2: Mitochondria as a signaling organelle. (Source: Nature Reviews Genetics, 2013).

2.3.1. Mitochondria as a signaling organelle: A historical account

In 1990s, several groups laid down foundations for the concept of mitochondria as a signaling organelle that communicated with the cytosol. In 1993, microdomains with high Ca^{2+} close to IP3-sensitive channels sensed by neighboring mitochondria were suggested (Rizzuto et al., 1993). A significant discovery happened in the field of research in mitochondria in 1996, when Xiaodong Wang and colleagues, using biochemical approaches, found that cytochrome c is released from mitochondria to initiate cell death in mammalian cells (Liu et al., 1996a). In the same year, Navdeep Chandel and colleagues reported mitochondrial release of reactive oxygen species (ROS) as a signaling molecule to activate hypoxic gene expression (Chandel et al., 1998). In 1999, Chen and colleagues showed how A-kinase-anchoring proteins (AKAPs) were localized to the mitochondrial outer membrane, which allowed cAMP-dependent protein kinase (PKA) to phosphorylate substrates on the outer mitochondrial membrane (Harada et al., 1999) (Chen et al., 1997).

In the same year, the group of Martinus demonstrated mitochondrial dysfunction mediated induction of mitochondria-specific heat shock proteins that promoted cytosolic calcium-dependent signaling (Martinus et al., 1996). Similarly, Ca^{2+} mediated retrograde signaling was found to be involved in the skeletal myocytes in response to mitochondrial genetic and metabolic stress (Biswas et al., 1999). These studies led to the evolving concept of mitochondria acting as a signaling organelle by releasing proteins, ROS, metabolites, or by serving as a scaffold to configure signaling complexes. Up to now, multiple other mechanisms of mitochondrial signaling have been discovered by which mitochondria cross-talk with rest of the cell. These involve the release of metabolites, mitochondrial motility and dynamics, and interaction with other organelles, such as endoplasmic reticulum in signal regulation.

2.3.2. Mitochondrial ROS in signaling

Mitochondrial ROS in signaling was earlier believed to be produced under pathological conditions that had damaging functions in the cell (Shigenaga et al., 1994). The free radical theory of aging proposed ROS mediated damaged mitochondria to be responsible for the ageing process (Harman, 1956). However, in late 1990s, ROS emerged as a signaling molecule that established communication between mitochondria and rest of the cell even under normal physiological conditions. In hypoxic conditions, mitochondria was shown to produce excessive ROS that resulted in stabilization of hypoxia inducible factors (HIFs) and the induction of genes responsible for metabolic adaptation to low oxygen (Chandel et al., 1998; Chandel et al., 2000a). Subsequently, mtROS were shown to regulate cellular metabolism via redox-dependent activation of JNK1, NF-kappa B activation and tumor necrosis factor receptor signaling (Chandel et al., 2001; Chandel et al., 2000b; Nemoto et al., 2000). In the context of tumorigenesis, mtROS were reported to play a dual role, by promoting or suppressing the cell survival (Ras-Raf-MEK1/2- ERK1/2 signaling) and cell death (p38 MAPK) pathways (Han and Sun, 2007). Interestingly, these two pathways have opposite consequences as they lead to cellular proliferation and apoptosis, respectively. In addition to that in the past decade, mtROS have been shown to regulate a wide range of biological processes, including oxygen sensing, autophagy, epigenetics, stem cell

proliferation and differentiation, innate and adaptive immune responses and hormone signaling (West et al., 2011), (Collins et al., 2012), (Sena and Chandel, 2012).

Mitochondria during electron transfer process are known to produce ROS. There are a total of eight sites in the mitochondrial inner membrane and matrix that have been associated in the production of these transient ROS. The process of generation of these ROS is mostly governed by: concentration of oxygen available to mitochondria, the redox state of the different electron transport chain complexes and mitochondrial membrane potential (Murphy, 2009), (Brand, 2010). The mtROS mediated signaling generates diverse biological outcomes depending upon the gradient of their concentration. Their generation in the cell in an unregulated way leads to the oxidation of nucleic acids, proteins, and lipids in mitochondria, and triggers the release of cytochrome c that ultimately results into the activated caspase-3 mediated apoptosis (Ricci et al., 2004). On a contrary note, recent evidence in yeast and mice suggests, an increase in mtROS could initiate cellular stress pathways that diminish tissue degeneration, stimulate healthy aging and increase lifespan (Hekimi et al., 2011; Liu et al., 2005; Schulz et al., 2007). These studies have put a question mark to the "mitochondrial" and "free radical" theories of aging by implicating ROS as pro-longevity signals as opposed to damaging pro-aging agents, as viewed for long. Ristow and colleagues have shown that reduced glucose availability lead to an increased mitochondrial respiration and mtROS production that delayed worm aging (Schulz et al., 2007). The anti-aging effects of mtROS signaling have been shown in reduced insulin/IGF signaling and D-glucosamine supplementation (Weimer et al., 2014; Zarse et al., 2012).

Mitochondrial dysfunction that arose due to: inhibition of mitochondrial ETC or by certain mutations or by inactivation of mitochondrial SOD2, increased the worm lifespan and was causally linked to increased mtROS production (Dancy et al., 2014).

Hekimi and colleagues have recently shown that this initiated a distinct form of activation of apoptotic signaling cascade to stimulate protective stress responses rather than apoptosis (Yee et al., 2014). These mtROS-mediated responses have suggested that a new paradigm of eliciting an adaptive homeostatic response emerges to the canonical stress-response pathways, such as DNA repair and apoptosis, to sense mtROS instead of the emergency and cell death responses for which they were defined originally.

Based on these studies, an emerging model of mtROS and signaling has been suggested where low levels (picomolar to nanomolar range) of mtROS maintain homeostatic biological processes; whereas, slightly elevated levels initiate pathways for adaptation to stress and the extreme elevated levels trigger cell death or senescence (Figure. 2.3).

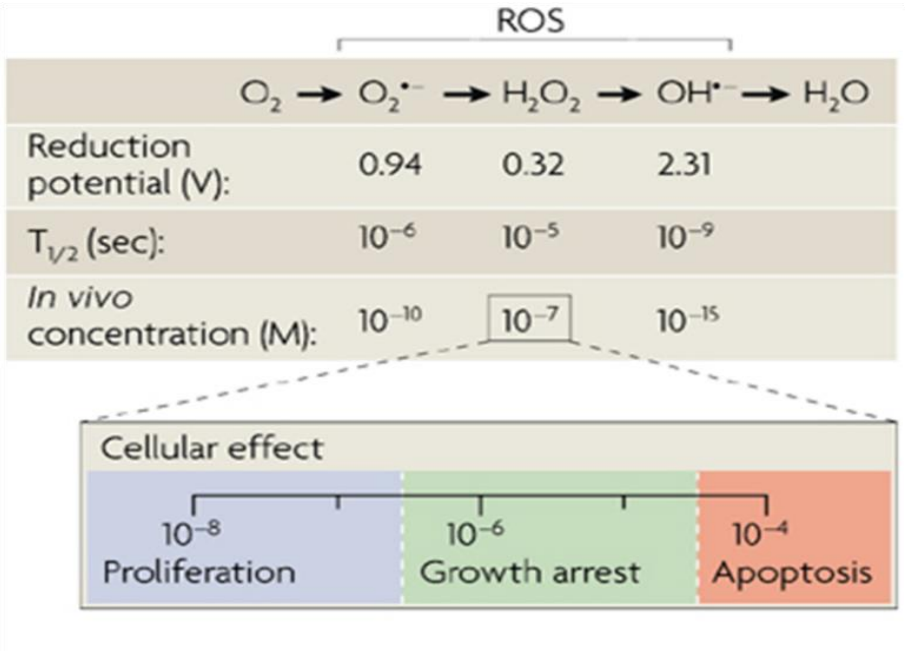

Figure 2. 3: Gradient of ROS levels governs the cellular effect. O2°-, OH°- represents superoxide and hydroxyl radical. (Source: Nature review genetics, 2012)

2.3.3. Mitochondrial cytochrome c release regulates signaling

Cytochrome c is an essential component of the electron transport chain that participates as an electron carrier in the life-supporting function of ATP synthesis. However, when the cell detects an apoptotic stimulus of DNA damage, or the presence of unfolded proteins, or metabolic stress, cytochrome c is released into the cytosol triggering intrinsic apoptotic pathway (Kluck et al., 1997; Liu et al., 1996b; Yang et al., 1997). The release of cytochrome c and cytochrome-c-mediated apoptotic signal molecules are controlled by multiple layers of regulation, the most prominent players being members of the B-cell lymphoma protein-2 (BCL2) family. Certain caspases have also been shown to act upstream of mitochondria to regulate cytochrome c release and thus regulate intrinsic apoptosis. Mitochondrial dynamics (elongated or fragmented) also has been known to regulate the process of cytochrome c release by specialized proteins involved in

mitochondrial fission and fusion. Death-associated protein kinase-related protein-1 (DRP1), a mitochondrial fission protein, promotes apoptosis while optic atrophy protein-1 (OPA1) and mitofusin protein (Mfn1/2) have anti-apoptotic property. Downregulation of OPA1 has been shown to result in fragmentation of the mitochondrial network and drastic disorganization of the cristae, thus facilitating cytochrome c release (Pellegrini and Scorrano, 2007). Under normal conditions, cytochrome c and second mitochondria-derived activator of caspase (SMAC), remain sequestered in the mitochondria. In this stage the permeability transition pore (PTP) is closed, while the pro-apoptotic B-cell lymphoma protein-2 (BCL2) family members, such as BAX, BID and BAK, are prevented from carrying out their functions by anti-apoptotic BCL2 family (BCL2 and BCL-XL) molecules. Caspases in the cytosol remain as uncleaved inactive procaspases and the apoptotic protease activating factor-1 (APAF1) is present in its auto inhibited monomeric form. Following an apoptotic stimulus, BID is cleaved to yield truncated (t) BID; and tBID in turn activates BAX and BAK by inducing their oligomerization to form pores in the outer mitochondrial membrane (OMM). Cytochrome c exits the mitochondrion through the pores of PTP and/or other channels. It is believed that the release occurs in two stages: mobilization and then translocation through the outer mitochondrial membrane. Once in the cytosol, cytochrome c engages with apoptotic protease-activating factor-1 (APAF1), enabling its heptamerization and formation of the apoptosome. Apoptosome then recruits and activates the inactive procaspase-9. Activated caspase-9 then activates the executioner caspases-3 and -7, which are the final mediators of the intrinsic apoptotic pathway (Pellegrini and Scorrano, 2007).

2.3.4. Mitochondrial Ca^{2+} mediated signaling

Calcium (Ca^{2+}) accumulation in energized mitochondria has emerged as a biological process of utmost physiological relevance. Ca^{2+} uptake in mitochondria has its implication in buffering cytosolic Ca^{2+} levels that regulates cell metabolism, cell survival and other cell-type specific functions. During the process of electron transfer, H^+ ions translocate across the inner mitochondrial membrane (IMM), generating an electrochemical proton gradient ($\Delta\mu H^+$), whose major component is the membrane potential ($\Delta\Psi$) difference. On the basis of the Nernst equation, the resulting $\Delta\Psi$ also represents a very large driving force

for Ca^{2+} uptake. Uptake of Ca^{2+} inside the mitochondrial matrix is directly proportional to the mitochondrial membrane potential. This uptake occurs through the ion-impermeable inner mitochondrial membrane (IMM) via mitochondrial Ca^{2+} uniporter (MCU), which rapidly accumulates Ca^{2+} across the steep electrochemical gradient. Ca^{+2} accumulation in mitochondria regulates intrinsic functions of the organelle, including the major mitochondrial function of ATP production. Three of the TCA cycle enzymes: the pyruvate dehydrogenase, regulated by a Ca^{2+}-dependent phosphatase, α-ketoglutarate- and isocitrate-dehydrogenases are regulated by direct binding of Ca^{2+} to these enzymes (Hansford, 1994; McCormack et al., 1990). In the intrinsic apoptosis pathway mediated by the release of cyt c, the permeability transition pore (PTP) opening is one of the primary events. Multiple studies have shown that the most important trigger for PTP opening is Ca^{2+}, which acts in conjunction with a variety of apoptotic signals in living cells (Davidson et al., 2012). Ca^{2+} has also been shown to play an important regulatory role in autophagy; Ca^{2+}/calmodulin-dependent kinase kinase-β (CaMKKβ) activating AMP-activated protein kinase (AMPK) ultimately leads to mammalian target of rapamycin (mTOR)-dependent autophagy (Hoyer-Hansen et al., 2007). Mitochondrial dysfunction that arises due to mtDNA damage or decrease in electron transport chain or mtDNA depletion results into a drop in ΔΨ. The drop in ΔΨ prevents mitochondrial Ca^{2+} uptake and generates an elevated cytosolic Ca^{2+} level, which in turn activates calcineurin (a phosphatase). Activated calcineurin governs diverse cellular outcomes, resulting in transcription activation/repression of large sets of genes involved in cellular metabolism, mitochondrial transcription and biogenesis, cell survival, apoptosis and cytoskeletal organization.

2.4. DNA Methylation

2.4.1. Biological relevance of DNA Methylation

Addition of methyl group at C5 position of the cytosine in DNA produces 5-methyl 2'-deoxy cytosine (5-mC), which is known as DNA methylation. Epigenetic modification in the form of DNA methylation is conserved among most plants, animals and fungal models (Feng et al., 2010). DNA methylation is one of the well-studied epigenetic mechanisms that regulates gene-expression and is involved in several important physiological processes, including X chromosome inactivation, imprinting and the silencing of germline

specific genes and repetitive elements. Methylation of nuclear genome is the marker of transcriptional silencing. During development, most of the CpG dinucleotides in mammalian genome persist in methylated form, but CpG islands found at promoter regions of several housekeeping or developmentally regulated genes are constitutively hypomethylated. Promoters of genes lacking methylation in CpG region are generally in transcriptionally permeable configuration (Ramirez-Carrozzi et al., 2009). This is due to unstable nucleosomal assembly in CGI (CpG Island) regions which are devoid of methylation. On methylation, MBD (Methyl CpG Binding Domain) proteins either recruit corepressor complex or directly inhibit transcription factor binding, ultimately leading to transcription repression (Bogdanovic and Veenstra, 2009; Klose and Bird, 2006). In mouse and humans, approximately 60 to 70% of genes possess CpG islands in their promoter regions. A maximum number of these CpG islands remain unmethylated independent of the transcriptional activity of the gene, in both differentiated and undifferentiated cell types (Weber et al., 2007).The CpG islands that are located in intragenic and transposable element regions are enriched in DNA methylation (Figure. 2.4). The role of CpG methylation in gene bodies is largely unknown, but recent evidences have shown their involvement in regulating splicing and in suppression of the activity of intragenic transcriptional units from cryptic promoters or transposable elements (Illingworth et al., 2010; Maunakea et al., 2010).

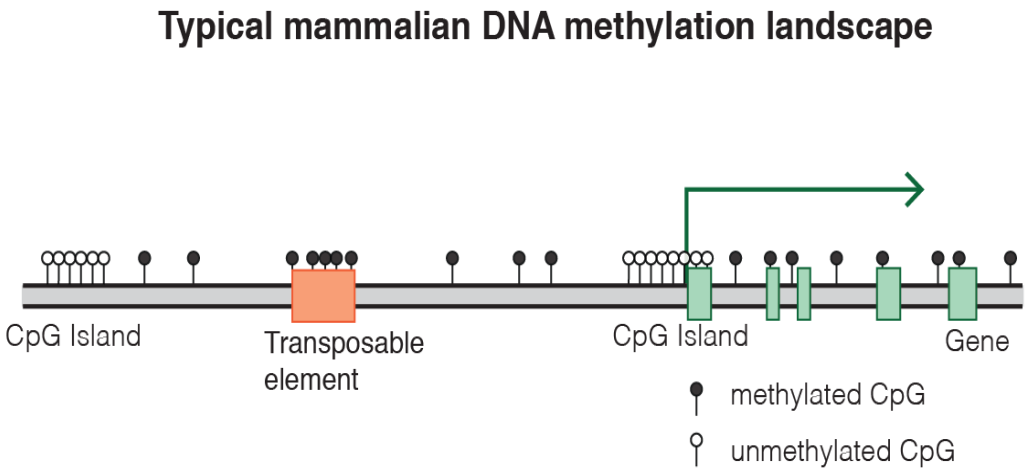

Figure 2.4: Mammalian DNA methylation landscape. (Source: Mariuswalter et. al., 2016).

Earlier, it was believed that cytosine methylation primarily exists in the CpG regions only and is absent at non-CpG regions in diverse somatic tissue types of mammals (Ramsahoye et al., 2000). However, recent reports have revealed that non-CG methylation (mCH) is abundant and non-randomly present in the genome of pluripotent and the brain cells; and is distributed at low levels in many other human cells and tissues (He and Ecker, 2015).

2.4.2. DNA Methyltransferases

DNA Methyltransferases are the enzymes that transfer the methyl group from a cofactor molecule S Adenosyl-L-methionine (SAM) to the C5 position of the cytosine in the DNA, generating 5-methyl 2'deoxy-cytosine (5-mC) and S-Adenosyl-L-homocysteine (SAH). These enzymes belong to a common DNMT family that consists of a total of four genes; DNMT1, DNMT3A, DNMT3B and DNMT3L, and share a common structural organization (Figure 2.5). Their N-terminal region contains regulatory domain, while the C-terminal region consists of catalytic domain which mediates the methyl group transfer (Jurkowska et al., 2011). DNMT3L is a catalytically inactive enzyme and has a role in assisting DNMT3A and DNMT3B to bind to DNA.

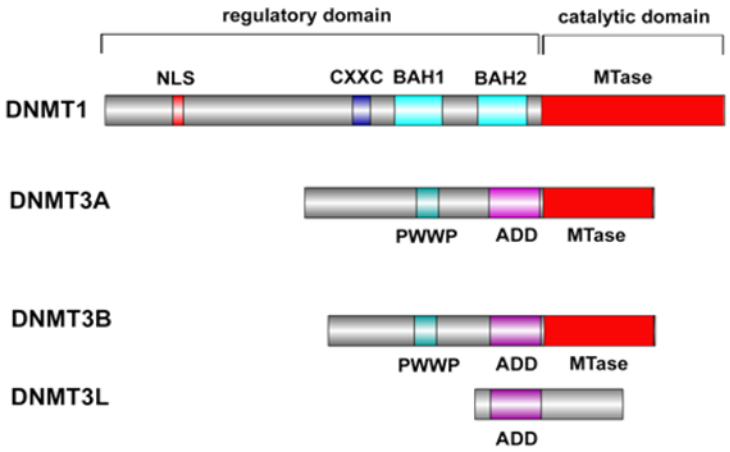

Figure 2. 5: Types of DNA Methyltransferases with important structural elements.NLS, nuclear localization signal; CXXC, a cysteine rich region; BAH, a bromo-adjacent homology domain; PWWP, a proline-tryptophan-tryptophan-proline domain; ADD, an ATRX-DNMT3-DNMT3L-type zinc finger domain; Mtase, a methyltransferase domain. (Source: atlasgeneticsoncology.org).

Further, these enzymes are categorized into: De novo methyltransferase and maintainence methyltransferase. DNMT3A and DNMT3B belong to de-novo methyltransferase and are responsible for establishing methylation patterns in embryonic stages. DNMT1 is a maintainence methyltransferase enzyme that preferentially methylates hemi-methylated sites in DNA and is responsible for maintaining methylation patterns in newly synthesized daughter strand during replication (Goyal et al., 2006). DNMT1 methylates hemi-methylated DNA either in cooperation with or without DNMT3A and DNMT3B (Jones and Liang, 2009).

Functions of DNMTs have been widely studied in mice by using gene knockout approach. Mice knocked out for any of the DNMTs have severe developmental abnormalities. Mice that lack DNMT1 loose about 90% of their DNA methylation and die early in embryonic stage (Bonfini and Karlovich, 1992). Mouse embryonic stem cells (ESC) deficient for DNMT1 or for both DNMT3a and DNMT3b have extremely elongated telomeres compared to the wild-type control, suggesting their role in telomere integrity and maintainence (Gonzalo et al., 2006).

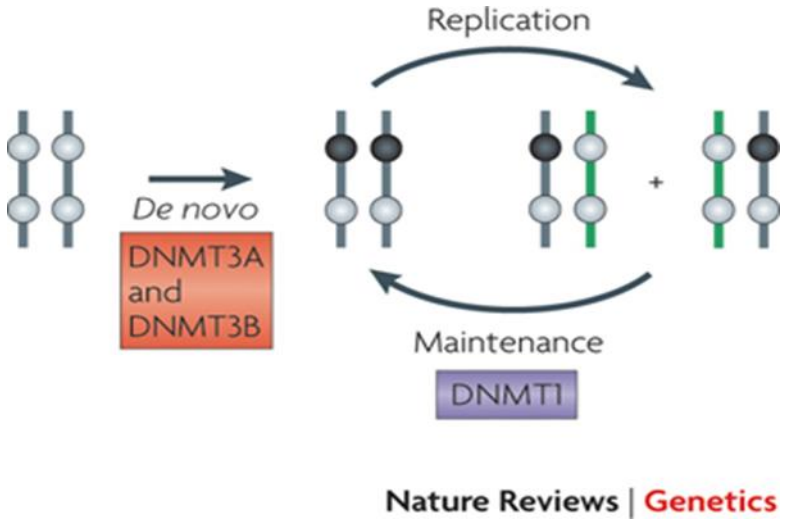

Figure 2.6: Schematic representation of establishment and maintenance of DNA methylation. DNMT3A and DNMT3B are De-novo methyltransferase; while, DNMT1 is maintenance methyltransferase. (Source: Nature Reviews Genetics, 2009)

Hypomorphic DNMT1 activity has been associated with highly proliferative T-cell lymphomas in a mouse model showing a potential relationship between the expression

levels of this enzyme and cancer susceptibility, possibly through regulation of genomic stability (Gaudet et al., 2003). However, contrary to this, when a DNMT1 hypomorphic mutation was introduced into Apc (Min/+) mice, it suppressed later stages of intestinal tumorigenesis, but induced early lesions in the colon and liver through the mechanism of loss of heterozygosity (LOH) (Yamada et al., 2005). These studies together suggested for a dual role of DNA hypomethylation in the process of tumorigenesis that ultimately depends upon different environments.

2.5. Mitochondria and Epigenetic regulation

2.5.1. mtDNA methylation-Early studies

The very first study conducted in 1971 reported mitochondrial DNA methylation in loach embryos, using Thin Layer Chromatography (TLC)-radiography as an experimental approach. Two years later, in 1973, a subsequent study found mtDNA to have a low percentage (0.2 to 0.6%) of methylated cytosines in cultured mouse fibroblasts and baby hamster kidney cells (Nass, 1973). The very next year, in 1974, Dawid and colleagues reported absence of this epigenetic modification in frogs and HeLa cells (Dawid, 1974). In 1977, Vanyushin and Kirnos, reported 1.5 to 3.2 mole percentage of methylated cytosines within heart and liver tissues of various vertebrates, using TLC resolved method, followed by spectrophotometric quantification. Two years later, in 1978, Groot and Kroon found the absence of methylation in mtDNA of several organisms including yeast, neurospora, rat and calf (Groot and Kroon, 1979). However, several studies thereafter suggested the occurrence of low levels of methylation in mitochondria in different species (Pollack et al., 1984; Shmookler Reis and Goldstein, 1983). One of the reasons behind the discrepancy in the observation of mtDNA methylation by these groups was the poor methylation quantification techniques that failed to reproduce results. Collectively, these studies in the past put the epigenetic process of mtDNA methylation in dilemma and were more or less ignored for several years thereafter.

2.5.2. Resurgence in the field of mtDNA methylation

Research in the field of mitochondrial genome methylation did not gain much importance for several years until Shock et al. (2011) demonstrated the presence of a methyltransferase

enzyme, mtDNMT1, inside mitochondria. They showed that an upstream sequence to the known transcription start site of DNMT1 was also a part of the transcript. And, this upstream sequence possessed a start codon in the open reading frame to the known start codon, generating an upstream open reading frame (uORF). The uORF was shown to encode for a mitochondrial targeting sequence which when ligated at the N-terminal of a reporter construct, GFP, localised GFP to mitochondria. This particular report gave birth to the area of mtDNA methylation research. Thereafter, a number of reports in favor of this epigenetic modification continued to increase; and found differential methylation at certain CpG regions of mitochondrial genome in association with several pathophysiological conditions.

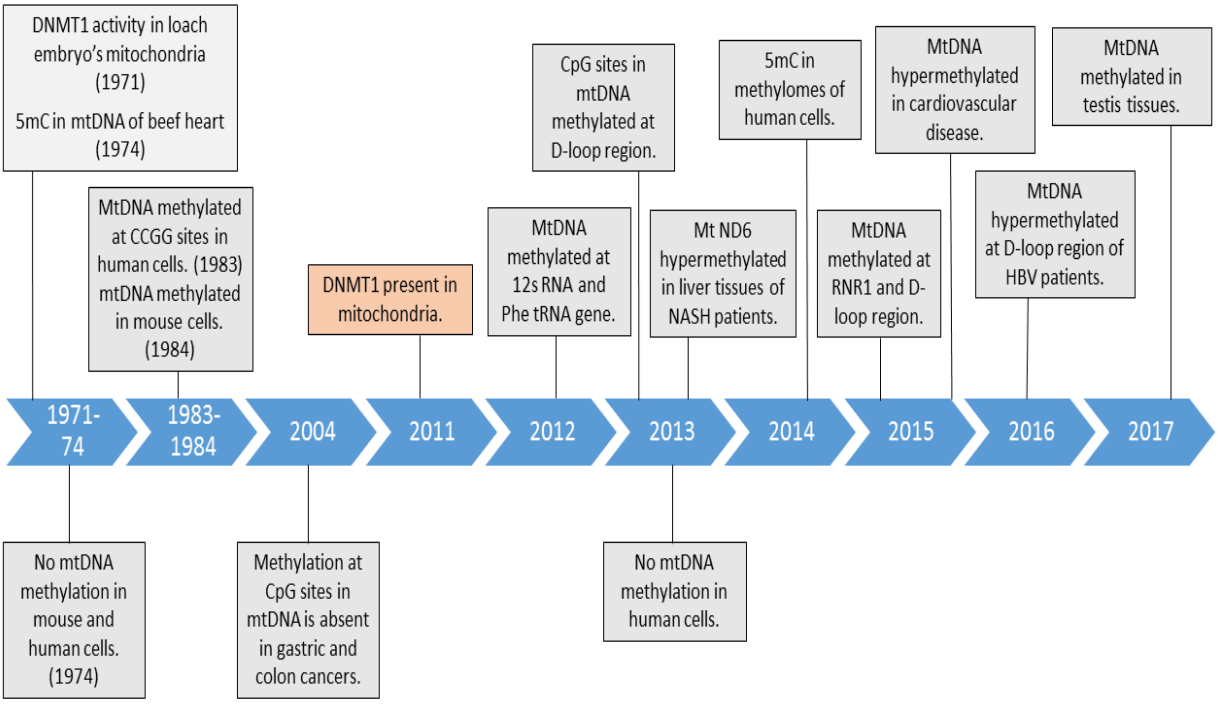

Figure 2.7: An overview of reports regarding presence and absence of mtDNA methylation through the advancing decades.

In 2013, Hyang Byun and group had reported the environmental conditions of long term exposure to air borne pollutants to be associated with mtDNA methylation at 12S rRNA and Phe-tRNA genes and the D-loop area (Byun et al., 2013a). In addition to the methylation at CpG sites in mitochondrial genome, there were some non-CpG sites in D-

loop region that were also found to be methylated in both mice and human tissues (Bellizzi et al., 2013). In the same year, Pirola and colleagues demonstrated hypermethylation of the mt-ND6 in liver tissues of non-alcoholic steato-hepatitis (NASH) patients but not in the patients with simple steatosis. The transcript levels and the protein expression of ND6 gene was significantly decreased in non-alcoholic steato-hepatitis, suggesting that the expression of this mitochondrial gene, which is regulated by an epigenetic modification, could play an important role in the pathogenesis of the disease progression (Pirola et al., 2013). In 2014, a study done on methylated DNA immunoprecipitation datasets, covering 39 different human cell and tissue types, showed the presence of methylated cytosine within mitochondria, signifying a universal physiological role of this modification in mitochondria (Ghosh et al., 2014). In 2015, Janssen and group reported mtDNA methylation at mt-RNR1 and D-loop region in the placental tissue in positive association with airborne pollutant (PM2.5) exposure during the gestation period (Janssen et al., 2015). In the same year, Baccarelli and the colleagues showed hypermethylation of mitochondrial genes (COI, COII, COIII, tRNAleu, ATP6, ATP8 and ND5) in cardiovascular disease patients (Baccarelli and Byun, 2015). Studies indicated an inverse co-relation of mtDNA methylation with the transcription. In this regard, Gao et al. found de-methylation in the D-loop region of mtDNA to be associated with the gene expression in colorectal cancer tissues (Gao et al., 2015). A study done on chronic HBV (Hepatitis B Virus) patients revealed higher levels of methylation in the D-loop region of the patient taking nucleoside analogue (for the inhibition of viral replication) in comparison to healthy controls (Madeddu et al., 2016). While writing this thesis a report appeared in 2017, which suggested the occurrence of methylation of mtDNA in the gene regions of immature testis of Chinese mitten crab, *E. sinensis* (Li et al., 2017).

The regulation of the mtDNA methylation, apart from DNMT1 expression, has been suggested to be influenced by the availability of S-adenosyl methionine (SAM); which was found to regulate the methylation levels in cervical cancer cells. The SLC25A26 gene, encoding for the mitochondrial carrier that catalyzes the import of S-adenosylmethionine (SAM) into the mitochondrial matrix, when overexpressed in CaSki cells increased mitochondrial SAM availability and promoted hypermethylation of mtDNA, leading to decreased expression of key respiratory complex subunits, reduction of mitochondrial ATP

and release of cytochrome c (Menga et al., 2017). Same group had earlier reported lower levels of mtDNA methylation in Down Syndrome (DS) patients in comparison to the control samples, correlating with lower SAM levels in the cytosol of DS patients (Infantino et al., 2011). These observations highlighted the importance of SAM availability, suggesting that its synthesis and transport to mitochondria could represent key regulatory steps of mtDNA methylation.

2.5.3. MicroRNA and mitochondrial epigenetic regulation

MicroRNAs (miRNAs) constitute a class of non-coding RNAs that play an important role in epigenetic regulation of gene expression. These RNA molecules act at the post transcriptional level, and are known to fine–tune the expression of ~ 30% of all mammalian protein encoding genes (Sioud and Cekaite, 2010). Mature microRNAs are short, single stranded RNA molecules approximately 22 nucleotides in length. These are sometimes encoded by multiple loci, some of which are organized tandemly in co-transcribed clusters. RNA polymerase II transcribe microRNA genes to generate primary transcripts (pri-microRNA) that are processed by a protein complex which contains RNase III enzyme, Drosha, resulting in an approximately 70 nucleotide precursor microRNA (pre-microRNA). The precursor is transported to the cytoplasm to be processed by a second RNase III enzyme, DICER, finally resulting in a mature microRNA of approximately 22 nucleotides. The mature microRNA incorporated into a ribonuclear particle ultimately forms the RNA-induced silencing complex, RISC, mediating gene silencing.

MicroRNAs mediate post-transcriptional gene silencing by binding to the 3'UTR of the targeted mRNA. This interaction either initiates mRNA degradation and/or prevents protein synthesis. Since most target sites on the mRNA have only partial base complementarity with their corresponding microRNA, individual microRNAs may target as many as 100 different mRNAs. Moreover, individual mRNAs may consist of multiple binding sites for different microRNAs, resulting in a complex regulatory network.

MicroRNAs have been shown to be involved in a diverse range of biological processes, such as cell cycle control, apoptosis and several developmental and physiological processes including stem cell differentiation, hematopoiesis, hypoxia, cardiac and skeletal muscle development, neurogenesis, insulin secretion, cholesterol metabolism, aging, immune

response and viral replication (Booton and Lindsay, 2014; Guay and Regazzi, 2015; Hayes and Chayama, 2016; Jiangpan et al., 2016; Maegdefessel, 2014; Paul et al., 2017) . In addition, highly tissue-specific expression and distinct temporal expression patterns during embryogenesis suggest that microRNAs play a key role in differentiation and maintenance of tissue identity (Fogel et al., 2015; Taylor and Gilleard, 1990). Since, dysfunction of mitochondria is related to a variety of pathological processes and diseases, for the proper functioning of a mitochondrion, it is expected that miRNA could have a role in regulating mitochondrial biology too.

Mitochondrial DNA (mtDNA) mutations and deletions arise as a result of dysfunction of the mitochondrial respiratory chain and have been reported to contribute to the aging process. The decreased expression of mitochondrial genes and disrupted mitochondrial structure has been associated with abnormal human development. It is essential that both the nuclear and mitochondrial genomes crosstalk to contribute to mitochondrial protein synthesis, assembly and its function. Thus, communication from the nuclear genome to the mitochondrion involves proteins that are translated in the cytosol and imported into the mitochondrion. Although, miRNAs are transcribed in the nucleus and transported into cytoplasm, which is a primary site of action, however, there is growing evidence associating miRNAs with other organelles or unstructured cytoplasmic foci, such as mitochondria, endoplasmic reticulum (ER), processing bodies (P-bodies), stress granules, multivesicular bodies, and exosomes (Leung, 2015). It could be suggested from these recent observations that miRNA-mediated gene regulation may be controlled within different cellular compartments, and that this miRNA-organelle crosstalk allows for more selective responses to specific cellular demands (Shinde and Bhadra, 2015). Several studies have demonstrated the presence of miRNAs either within (Latronico and Condorelli, 2012) or associated with (Carrer et al., 2012; Sripada et al., 2012; Yamamoto et al., 2012) mitochondria isolated from various cell types and tissues, including the CNS (Wang and Springer, 2015). In addition, the miRNA machinery proteins, Argonaute (AGO) and Dicer have been detected in mitochondria (Bandiera et al., 2013), indicating the presence of an active miRNA ribonucleoprotein complex (miRNP) (Dasgupta et al., 2015). The majority of these mitochondria associated miRNAs are known to be nuclear-encoded, while a few are predicted to originate from the mitochondrial genome (Shinde and Bhadra, 2015).

Given the small genome of mitochondria and the presence of minimal non-coding DNA, the characterization and function of this group of intra-mitochondrial miRNA requires further investigation.

One of the presumed functions of mitochondrial miRNA is the regulation of mitochondrial gene expression. In support of this, studies performed using muscle cells and heart tissues have identified nuclear-encoded miRNAs in mitochondria that directly regulate mitochondrial proteins. For example, miR-181c is enriched in mitochondria and it targets cytochrome c oxidase subunit 1 (COX1) in rat cardiomyotubes (Das et al., 2014). Another nuclear-generated mitochondrial miRNA, miR-1, also targets COX1 and has been found to increase in mitochondria during muscle cell differentiation (Zhang et al., 2014). Surprisingly, miR-1 was shown to enhance rather than inhibit COX1 protein translation. These authors suggested that this unconventional action of miR-1 required AGO2 but not GW182 (glycine-tryptophan protein of 182 kDa), which is essential for cytoplasmic miRNA gene repression but is absent in mitochondria. In a separate study, computational analysis of mitochondria enriched miRNAs isolated from human skeletal muscle cells predicted 80 putative target sites in the mitochondrial genome (Barrey et al., 2011). Recently, it has been shown that the deficiency of miR-133a in mice resulted in impaired exercise tolerance, mitochondrial biogenesis, and muscle fibre maintenance (Nie et al., 2016). A report in January 2017 showed the role of miR-199a-3p in enhancement of breast cancer cell sensitivity to cisplatin by targeting mitochondrial transcription factor, TFAM (Fan et al., 2017). Similarly, a recent report in February 2017, found microRNA-200a-3p to be involved in enhancing the process of mitochondrial elongation by down-regulating mitochondrial fission factor (Lee et al., 2017).

3. RATIONALE OF THE STUDY AND AIMS & OBJECTIVES

RATIONALE OF THE STUDY AND AIMS & OBJECTIVES

3.1. Rationale

Research to date has successfully proven the presence of methylation in mitochondrial DNA (mtDNA). However, none of these studies has provided an insight into the mechanistic details of this epigenetic process and its role in mitochondrial biology. The emerging field of mitochondrial epigenetics allowed in this study to look into genetic differences among different human cancer cell lines belonging to five most prominent cancer types worldwide and used globally as *in-vitro* experimental models, for CpG positions and richness. Knowing that the mitochondria undergoes a rapid change in its structure and function under various pathophysiological conditions and stresses, an attempt was made to understand how mtDNA methylation is affected in response to nutritional and oxidative stress. Further, a direct approach of ectopic overexpression of specific isoforms of DNMT1 was used to study their localization in mitochondria and their influence on the mitochondrial biology epigenetically.

The emerging evidences supporting the role of miRNA in regulating mitochondrial gene expression suggested identifying bioinformatically novel microRNAs targeting key mitochondrial genes (encoded by the nuclear genome) involved in mitochondrial biogenesis, thus regulating the biogenesis of this organelle at another level of epigenetic control.

With this background, the study was designed with the following aims and objectives:

3.2. Aims and Objectives

- Explore whole mitochondrial genome for the presence of CpG positions in different human cell lines.

- Assess the methylation status of the defined CpG sites and evaluate their status under experimental conditions of oxidative stress.

- Evaluate the intermediate phenotypes related to mitochondrial biology, such as mitochondrial mass, copy number variations, transcript levels of chosen mitochondrial genes, membrane potential, ATP production rate etc, resulting from differential methylation status of the mt genome.

- If possible, explore the role of miRNA in mitochondrial biology or as yet unknown mt-miRNA in epigenetic regulation of mitochondrial biogenesis.

4. MATERIALS AND METHODS

MATERIALS AND METHODS

4.1. Whole mitochondrial genome sequencing

Whole mitochondrial genome of 10 different human cell lines belonging to five most prominent cancer types worldwide was sequenced. Genomic DNA from these cell lines (Table 4.1) was isolated using QIAamp DNA Blood Mini Kit (Qiagen# 51304).

Table 4. 1: Human Cancer Cell lines used in the study

	Cancer Type	Cell Lines
1.	Breast	MCF-7 and MDAMB-231
2.	Lung	A549 and H1299
3.	Prostate	PC-3 and LNCaP
4.	Colon	HCT 116 and HT 29
5.	Cervix	HeLa and SiHa

Twelve overlapping sets of primers (Figure 4.1) were designed to cover the entire mitochondrial genome. Genomic DNA from each of the cell line (Figure 4.2A) was used as a template to carry out PCR for whole mitochondrial genome amplification, using these 12 different overlapping sets of primers. PCR conditions were optimized for each of the 12 sets (details of the primer position, sequence and their annealing temperature is mentioned in appendix Table A1).

A representation of whole mitochondrial genome amplification of A549 cells is shown in Figure 4.2B. After amplification, the PCR products were purified by Exonuclease I (NEB# M0293L) and Shrimp Alkaline Phosphatase (NEB# M0371L) treatment to degrade left over primers and dNTPs, respectively. The amplicons were then used as a template to carry out sequencing reactions using single internal primers (details of primers used and the reaction conditions are provided in appendix Table A1) and BDT master mix (ABI PRISM Big Dye terminator cycle sequencing ready reaction kit version 3.1 from Applied Biosystems), generating single stranded DNA molecules of varying lengths. Subsequently, each PCR product in the 96 well plates was prepared for capillary gel electrophoresis by cleaning and washing. PCR product (10µl) in each well was added with: 2µl of 3M CH_3COONa, 2µl of 125mM EDTA (pH 5) and 65µl of absolute ethanol (Merck). Plates were covered by septa, invert mixed 5 times and incubated at RT for 5 mins. Plates were then spun at 3300 rpm for 30 mins to pellet DNA; the supernatant was decanted on lint free paper by inverting the plates and pop spun at 700 rpm. The pelleted DNA was then washed with 100µl of 70% ethanol by inverting and mixing the plate 5 times, followed by invert spun on lint free paper at 3300 rpm for 20 mins. The washing step was repeated for one more time. 10 µl High Dye Formamide (HDF) was added to each well, followed by incubation of the plate in PCR machine at 95^{o}C and 4^{o}C for 5 min each. The plates were then kept in DNA Sequencer (ABI 3130xl genetic analyzer) for capillary based electrophoresis. The data was collected and analyzed using SeqScape analysis software against reference mitochondrial genome rCRS (revised Cambridge Reference Sequence).

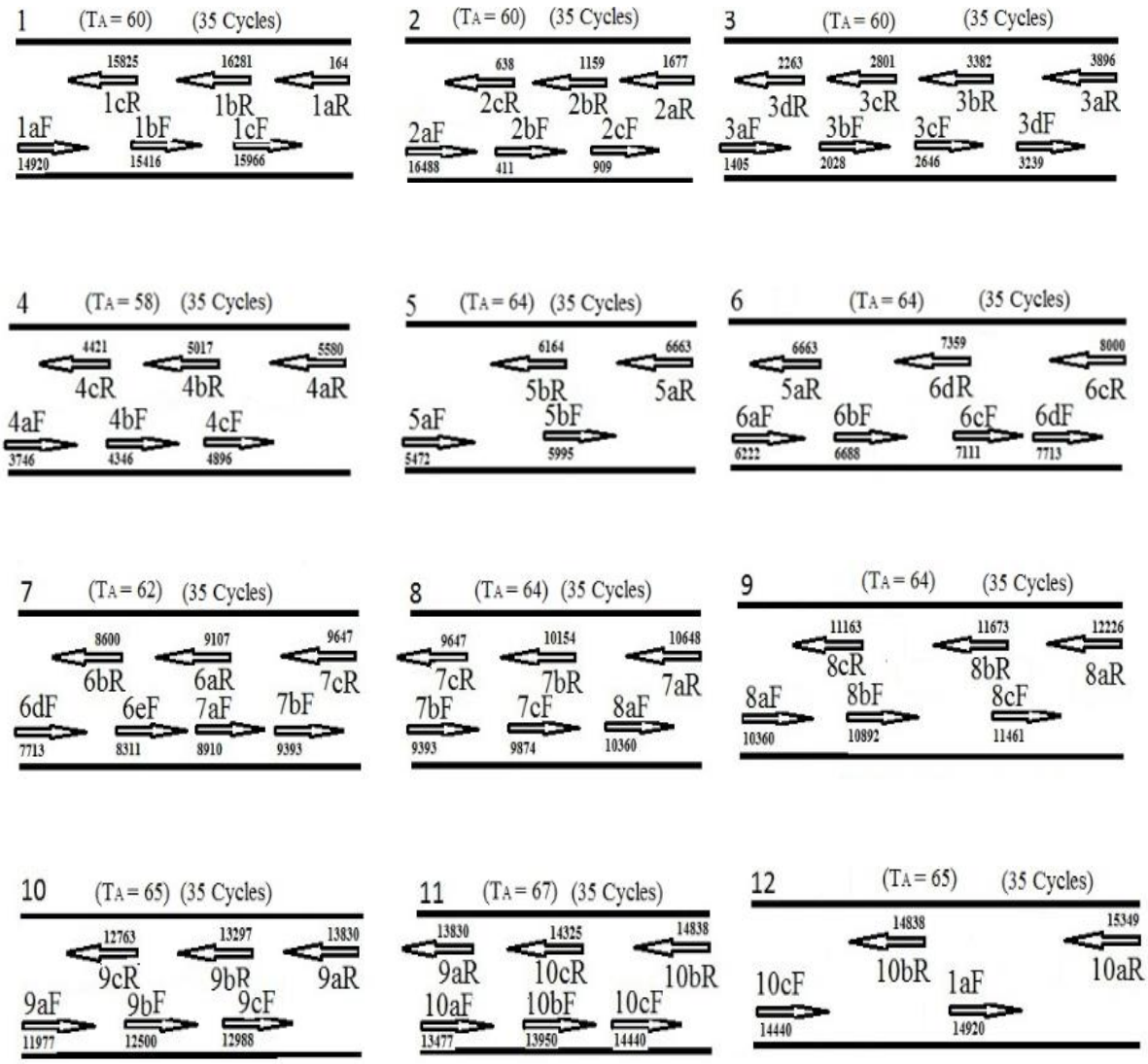

Figure 4.1: Different sets (numbered from 1 to 12) of overlapping sets of primers used for mitochondrial genome sequencing. Inside each set are sequencing primers (marked as arrow) at every 500bp with their primer names and mitochondrial DNA positioning. PCR for each of these sets was carried out with the annealing temperature (mentioned on the top as T_A).

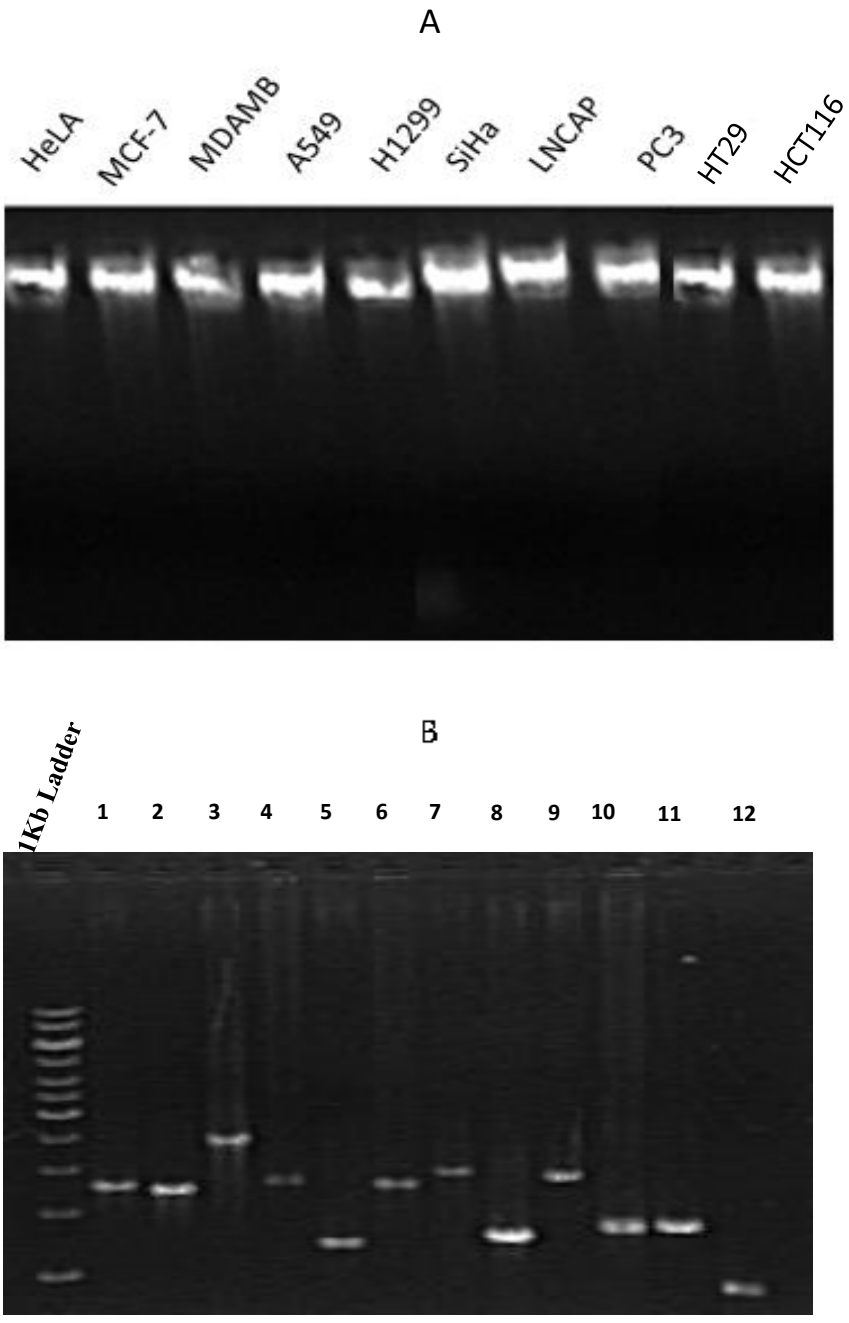

Figure 4.2: Amplification of whole mitochondrial genome. (A) Gel image of genomic DNA of 10 different cell lines (HeLa, MCF-7, MDAMB-231, A549, H1299, SiHa, LNCAP, PC3, HT29 and HCT116). (B) Representation of whole mitochondrial genome amplification of A549 cells using 12 different primer sets.

4.2. Cloning and Site Directed Mutagenesis

Of the three isoforms of DNA methyltransferaseI (DNMT1) - DNMT1-iso1, DNMT1-iso2 and DNMT1-iso3, the DNMT1-iso1 is the longest and contains a total of 40 exons. Whereas, DNMT1-iso3 is the shortest and contains a total of 25 exons, lacking initial 15 exons in comparison to isoform1 (Figure. 4.3A). Since, an additional upstream open reading frame (uORF) had been reported to be the part of transcript of DNMT1 (Figure. 4.3B), constructs were generated of DNMT1 isoform1 and 3 with uORF and other known strong mitochondrial localization signal (MLS of COVIII) sequence.

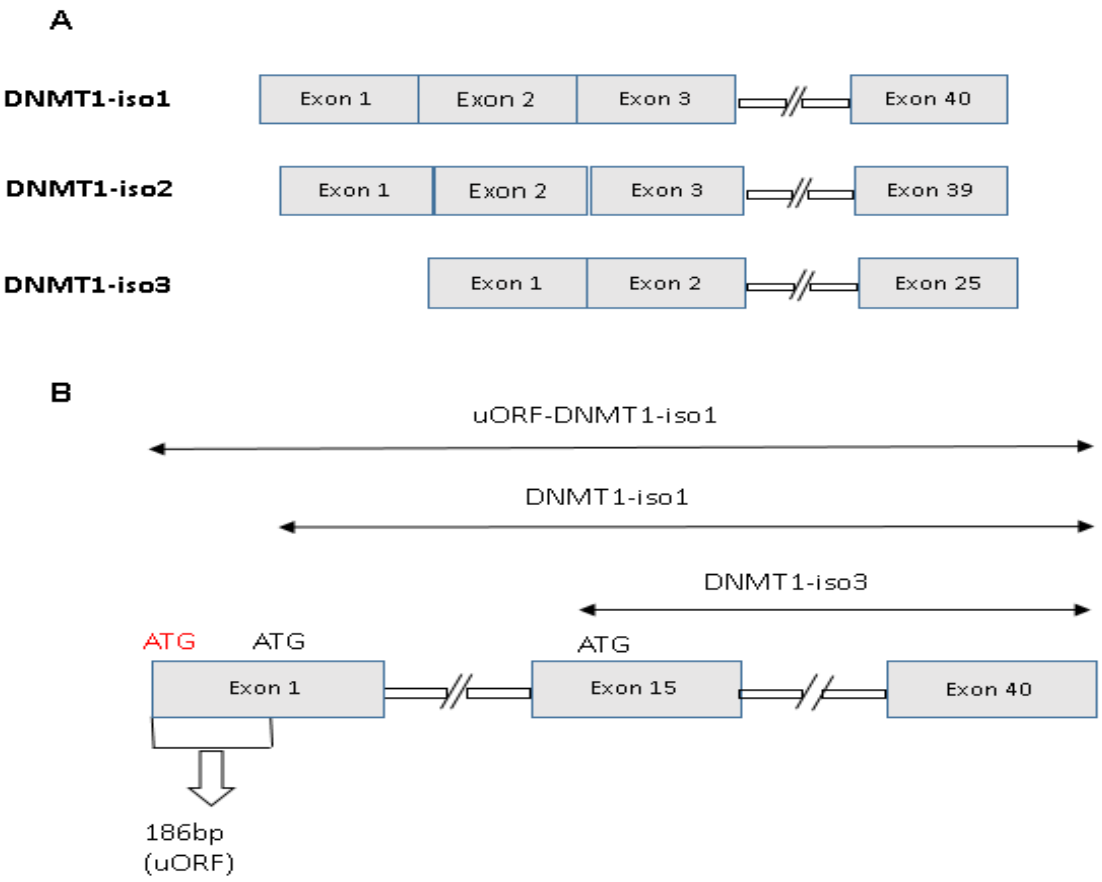

Figure 4.3: The schematic diagram of different isoforms of DNMT1. (A) Depicting their structure. (B) Showing the positions of start codons within DNMT1 isoform1, 3 and the upstream open reading frame (uORF).

DNMT1 isoforms alone or in frame with uORF (upstream open reading frame) sequence were cloned in pcDNA3.1myc/his A (-) vector (Invitrogen # V855-20), using a three-step cloning strategy (Figure 4.4): (i) where the uORF sequence was cloned at Nhe1 and EcoR1

sites to generate pcDNA3.1-uORF construct, (ii) DNMT1 isoforms cloning in the recombinant construct pcDNA3.1-uORF at EcoR1 and Kpn1 restriction sites, (iii) followed by deletion of EcoR1 restriction site located in-between uORF and DNMT1 isoforms, by site directed mutagenesis [using Q5® site-directed mutagenesis kit (NEB # E0554S)] to obtain the resultant constructs of pcDNA3.1 with uORF in frame with DNMT1 isoforms.

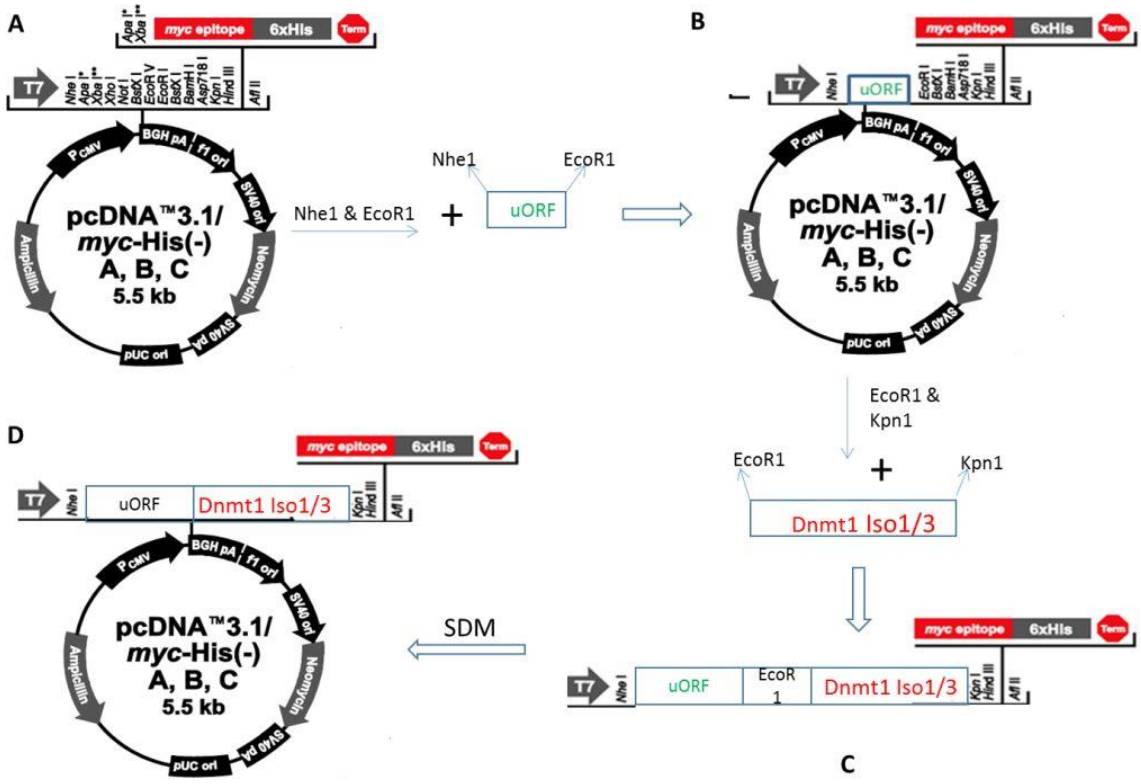

Figure 4.4: Cloning Strategy to clone DNMT1-Isoforms 1 and 3 with uORF sequence. (A) The vector backbone of pcDNA3.1-myc-his was double digested with NheI & EcoRI; similarly the PCR product for uORF sequence was digested with the same set of restriction enzymes. (B) Ligation of the digested uORF PCR product to the vector to generate pcDNA3.1-uORF-myc-his. (C) Digestion of (B) construct with EcoRI and KpnI restriction enzymes and ligation with double digested (EcoRI and KpnI) PCR product of DNMT1-Isoforms 1 or 3 to generate pcDNA3.1 uORF-DNMT1-Isoforms 1 & 3 vectors. (D) Deletion by site directed mutagenesis of the EcoRI restriction site in-between uORF and DNMT1

sequence to generate the final clone of uORF in frame with DNMT1-Isoforms 1 and 3 independently.

DNMT1 isoforms 1 and 3 (Figure 4.5A and 4.5B) were amplified using pcDNA3/myc-DNMT1 vector (obtained from addgene).

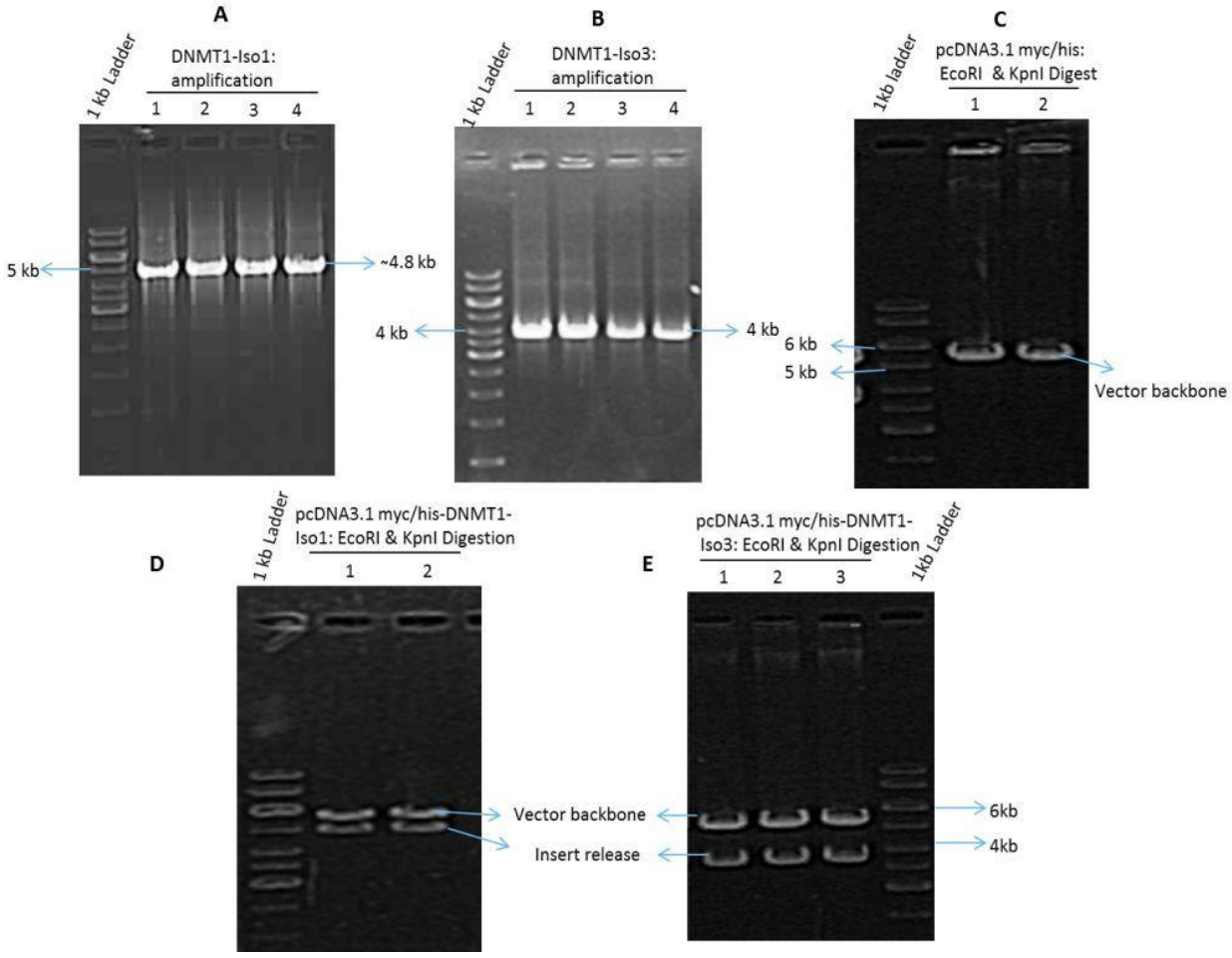

Figure 4.5: Validating the recombinant clones of DNMT1-Isoforms 1 and 3, cloned in pcDNA3.1 myc-his vector. (A) and (B) PCR to amplify DNMT1-Isoforms 1 and 3, respectively. (C) Double digestion of pcDNA3.1 myc-his vector backbone with EcoRI and KpnI restriction enzymes. (D) and (E) clone confirmation of DNMT1-Isoform 1 and 3 in pcDNA3.1 myc-his vector by insert release with EcoRI and KpnI double digestion, respectively.

The pcDNA3.1 myc-his vector was digested at EcoR1 and Kpn1 restriction sites (Figure 4.5C), the vector backbone was gel eluted, purified and ligated with DNMT1 isoforms. The resultant constructs were checked for the DNMT1-isoform1 and isoform3 by insert release (Figure 4.5D and 4.5E).

To generate the constructs of DNMT1 isoforms in frame with uORF sequence, the pcDNA3.1 myc-his vector was digested with Nhe1 and EcoR1 restriction enzymes (Figure 4.6A).

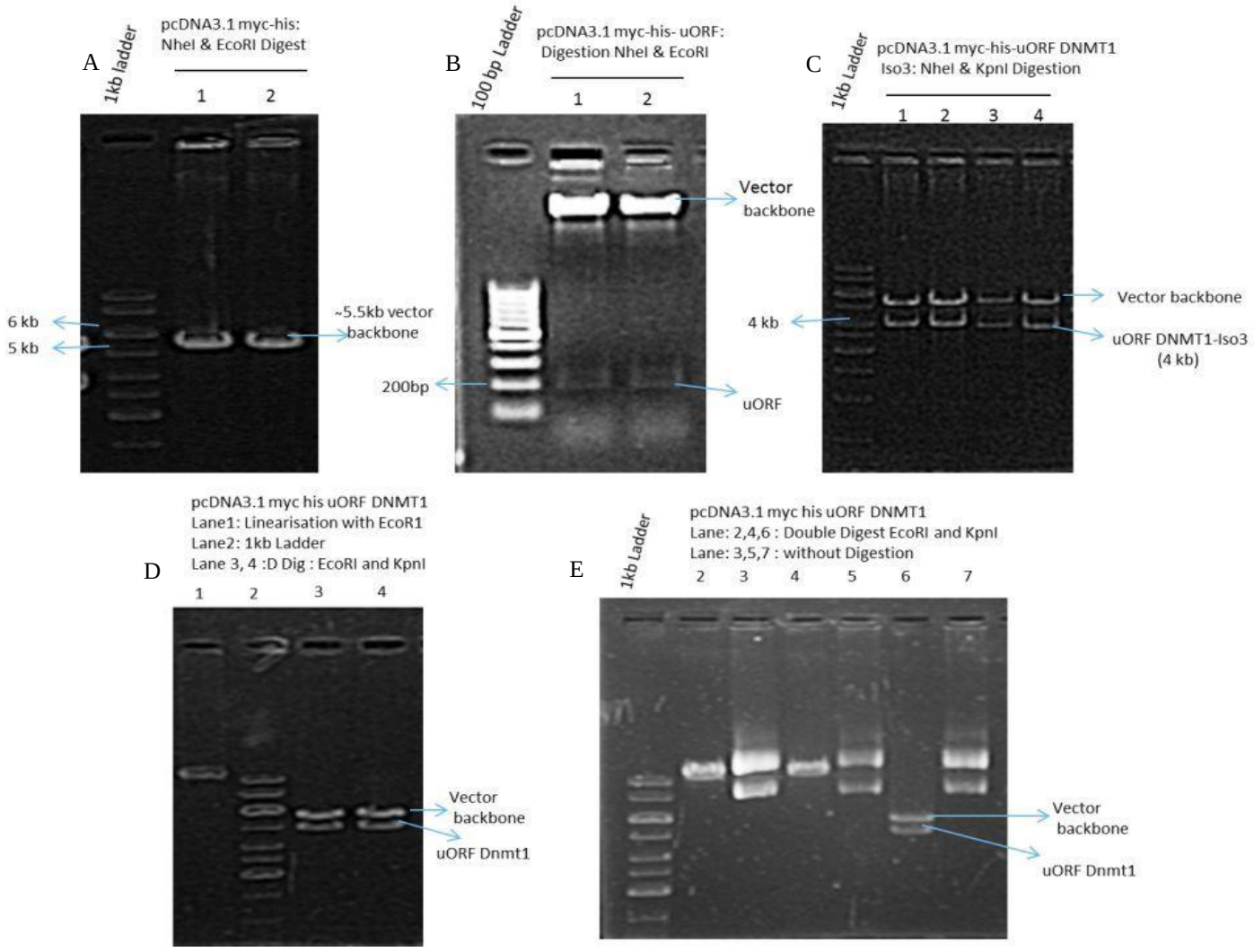

Figure 4.6: Validating the clones of DNMT1-Isoform 1 and 3 with uORF into pcDNA3.1 myc-his vector. (A) Double digestion of pcDNA3.1 myc-his vector with Nhe1 and Kpn1 *and (B) Cloning of uORF sequences in the double digested vector. (C) and (D) Double*

digestion of pcDNA3.1 myc-his vector backbone with EcoRI and KpnI restriction enzymes for the clone confirmation of DNMT1 isoforms 1 and 3 respectively.

The vector backbone was gel eluted, purified and ligated with uORF PCR product to generate pcDNA3.1 myc his-uORF recombinant (Figure 4.6B). The DNMT1-isoform1 and isoform3 was cloned into the recombinant plasmid to yield pcDNA3.1 myc his –uORF-DNMT1-isoform3 and pcDNA3.1 myc his-uORF-DNMT1-isoform1 (Figure 4.6C and 4.6D), which was later confirmed by double digestion with EcoR1 and Kpn1 restriction enzymes (Figure 4.6E).

For mitochondrial localization, DNMT1 isoforms were cloned into Sal1 and Not1 restriction sites of pCMV-myc-mito vector (Invitrogen # V822-20) with N-terminal mitochondrial targeting sequence (MTS) and C-terminal myc epitope (Figure 4.7).

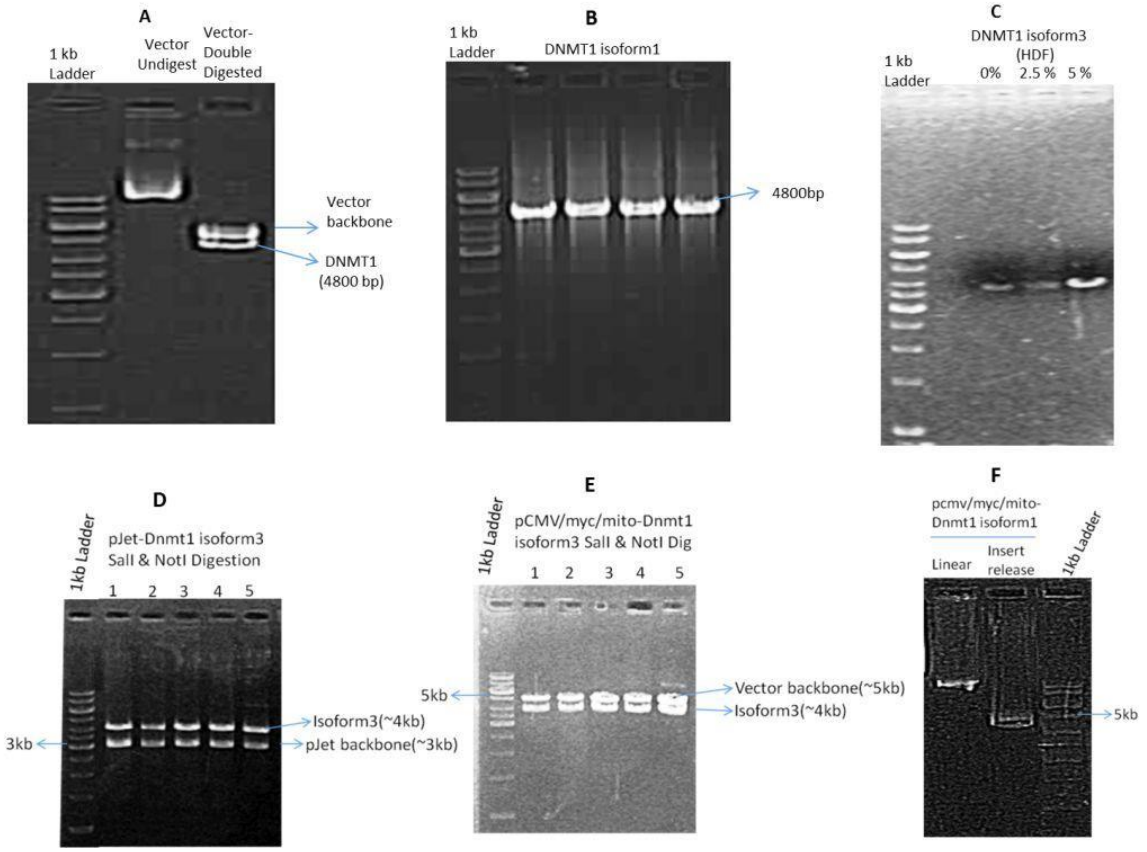

Figure 4. 7: Validating the clones of DNMT1-Isoforms 1 and 3 in pCMV-myc-mito vector. (A) Checking cloned insert (DNMT1) in the vector from addgene. (B) and (C) PCR

amplified products of DNMT1-Isoforms 1 and 3, respectively. (D) Sub-cloning of DNMT1-Iso3. (E) and (F) Cloning of DNMT1-Iso1 and Iso3 in pCMV-myc-mito vector, respectively.

DNMT1 isoforms 1 and 3 (Figure 4.7A and 4.7B) were amplified using pcDNA3/myc-DNMT1 vector (obtained from addgene), and sub-cloned into pJET1.2 vector (Figure 4.7C and 4.7D). The DNMT1 isoforms 1 and 3 was double digested with Sal1 and Not1 restriction enzymes and cloned into pCMV-myc-mito vector (Figure 4.7E and 4.7F). All the generated constructs were confirmed by sequencing, using ABI 3130xl genetic analyzer.

4.3. Bacteria and culture conditions

4.3.1. Strains

DH5α (Invitrogen, Darmstadt, Germany) or TOP10 (Invitrogen, Darmstadt, Germany) chemically competent bacterial strains were used for, transformation of plasmid DNA, ligation mixtures and amplification of positive recombinant vector.

4.3.2. Culture conditions

Bacterial cultures were grown in suspension cultures in LB media (Sigma-Aldrich, München, Germany), supplemented with either 50µg/ml kanamycin (Sigma-Aldrich, USA) or 100µg/ml ampicillin (Sigma-Aldrich, USA) or 50µg/ml spectinomycin (Sigma-Aldrich, USA). For a selection of transformed vs untransformed, the bacterial cells were plated on 2% LB-agar plates containing 50µg/ml kanamycin or 100µg/ml ampicillin or 50µg/ml spectinomycin.

4.3.3. *Preparation of competent cells*

To prepare the competent cells, E. coli strain DH5α was plated on 2% LB-agar-nalidixic acid plates and incubated overnight at 37^{o}C. Next day, a single bacterial colony was picked and transferred to 3 ml of LB broth medium. The culture was incubated for 6 hours at 37^{o}C with vigorous agitation. 1% of this culture was transferred to 50 ml of SOB medium and incubated overnight at 18^{o}C with moderate shaking. Next day, when OD600 of culture reached to 0.55, the culture was transferred to sterile, ice-cold 50ml polypropylene tube

and incubated on ice for 10 minutes. Bacterial cells were recovered by centrifugation at 2700g for 10 minutes at 4^{o}C. Then the medium was decanted and pellet dried by inverting tubes on a pad of paper towels for 1 minute to remove the last traces of media. Each pellet was suspended in 16ml of ice-cold inoue transformation buffer by swirling and gentle vortexing, and cells recovered by centrifuging at 2700 g for 10 minutes at 4^{o}C. The supernatant was poured off and the pellet was dried on a pad of paper towels for 1 minute. Pellet was re-suspended by swirling and gentle vortexing in 4ml of ice-cold transformation buffer. Finally, 200µl of DMSO was added and mixed by gentle vortexing. Cell mix was incubated on ice for 30 minutes and aliquots of 100µl were made by dispensing the mix in ice chilled, sterile 1.5 ml micro-centrifuge tubes. Aliquots of competent cells were snap frozen by bathing in liquid nitrogen and stored at -80^{o}C for later use. Transformation efficiency was measured by transforming cells with 10pg of pUC19 (Invitrogen, USA) vector. Next day colonies were counted and transformation efficiency was calculated by following formula: Colonies/µg/Dilution.

4.3.4. Transformation of competent cells

The competent cells were thawed on ice for 20 minutes prior to the addition of ligation mixture. After 30 minutes incubation on ice, cells were heat shocked at 42^{o}C for 90 seconds followed by incubation on ice for 2 minutes. Cells were suspended in 900µl of SOC medium and kept in an incubator-shaker at 37^{o}C to allow the bacteria to recover and express the antibiotic resistance marker encoded by the plasmid. After 45 minutes of incubation, cells were pelleted down by centrifugation. Supernatant was discarded and pellet re-suspended in 100 µl of LB and plated over 2% LB-agar plates containing 50µg/ml kanamycin or 100µg/ml ampicillin or 50µg/ml spectinomycin. The plates were incubated at 37^{o}C in an incubator shaker in an inverted position for 12-16 hours and colonies were screened by colony PCR, using forward primer of vector and reverse primer of the insert.

4.3.5. Plasmid isolation

Plasmids were isolated from overnight grown cultures using the QIAprep Spin Miniprep Kit (Qiagen) according to the manufacturer's recommendations. Briefly, 5ml of overnight grown bacterial cultures were centrifuged for 2 minutes at 13000rpm. The bacterial pellets

were suspended in 250µl of ice-chilled buffer P1 containing ribonuclease A (Qiagen). Subsequently, 250µl of buffer P2 was added and suspension mixed by inverting the tubes followed by 5 minutes' incubation at room temperature. To stop lysis, 350µl of ice-chilled buffer N3 was added and suspension mixed by inverting the tubes. The solution was centrifuged for 10 min at 12,000 g. The supernatant was loaded to QIAprep Spin Columns and centrifuged at 8000rpm for 1 minute, followed by washing with 700µl of PB buffer. DNA was eluted in 60 µl H2O and quantitated by NanoDrop 2000c spectrophotometer (ThermoFisher Scientific, USA).

4.4. Cell cultures and exposure to stress

H1299 and HCT116 cell lines were grown in DMEM medium supplemented with 10% Fetal Bovine Serum (FBS), containing appropriate antibiotics (Pencillin and Streptomycin) in a humidified incubator at 37^0C and 5% CO2. Nutritional stress was induced by starving the cells in culture either to low serum (0.5% FBS) or low glucose (1mM) for 18h; whereas, oxidative stress was induced by treating the cells in culture with different doses of H2O2 (100 µM and 500 µM) and CoCl2 (100 µM and 500 µM) for 18h. Cells were transfected with the desired constructs at 70-80% confluency using Lipofectamine 3000 reagent as described in the next section (4.4).

4.5. Transfection using Lipofectamine 3000

On the first day prior to the transfection, cells were seeded into 6 or 12 well plates, as per experimental requirement (Day1); and incubated in humidified incubator for 24 hrs. After 24hrs, morphology of cells was monitored and their confluency observed upto 70 to 80%. The medium from the plates was removed and replaced by fresh antibiotic free DMEM. Afterwards, transfection was carried out by using Lipofectamine 3000 reagent (ThermoScientific # *L3000015*). In an eppendorf tube, 2.5 ug or 1 ug plasmid DNA was diluted with 120ul or 60ul optiMEM medium followed by addition of 5ul or 2ul Lipofecatmine P3000 solution. In a separate tube Lipofectamine 3000 reagent was diluted in 120ul or 60ul optiMEM medium. The diluted DNA was added to the reagent containing tube and the mixture was kept for 20 minutes at room temperature. The mixture from the eppendorf tube was added evenly throughout the wells. The plates were swirled very slowly for uniform distribution and were kept in the incubator at 37^0C. After 12 hours, the

medium was replaced with complete DMEM medium. The plate was kept back in the incubator at the same temperature. After 48 hours, cells were harvested for the desired experiment.

4.6. Virus production and stable cell generation

Stable cells were generated using lentiviral particles. Lentiviral particles were produced by co-transfecting HEK293-T cells with transfer plasmid along with psPAX2 and pMD2.G, using Lipofectamine 3000 reagent. Fifteen hours after transfection, the medium was replaced with fresh DMEM. Supernatant containing virus particles was collected twice at 36h and 50h after transfection. The viral supernatant was filtered through a 0.45-µm filter and kept either at 4°C to use on the same day or stored at -80^{0}C for long term storage. For virus infection, H1299 cells were plated in polybrene (8µg/ml) containing DMEM and simultaneously infected with virus supernatant for 12h and kept in an incubator at 37^{0}C. Cells were selected after 24 hrs of infection with puromycin (2µg/ml) containing medium. The ectopic expression of the puromycin resistant cells was monitored by RT PCR analysis or Western blot.

4.7. RNA Isolation and Real-Time PCR

Total cellular RNA was isolated using Tri Reagent (Sigma # 93289-25ML). Reverse transcription reaction was performed for cDNA conversion, using Revert-Aid reverse transcription kit (Thermo scientific # K1621). PCR reactions were carried out with 75ng of cDNA as template, using PowerUp SYBR Green Master Mix (Thermo Scientific #A25742) on Real Time Detection System (CFX-96, Biorad # 1855195). All primers used for gene expression analysis in this study are listed in the Appendix TableA1.

4.8. 5’ Rapid amplification of cDNA ends (5’ RACE)

5’ RACE experiment was carried out to identify 5’end of DNMT1 gene using SMARTer RACE 5’/3’ Kit (Clontech # 634858). Briefly, RNA was converted to cDNA using 5’-CDS A as forward primer and gene specific internal primer as reverse primer (sequence detail provided in the Appendix Table A1). This cDNA was used to amplify 5’region of DNMT1.

Amplicons were cloned into pJET1.2 vector (Fermentas # K1231) and confirmed by sequencing (primer sequence provided in Appendix TableA1).

4.9. Confocal Microscopy and Immunostaining

4.9.1. In-silico localization prediction

The cDNA sequence of DNMT1-isoforms 1 or 3 fused in frame with, either uORF of DNMT1 gene or mitochondrial targeting sequence of human cytochrome c oxidase subunit VIII at their 5'end, were assessed for their potential to localize in different subcellular compartments, using PSORT II localization prediction program (*http://psort.hgc.jp/form2.html*).

4.9.2. Overexpressed protein localization

Cover slips were sterilized by soaking them in absolute ethanol and then dried in front of flame using a forcep. These sterilized cover slips were then placed in the required number of wells of 12 well plate. Cells (10^5) were seeded onto each cover slip. The dishes were incubated at 37^{o}C, 5% CO2 for 18 hours. The following day, transfection (as described earlier) with different constructs was performed using these cells. After 48h of transfection, cells were incubated with 1nM Mitotracker Red in DMEM medium for 20min at 37^{o}C, to stain mitochondria. Cell fixation was carried out 3.7% paraformaldehyde solution in PBS for 20min. Blocking and permeabilization was carried out together in PBS containing 5% BSA and 0.1% triton X 100. Permeabilized cells were incubated overnight with desired antibodies at 4^0C, followed by washing and incubation with Alexa-488-linked secondary antibody at RT for 1h. Thereafter, nuclei were stained with 1nM DAPI in PBS for 20min at room temperature. Mounting was done in presence of prolong gold anti-fade reagent (Invitrogen, USA). Images were captured with 60x oil immersion objective lens on Andor Spinning Disc confocal microscope equipped with iXon Ultra 897 EMCCD camera. Pearson coefficient for mitochondrial co-localization was calculated for multiple images, using NIS viewer software.

4.9.3. Immunostaining for 5 methyl cytosine

Cell seeding and transfection was done as described in the previous section (Section 4.8.2). Cell fixation was carried out with ice-chilled methanol at -20^{o}C for 10 minutes. Cells were permeabilized with ice-chilled acetone for 1min at -20^{o}C.

These cells were rehydrated in PBS and treated with 2N HCl for 30min at 37^{o}C. Cells were then washed twice with 0.1M borate buffer (pH 8.5) and blocked with 1% BSA in PBS. Further, cells were stained with 5 methyl cytosine antibody (Sigma # SAB4800001**)** at RT in dark for 1h, followed by washing and incubation with Alexa-488-linked-secondary-antibody at RT for 1h. Later steps were similar as mentioned already for DNMT1 immunostaining (mentioned in the section 4.8.2).

4.10. Methylation analysis

4.10.1. Gradient gel electrophoresis

Pure mitochondrial DNA was isolated (Figure. 4.8A) using Mitochondrial DNA Isolation Kit (Biovision# K288). The purity of mtDNA was established by setting a PCR reaction (Figure. 4.8B) with both mitochondrial gene and nuclear gene, using total genomic DNA (containing both nuclear as well as mtDNA). Isolated mtDNA was subjected to MspI and HpaII (Fermentas# K14441) restriction enzyme digestion at 37^{o}C for 3 hrs. MspI and HpaII are isoschizomers; MspI is a methyl insensitive enzyme that cuts both within methylated as well as unmethylated "CCGG'' sites, while, HpaII cuts within only unmethylated "CCGG" sites.

Whole mitochondrial genome when analyzed contained 23 sites for MspI/HpaII restriction enzyme (Table 4.3); suggesting to expect 23 fragments generated after restriction digestion, ranging from 2396 to 24 bp. For positive control experiments, DNA was methylated *in-vitro* using M.SssI methylase enzyme (NEB# M0226S) at 37^{o}C for 1 hr. The restriction digested mtDNA was subjected to gradient TBE PAGE (4-20%) gel electrophoresis (Invitrogen# EC62252BOX) at 60V for 1 hour. Surprisingly, we were unable to get those 23 fragments and ended up with getting a smearish pattern of undistinguished bands (Figure. 4.8C, D). However, we got a preliminary impression about occurrence of mtDNA

methylation, which was further established with more quantitative, Methyl Sensitive Resrtiction qPCR (MSRP) approach.

Table 4. 2: Total MspI/HpaII restriction enzyme sites in mtDNA with their coordinates and with the expected sizes of the fragments after restriction digestion

#	Ends	Coordinates	Length (bp)
1	HpaII-HpaII	9293-11688	2396
2	HpaII-HpaII	13713-15925	2213
3	HpaII-HpaII	932-3077	2146
4	HpaII-HpaII	3247-4711	1465
5	HpaII-HpaII	12124-13364	1241
6	HpaII-HpaII	8151-9292	1142
7	HpaII-HpaII	7205-8112	908
8	HpaII-HpaII	105-931	827
9	HpaII-HpaII	15926-16453	528
10	HpaII-HpaII	5243-5742	500
11	HpaII-HpaII	5767-6262	496
12	HpaII-HpaII	11689-12123	435
13	HpaII-HpaII	4847-5242	396
14	HpaII-HpaII	6851-7204	354
15	HpaII-HpaII	13365-13712	348
16	HpaII-HpaII	6263-6571	309
17	HpaII-HpaII	3078-3246	169
18	HpaII-HpaII	6689-6850	162
19	HpaII-HpaII	4712-4846	135
20	HpaII-HpaII	6572-6688	117
21	HpaII-(RightEnd)	16454-16569	116
22	(LeftEnd)-HpaII	1-104	104
23	HpaII-HpaII	8113-8150	38
24	HpaII-HpaII	5743-5766	24

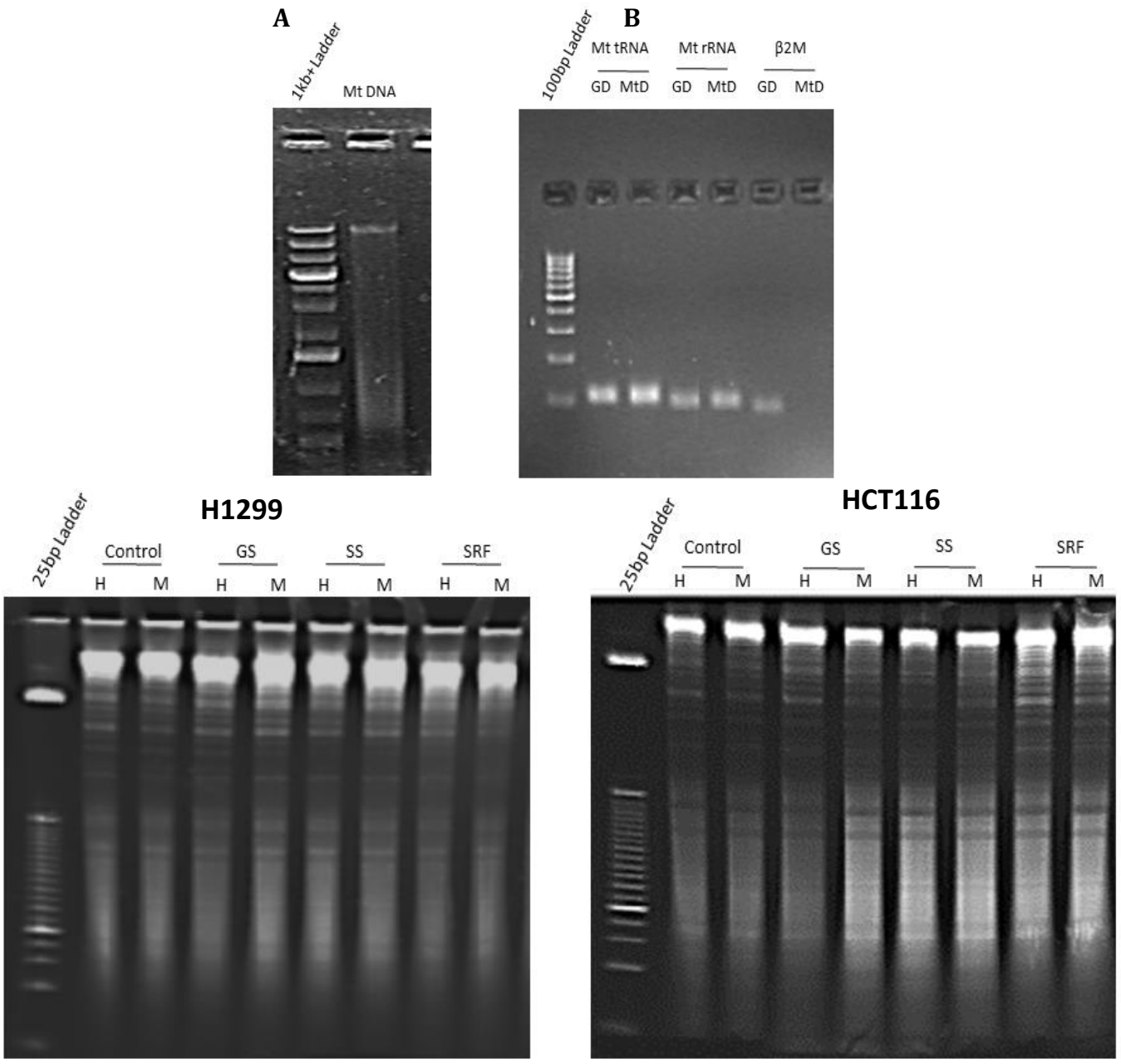

Figure 4.8: Representative gel images showing (A) isolated mtDNA. (B) Checked for purity from nuclear DNA contamination, by PCR using nuclear gene (β2M) and mtDNA gene (mt tRNA and 16s rRNA) specific primers. (C) and (D) gel images of TBE gradient (4-12%) electrophoresis of mtDNA from H1299 and HCT116 cells digested with MspI and HpaII restriction enzymes. GD: total genomic DNA; mtD: mtDNA; GS: glucose starvation (1mM); SS: serum starvation; M: MspI; H: HpaII.

4.10.2. Dot Blot Assay

Global mitochondrial DNA methylation was assessed, using Dot Blot experiments with 5 meC antibody (Sigma # SAB4800001**)**. Briefly, 50 ng of purified mtDNA was spotted on nitrocellulose membrane, dried and exposed to UV light for 5 mins. The membrane was blocked with 2% BSA in PBS on a rocker at RT for 2hr, followed by incubation with 5meC antibody at 4^{o}C overnight. Membrane was washed with PBST (0.1% Tween 20) thrice for 15 mins each on the rocker. Further, membrane was incubated with secondary anti-mouse HRP antibody at RT for 2 hrs. Again, the membrane was washed with PBST thrice for 15 mins each on the rocker. ECL reagents were used for visualization (Luminata Forte Western HRP substrate, Millipore) through chemiluminescence on the x-ray film which was developed and fixed as per routine procedures in the laboratory.

4.10.3. Methyl Sensitive Restriction qPCR (MSRP)

Genomic DNA was isolated using QIAamp DNA Blood Mini Kit (50) from Qiagen. Methylation at 6 specific CpG positions of mitochondrial genome was quantified using EpiJET DNA Methylation Analysis Kit (MspI/HpaII, # 1441). These 6 sites located in: the transcription termination factor binding region (TTF) at 3266, L-strand origin of replication (LSO) at 5766, membrane attachment site (MAS) at 15925, hypervariable region2 (HVR2) at 104, 12s rRNA at 931 and 16s rRNA at 3077 positions, respectively within the mitochondrial genome (NC_012920 as the rCRS), were chosen on the basis of their regulatory and structural importance from a total of 23 MspI/HpaII restriction sites within the whole mitochondrial genome. Briefly, 500ng of total genomic DNA was digested with MspI and HpaII restriction enzymes at 37^{0}C for 4h, followed by restriction enzyme inactivation by heating at 80 °C for 20 minutes. 25ng of each MspI and HpaII digested DNA was used as a template to carry out Real-time PCR for the above mentioned CpG positions, using mitochondrial DNA specific flanking primers (the sequence of all the primers are mentioned in appendix Table A1).

4.11. CHIP Assay

Chromatin immunoprecipitation was carried out by ChromaFlash High Sensitivity CHIP Kit from Epigentek (#P-2027). Briefly, cells in culture were harvested and washed with

PBS twice. For cross-linking, cells were then incubated for 10 min with 1% formaldehyde solution, containing 10ml DMEM medium, on a rocker. 1 ml of 1.25 M glycine was added and centrifuged at 1000 RPM for 5 min. Cell pellet was washed with ice-chilled PBS and lysed on ice for 10 min. Chromatin collected after centrifugation; incubated with CHIP buffer for 10 min, was sheared using probe-based sonication (Branson sonifier) for 10 cycles of 15 sec ON and 40 sec OFF at 25% power output. Chromatin was then used immediately or stored at -80^{0}C. The pre-incubated wells with 0.5 µg of DNMT1 antibody in antibody binding buffer (AB, provided in kit) for 1h were washed with 150ul of chip buffer (CB). Chromatin (2ug) for each of the sample was allowed to bind to the antibody coated wells at RT for 90mins on an orbital shaker. Afterwards, the solution was removed from the wells carefully and wells were washed with 200ul wash buffer (WB) for 2mins on an orbital shaker, repeating the washing step 4 times. The wells were then washed with DNA releasing buffer (DRB) simply by pipetting DRB in and out of the well. The antibody bound DNA was de-crosslinked with 40ul of DRB in each well. The de-crosslinked DNA was incubated at 42^{0}C for 30mins for RNase treatment. In each well, 2ul proteinase K was added and incubated at 60^{0}C for 45mins. The DNA was then incubated at 95^{0}C for 15 mins and was directly used as a template to carry out real time PCR to assess mtDNA binding sites of DNMT1 at multiple positions of the mitochondrial genome.

4.12. Western Blotting

For immunodetection, samples prepared by lysis of cell pellets in RIPA buffer and estimated for the concentration of proteins by bicinchoninic acid assay, using BSA as a standard (Pierce # 23227), were separated on 8-10% SDS–PAGE as required. The gel was then transferred onto a nitrocellulose membrane (NCM) via wet transfer method and was further processed using standard methods. The antigens were detected using primary antibodies (Anti-DNMT1 # ab13537, Abcam and beta-actin # A2228-100UL, Sigma) raised in mice, followed by secondary anti-mice immunoglobulins conjugated to HRP (1:10,000, Sigma). ECL reagents were used for visualization (Luminata Forte Western HRP substrate, Millipore).

4.13. Flow cytometry

Cells in culture were harvested; washed with PBS twice and pelleted. Cell pellets were resuspended in 450ul of serum free DMEM. Mitotracker Red CMX ROS (Invitrogen # M7512) or Mitotracker Green (Invitrogen # M 7514) was diluted 1000 fold by adding 1ul of 1mM stock solution to 1ml DMEM to give sub-stock solution with 1uM for each one of them. To assess mitochondrial membrane potential, 50ul of Mitotracker Red sub-stock solution was added to 450ul of cell suspension to give the final working concentration of 100nM. To assess mitochondrial mass, 50ul of Mitotracker Green sub-stock solution was added to 450ul of cell suspension to give the final working concentration of 100nM. Cell suspension was incubated at 37^0C for 30 min in dark to allow the dye to stain mitochondria. After that, cells were centrifuged; washed with PBS twice and suspended in PBS. The stained cell suspensions were run on flow cytometer BD FACS Calibure (BD Biosciences) system to monitor fluorescence in FL-1 and FL-2 channels for Mitotracker Green and Mitotracker Red, respectively. The values of mean fluorescence intensity recorded at respective channels was used to analyze the data using Cell quest pro software.

4.14. Bioinformatics analysis of miRNA mediated epigenetic regulation of mitochondrial biogenesis genes.

4.14.1. miRNA target prediction of the defined mitochondrial biogenesis genes

From the miRBase (Kozomara and Griffiths-Jones, 2014) website (Release 21), 2588 mature human miRNA sequences and 3′UTR sequences of key mitochondrial (nuclear genome encoded) biogenesis genes (5 genes, Table 4) were obtained from UCSC genome table browser (Karolchik et al., 2004).

A total of 4 standard and widely used miRNA target prediction programs: PICTAR (Anders et al., 2012), miRanda (Betel et al., 2010), PITA (Kertesz et al., 2007) and TargetScan (Garcia et al., 2011) were used. Experimentally validated miRNA targets for 5 genes from miRTarBase (Hsu et al., 2014) and miRecords (Xiao et al., 2009) databases were also retrieved.

The sequence was retrieved based on: clade- Mammal, genome- Human, Assembly- GRCh38/hg38, group- Genes and Gene Predictions, track- RefSeq Genes, table- refGene, Region- genome, ouput- sequence.

Table 4. 3: Mitochondrial biogenesis genes with their gene ID

Gene	EntrezID	RefseqID
NRF1	4899	XM_005250388
TFAM	7019	NM_003201
TFB2M	64216	NM_022366
NFE2L2	4780	NM_006164
PPARGC1A	10891	XM_005248133

4.14.2. Identification of highly regulating nodes in the Network

In a large integrated-network-constructed- of proteins/genes with a high degree (the number of edges per node) interaction with several other signaling proteins/genes, pointed towards a key regulatory role of hubs. It is believed that proteins/genes with many interacting partners in the network tend to play an important role in the cells; and these tend to be essential proteins or disease-associated proteins (Wu et al., 2012). Using Network analyzer, the plugin of Cytoscape v3.4.0 (Hernandez-Toro et al., 2007) and *Perl* programming version 5.18.2.2, the hub proteins communicating with many other significant proteins involved in several biological processes were identified, which were known to be associated with different diseases. An undirected network was constructed and analyzed in this study. The microRNA, hsa-miR-19b-2-5p, which acted as a hub and could target all the 5 genes involved in regulating nuclear coded mitochondrial biogenesis related gene products, were identified. These 5 genes were upregulated in the background of DNMT1-isoform3 overexpressing condition with hypermethylation and low expression of the mito-OXPHOS related genes, in our experiments in this work.

4.14.3. Functional annotation of microRNA network

To understand the functional role of proteins targeted by hsa-miR-19b-2-5p, its targets were identified using the same protocol as mentioned in the "miRNA target prediction section". Since single miRNA target could have a similar function, the GO (gene ontology) categories (Molecular function, Biological process, Cellular components) and the status/association of these proteins in diseases identified. The GO: biological process, molecular function and cellular components, were retrieved from WEB-based GEne SeT AnaLysis Toolkit (WebGestalt) (Wang et al., 2013); and each functional enrichment analyses was considered for the construction of pie diagrams that allowed better visualization of the functional categories, the pathways and diseases. For pathway analysis, the Wikipathways dataset was used and the results of the significance (p values) of the pathways and diseases analyzed.

4.14.4. Mitochondrial proteins and their regulation by microRNA

Despite the fact, the mitochondrion has its own genomic, transcriptomic and proteomic materials; it is not entirely autonomous to produce all the proteins required for its full functionality. Several essential cellular functions of mitochondria depend on a high degree of functional interaction between the nuclear and mitochondrial genomes. More than three thousand proteins have been identified in the mammalian mitochondria (Calvo et al., 2015); and there is a need to find out the proteins which regulate mitochondrial function and probably get regulated epigenetically through microRNA.

The mitochondrial proteins were retrieved from human mitochondrial protein databases (http://bioinfo.nist.gov/) and MitoProteome (http://www.mitoproteome.org/). A total of 1705 genes were identified within mitochondria. These proteins were subjected to miRNA target prediction. Same protocol as mentioned in the "miRNA target prediction section" was used. The GO functions and pathways were analyzed for those mitochondrial genes which were targeted by hsa-miR-19b-2-5p, using same protocol as mentioned in the "*Functional annotation section*".

4.15. Statistics

Statistical analysis was performed using Graph Pad Prism software. Data was represented as mean ± SD. Multiple comparison analysis was done by using 2 way ANOVA Sidak's test, while for the comparison of two samples, unpaired t-test was used. A difference was considered significant when $P<0.05$(*) or $P<0.01$(**) or $P<0.001$(***).

5. RESULTS

RESULTS

5.1. Whole mitochondrial genome sequencing and identification of CpG sites

Ten different human cancer cell lines (HeLa, MCF-7, MDAMB-231, A549, H1299, SiHa, LNCAP, PC3, HT29 and HCT116), belonging to five most prominent cancer types worldwide and involving a pair for each tissue type, were sequenced for a comparative study of CpG positions. Figures 5.1A and 5.1B depict the electropherograms with partial sequences of mtDNA of the paired breast cancer cell lines, MCF-7 and MDAMB-231. After mtDNA sequencing of the mentioned cell lines, the sequencing files were imported into SeqScape analysis software (Figure. 5.2), where these were analyzed for the CpG positions against rCRS mtDNA sequence. The total number of identified sites of CpG in each of these 10 cell lines were calculated (Table 5.1). Mitochondrial rCRS sequence when explored showed a total of 432 CpG sites. The differed CpG positions in the mitochondrial genome in comparison to rCRS in the studied cell lines were identified accordingly. A total of 13 positions within the mitochondrial genome with a variation at the CpG sites (Table 5.2), indicated the disruption of the CpG positions. Interestingly, both lung carcinoma cell lines (H1299 and A549) were conserved for CpG positions and showed all the 432 CpG positions present in rCRS. In both the breast cancer cell lines (MCF-7 and MDAMB-231), there was a disruption of the CpG position at 709 position. HCT116, HT29 and HeLa cell lines also showed disruption of the CpG sites at 3010, 11914 and 2699 positions, respectively. Similarly, CpG sites in SiHa (1168 & 1598) and LNCAP (4153 & 16126) were found disrupted. The mitochondrial genomic sequences exported from SeqScape software are tabulated for the observed variation at each position (provided in appendix section-Table A1) in comparison to revised Cambridge reference sequence (rCRS).

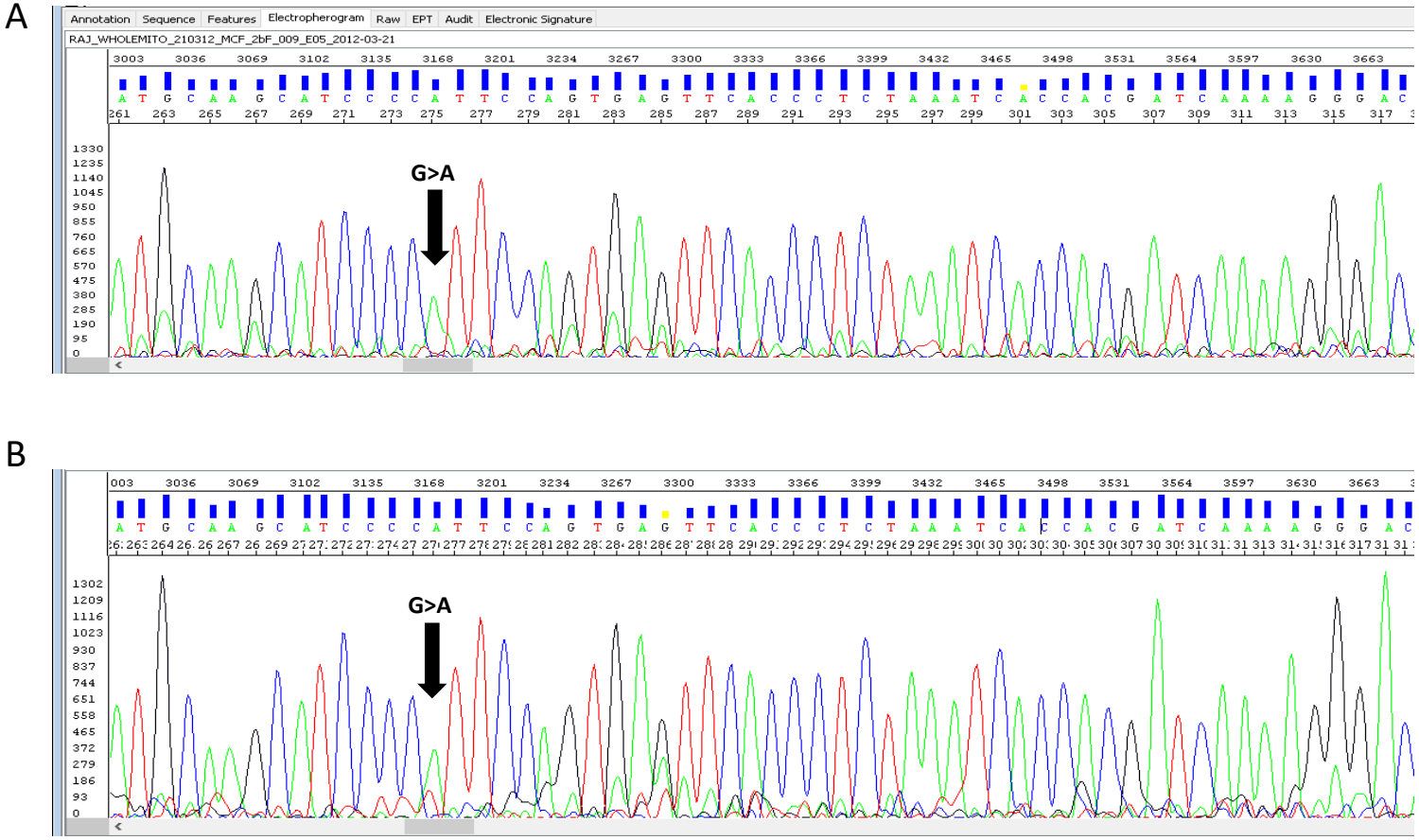

Figure 5. 1: Electropherograms representing partial mitochondrial DNA sequences from (A) MCF-7 and (B) MDAMB-231 cells.Adenine, Guanine, Cytosine and thymine are indicated as green, black, blue and red coloured peaks, respectively. The arrow depicts the variation (G>A) at 709 position in mtDNA disrupting the CpG site.

A

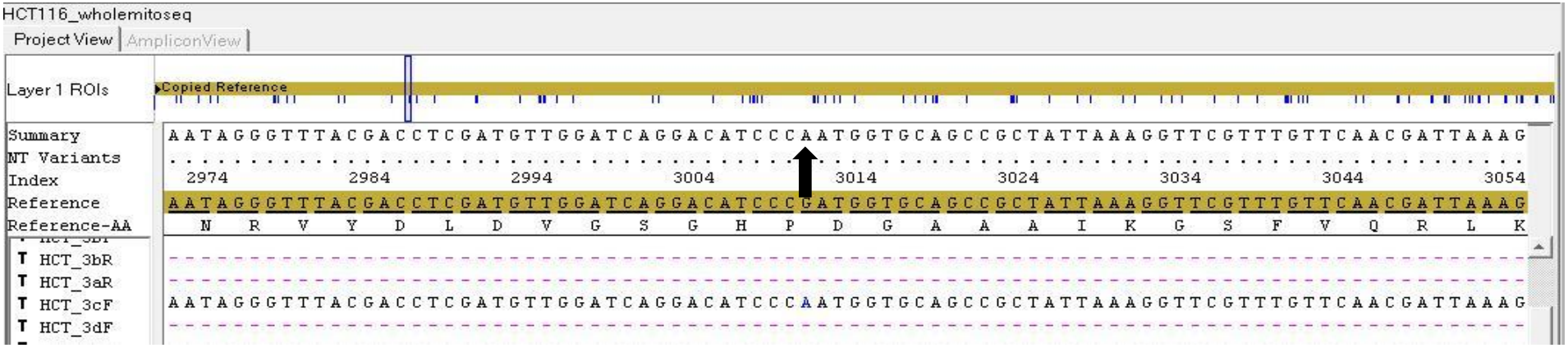

B

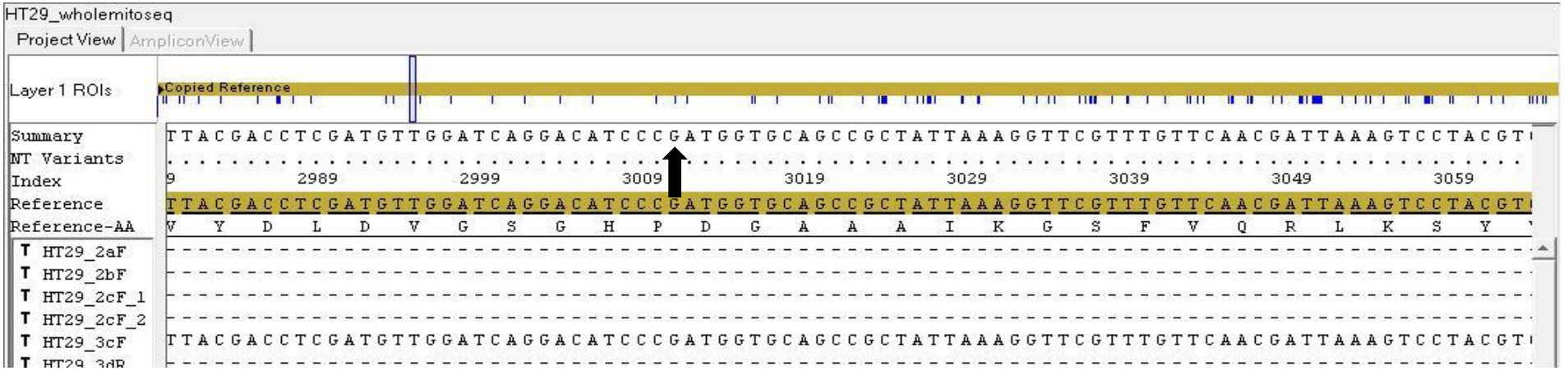

Figure 5. 2: Mitochondrial DNA sequence analysis against rCRS. (A) and (B) SeqScape screenshots representing partial mtDNA sequence for HCT116 and HT29 cell lines, respectively. The variation at 3010 position of mtDNA that results into disruption of CpG position is marked by an arrow.

Table 5.1: Total number of CpG sites in the studied cancer cell lines

Cell Lines	Tissue type	No. of CpG sites
A549	Lung	432
H1299	Lung	432
HCT116	Colon	431
HT29	Colon	431
MCF-7	Breast	431
MDAMB 231	Breast	431
HeLa	Cervical	431
SiHa	Cervical	430
LNCAP	Prostate	430
PC3	Prostate	431

Table 5.2: CpG site positions that differed from rCRS in the studied cancer cell lines

mtDNA position	Gene region	A549	H1299	HCT	HT29	MCF7	MDAMB	HeLa	SiHa	LNCAP	PC3
709	12s rRNA					G>A	G>A				INS G
1168	12s rRNA								A>G		
1598	12s rRNA								G>A		
2699	16s rRNA							C>T			
3010	16s rRNA			G>A							
4153	ND1									G>A	
5236	tRNA W										
5969	COI										
9449	COIII										
9912	COIII										
11914	ND4				G>A						
13968	ND5										
16129	7S DNA									G>A	

5.2. Mitochondrial DNA methylation status in control, nutritional and oxidative stress conditions

After the identification of the number of CpG sites in the studied 10 cancer cell lines, the purpose was to find out which one of these was methylated and differed in methylation status under nutritional (serum and glucose) and oxidative (H2O2 and CoCl2) stress conditions. Of a total of 430-432 identified CpG positions in different cell lines, 23 such sites were chosen *in-silico* as methyl sensitive, detected and differentiated by MspI and HpaII restriction enzymes (details provided in table 4.3, in materials and Methods section). Six of the 23 *in-silico* chosen CpG sites,were chosen for experimental studies in two (H1299 and HCT116) cell lines. These six sites (TTF: transcription termination factor, LSO: L-strand origin of replication, MAS: membrane attachment site, HVR2: hypervariable region, 12s rRNA and 16s rRNA) were conserved and had a possible role in the mitochondrial function. To our surprise, these sites behaved differently in terms of their methylation under glucose and serum starved, nutritional stress conditions (Figure. 5.3A). On glucose starvation, the CpG sites within TTF and LSO were significantly hypomethylated, whereas, the MAS CpG site was hypermethylated. However, under serum starvation, all of the CpG sites (TTF, LSO, HVR2, MAS, 12s and 16s rRNA) were hypomethylated and either attained the normal levels or hypermethylated when cells were refed with serum. Under oxidative stress conditions, the mtDNA was hypomethylated more extensively (Figure. 5.3B) in comparison to nutritional stress at these analyzed CpG positions. Within the oxidative stress conditions, CoCl2 treatment conditions affected the methylation of these CpG sites more profoundly. The hypomethylation at TTF site, was most prominent as compared to other analyzed sites under both (H2O2 and CoCl2) oxidative stress conditions. Similarly, CpG site within LSO, MAS and HVR2 region, was also hypomethylated, though not to the same extent as was observed for TTF site.

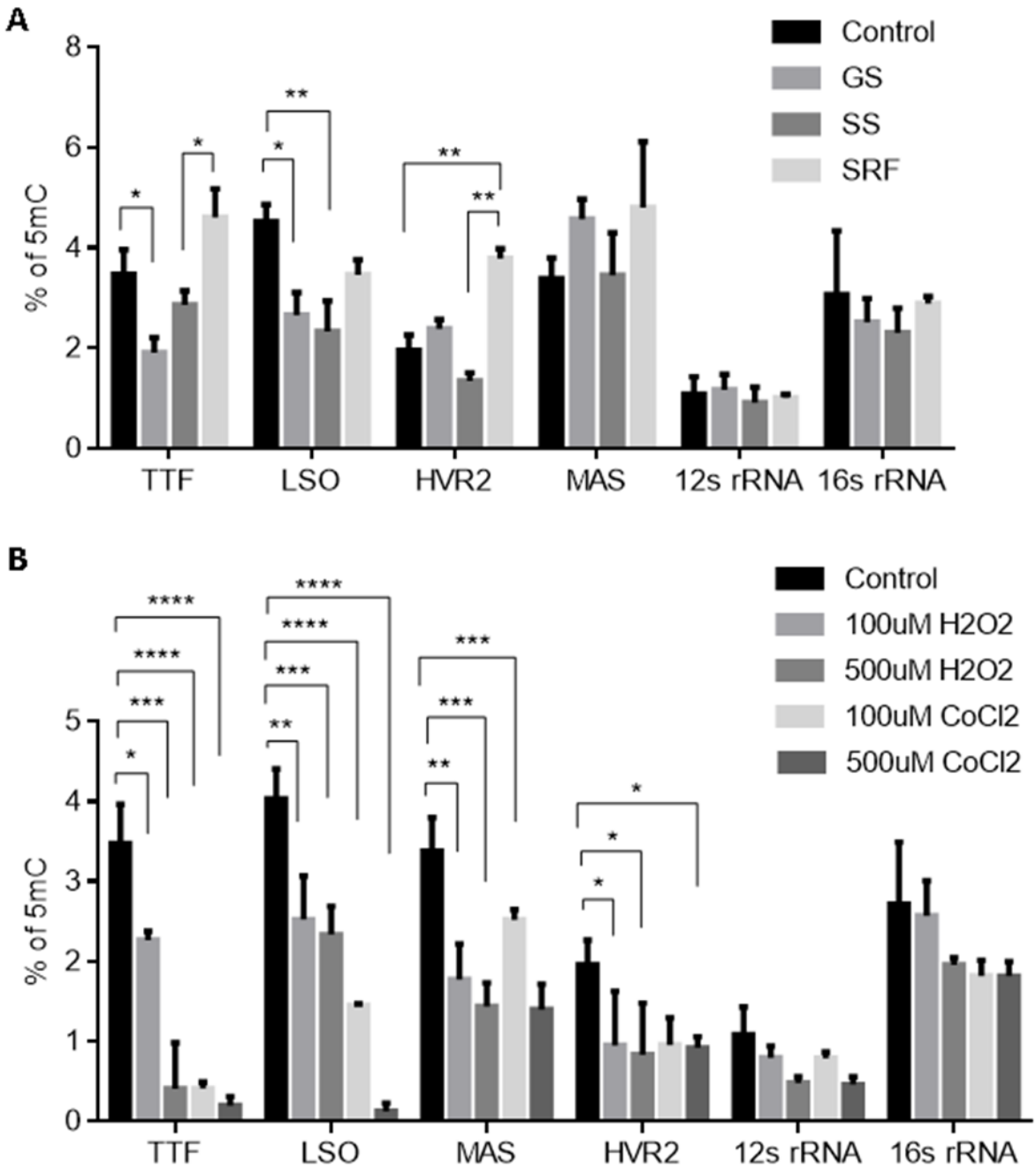

Figure 5.3: Mitochondrial DNA is hypomethylated under various conditions of nutritional and oxidative stress. % of 5mC at certain defined (TTF, LSO, MAS, HVR2, 12s rRNA and 16s rRNA) CpG sites of mitochondrial genome resulting from (A) nutritional and (B) oxidative stress conditions, respectively.

Since the status of mtDNA methylation varied between different stress conditions, it was pertinent to look at the expression of specific methyltransferases involved in methylation. Western blot analysis revealed downregulation in the expression profile of DNMT1-isoforms, especially isoform3, under all of these conditions. Interestingly expression profile correlated with the methylation status, under oxidative stress conditions (Figure. 5.4B), where it showed that it was further decreased in comparison to what was observed under nutritional stress conditions (Figure. 5.4B). Similarly, under serum starvation (SS) conditions, the expression of DNMT1 was downregulated, which was restored to that of normal level when cells were supplemented with serum (SRF).

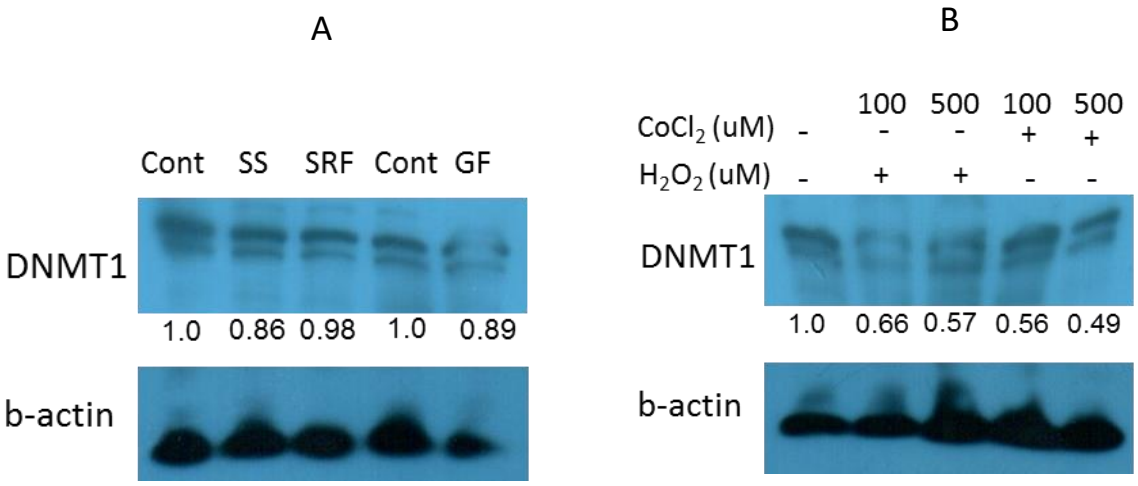

Figure 5.4: DNMT1-isoform3 is downregulated under conditions of nutritional and oxidative stress conditions. Western Blot scans of DNMT1 isoform expression profiles under (A) nutritional and (B) oxidative stress conditions. SS, SRF and GF stands for serum starvation, serum re-fed and glucose starvation respectively. H2O2 and $CoCl_2$ treated and non-treated are indicated with (+) and (–) sign respectively. Relative fold of expression of DNMT1-isoform3 is calculated by densitometry analysis on normalization with respective b-actin expression and indicated (in values) just below the DNMT1 scans.

It was evident from the previous results that mitochondrial DNA was hypomethylated accompanied with downregulation of DNMT1-isoform3, it was therefore essential to examine the health of mitochondria by measuring the mitochondrial activity per mass in response to both nutritional (Figure. 5.5A) and oxidative stress (Figure. 5.5B) conditions. We observed that under glucose starvation (GS), the mitochondrial activity per mass increased; while, under serum deprivation (SD), there was a decrease in mitochondrial activity, which was restored when cells were supplemented with serum (SRF). However, under oxidative stress conditions, the mitochondrial activity per mass decreased in accordance to the dose of the treatment and was affected the most in response to $CoCl_2$ treatment.

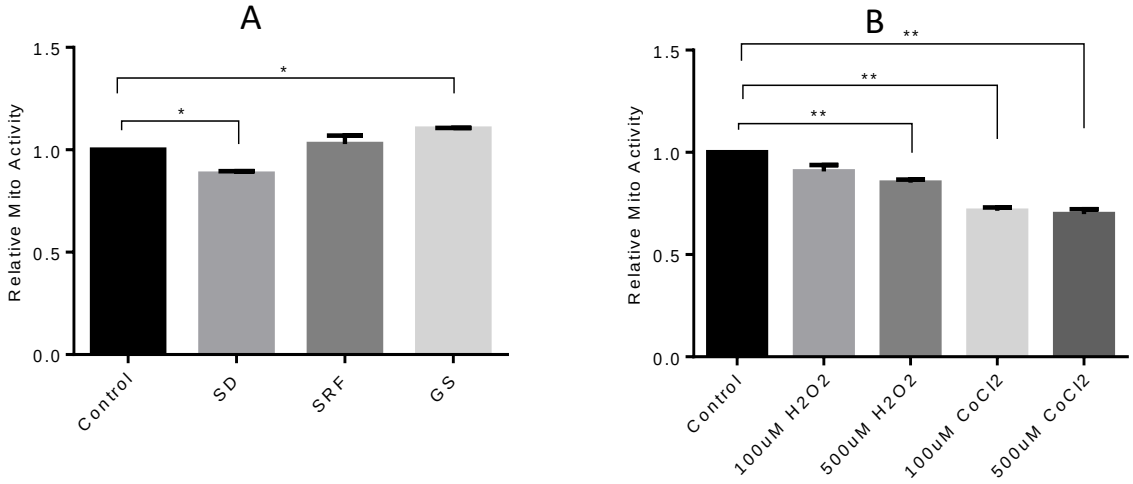

Figure 5.5: Mitochondrial activity per mass is decreased under nutritional and oxidative stress conditions. Relative mitochondrial activity per mass under (A) nutritional and (B) oxidative stress conditions. SS, SRF and GF stands for serum starvation, serum re-fed and glucose starvation respectively.

5.3. *In-silico* subcellular localization prediction of DNMT1-isoforms and their structure and expression analysis

In order to understand the biological relevance of mitochondrial DNA methylation, it was essential to identify the particular isoform of DNMT1 that localized into mitochondria and mediated the process of methylation. PSORTII localization prediction program (*http://psort.hgc.jp/form2.html*) was used to estimate the subcellular localization potential

of DNMT1-isoforms 1 and 3 either alone or with the presence of uORF/mitochondrial targeting sequence (Table 5.3). The DNMT1-iso1 sequence when fused with uORF sequence (reported earlier to act as MLS) predicted to localised inside the nucleus but not in mitochondria. On further addition of known strong mitochondrial targeting sequence of human cytochrome c oxidase subunit VIII at the 5'end of DNMT1-iso1 predicted most of it to be localised in the nucleus; however, 8.7% of it showed localisation in mitochondria. DNMT1-iso3 was also predicted to shown similar proportion for nuclear and mitochondrial localisation, however, in presence of additional MLS (human cytochrome c oxidase subunit VIII), the mitochondrial localisation was increased further and showed upto 40% of it to localise in mitochondria.

Table 5.3: Subcellular localization prediction of DNMT1-isoforms

	DNMT1-isoforms with or without additional signal sequence	Localisation prediction
1.	DNMT1-isoform1	82.6 %: nuclear 08.7 %: plasma membrane 04.3 %: cytoplasmic 04.3 %: cytoskeletal
2.	DNMT1-isoform1 with uORF	78.3 %: nuclear 13.0 %: plasma membrane 08.7 %: cytoskeletal
3.	DNMT1-isoform1 with MLS	65.2 %: nuclear 03.0 %: cytoskeletal 08.7 %: cytoplasmic 08.7 %: mitochondrial 04.3 %: plasma membrane
4.	DNMT1-isoform3	78.3 %: nuclear 08.7 %: cytoplasmic 08.7 %: mitochondrial 04.3 %: plasma membrane
5.	DNMT1 -isoform3 with uORF	69.6 %: nuclear 13.0 %: cytoplasmic 08.7 %: mitochondrial 04.3 %: cytoskeletal 04.3 %: plasma membrane
6.	DNMT1-isoform3 with MLS	56.5 %: nuclear 39.1 %: mitochondrial 04.3 %: cytoplasmic

It was pertinent from the *in-silico* prediction of subcellular localization that DNMT1-isoform1 with uORF sequence, failed to localize in mitochondria and exclusively present in the nucleus. We then examined the structure of DNMT1-isoform1 (Figure. 5.6A) and observed multiple patches of nuclear localization signal sequences (NLS) at their N-terminal that seemed to override the presence of MTS; and facilitated its targeting to the nucleus only. These nuclear localization signal sequences were found to be absent in the isoform3, as it lacked the portion of N-terminal region and represented the shortest isoform of DNMT1.

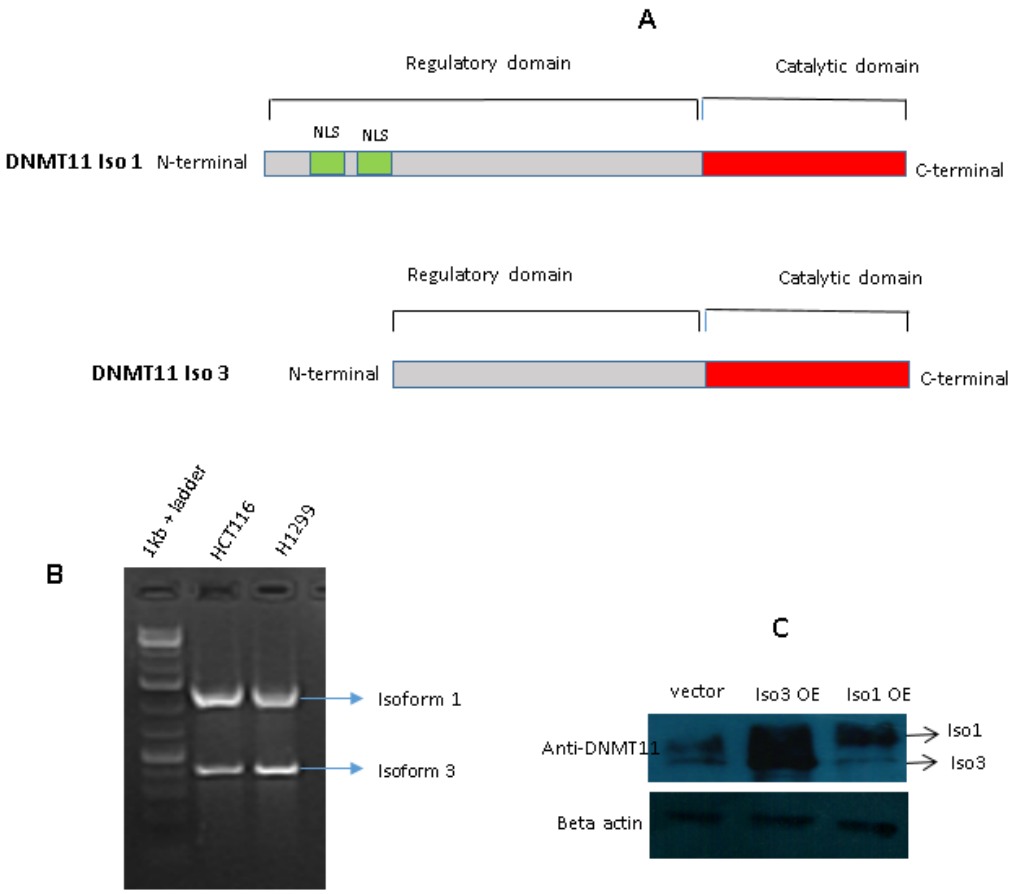

Figure 5.6: Structure and expression analysis of DNMT1-isoforms. (A) Structure of DNMT1-isoforms depicting presence of nuclear localization signal sequence elements exclusively in isoform 1. (B) 5' RACE PCR product with isoform 1 and 3. (C) Western blot of DNMT1-isoform1 and 3 overexpression.

We performed 5'RACE experiments to check the existence of DNMT1-isoforms and found that transcripts for both, DNMT1-isoform1 and 3 exists (Figure. 5.6B) in two different cell lines (H1299, HCT116). Both of these isoforms were confirmed for their expression by western blot (Figure. 5.6C).

5.4. DNMT1-isoform3 instead of isoform1 localizes to the mitochondria

After designing the expression vectors in different configurations (as detailed in the Materials and methods section) to express the two isoforms of DNMT1 in the cells and study which of these in actual, localize in mitochondria. The isoform of DNMT1 that possessed an additional upstream ORF which encoded for a mitochondrial targeting sequence (MTS) at the N-terminal, was suggested earlier to facilitate the localization of DNMT1 to mitochondria and methylate its genome. However, the overexpression of this isoform under similar conditions (Figure. 5.7Aii) in our experiments failed to target DNMT1 in the mitochondria. Experiments carried out to check the subcellular localization of DNMT1-isoform1 even with strong mitochondrial targeting sequence (Figure. 5.7Aiii) did not facilitate localization of DNMT1 within mitochondria, but showed an exclusive presence in the nucleus. On examination of DNMT1-isoform1 structure, we found multiple patches of nuclear localization signal sequences (NLS) that seemed to override the presence of MTS at N-terminal; and facilitated its targeting to the nucleus only. Incidentally, we found another isoform of DNMT1 (Figure. 5.7Aiv), the DNMT1-isoform3, not reported earlier, which localized to the mitochondria. The nuclear localization signal sequences were found to be absent in the isoform3, as it lacked the portion of N-terminal region and represented the shortest isoform of DNMT1. *In-silico* localization prediction by psortII program also found some of the fraction (8.7%) of the isoform3 to localize in human mitochondria. Further addition of strong mitochondrial localization signal sequence to isoform3, increased it probability to localize in mitochondria (Figure. 5.7Av & Avi).

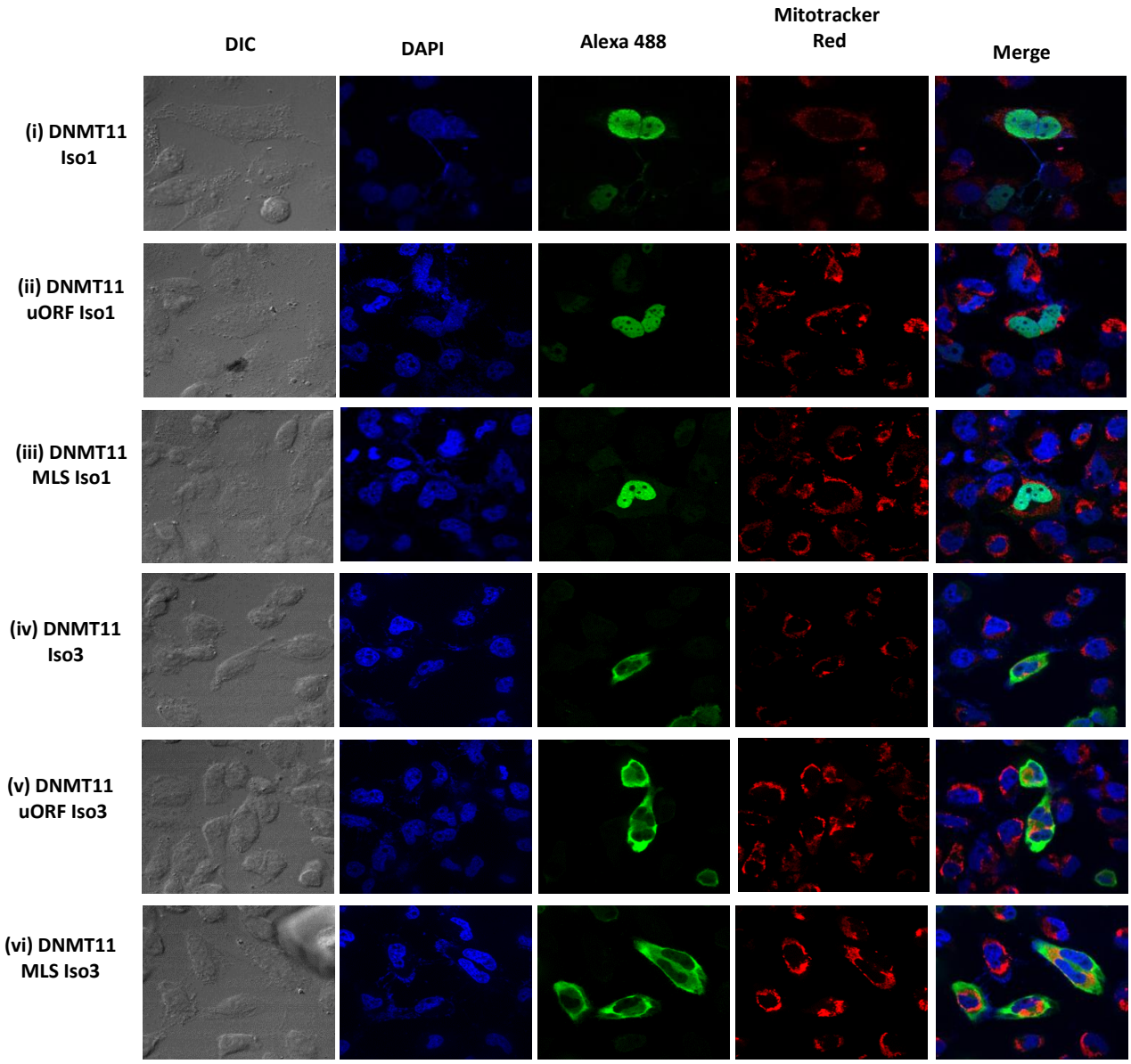

Figure 5.7: DNMT-isoform3 not isoform1 localizes to mitochondria. Representative confocal images of H1299 cells showing subcellular localization pattern of exogenously over-expressed DNMT1-isoform1 and 3 with or without any additional localization signal sequence. Nucleus, overexpressed protein and mitochondria were stained with DAPI, Alexa488 and Mitotracker red respectively.

Since it is the DNMT1-isoform3 not isoform1 that localized to mitochondria, we further trace the subcellular localization of DNMT1 isoforms with or without additional localization signal sequences at different time period of their expression. DNMT1-isoform1 failed to localize in mitochondria at all the time points analyzed in growing cells in culture (Figure. 5.8B; even after the addition of strong mitochondrial localization signal sequence, suggesting the absence of its localization to mitochondria (Figure. 5.9B). However, a change in the pattern of localization was observed for DNMT1-isoform3 between mitochondria and nucleus with advancing time after its exogenous expression (Fig 5.10B). This isoform exclusively localized to mitochondria and cytosol during 24 to 48 hrs of expression. In the later hrs, however, it localized in the nucleus and was gradually distributed throughout the cell. Inclusion of uORF sequence increased the potential of localization of the isoform3 in mitochondria with concomitant decrease in the nucleus (Figure. 5.11B). Further addition of strong mitochondrial localization signal sequence to isoform3, prevented its localization in the nucleus even in later hrs of expression (Figure. 5.12B). There was a negative co-relation for Pearson's coefficient for mitochondrial localization of DNMT1-isoform1 with or without upstream localization signal sequences (Figure. 5.13), whereas, for isoform3 this coefficient showed a positive correlation and increased in presence of additional targeting sequences.

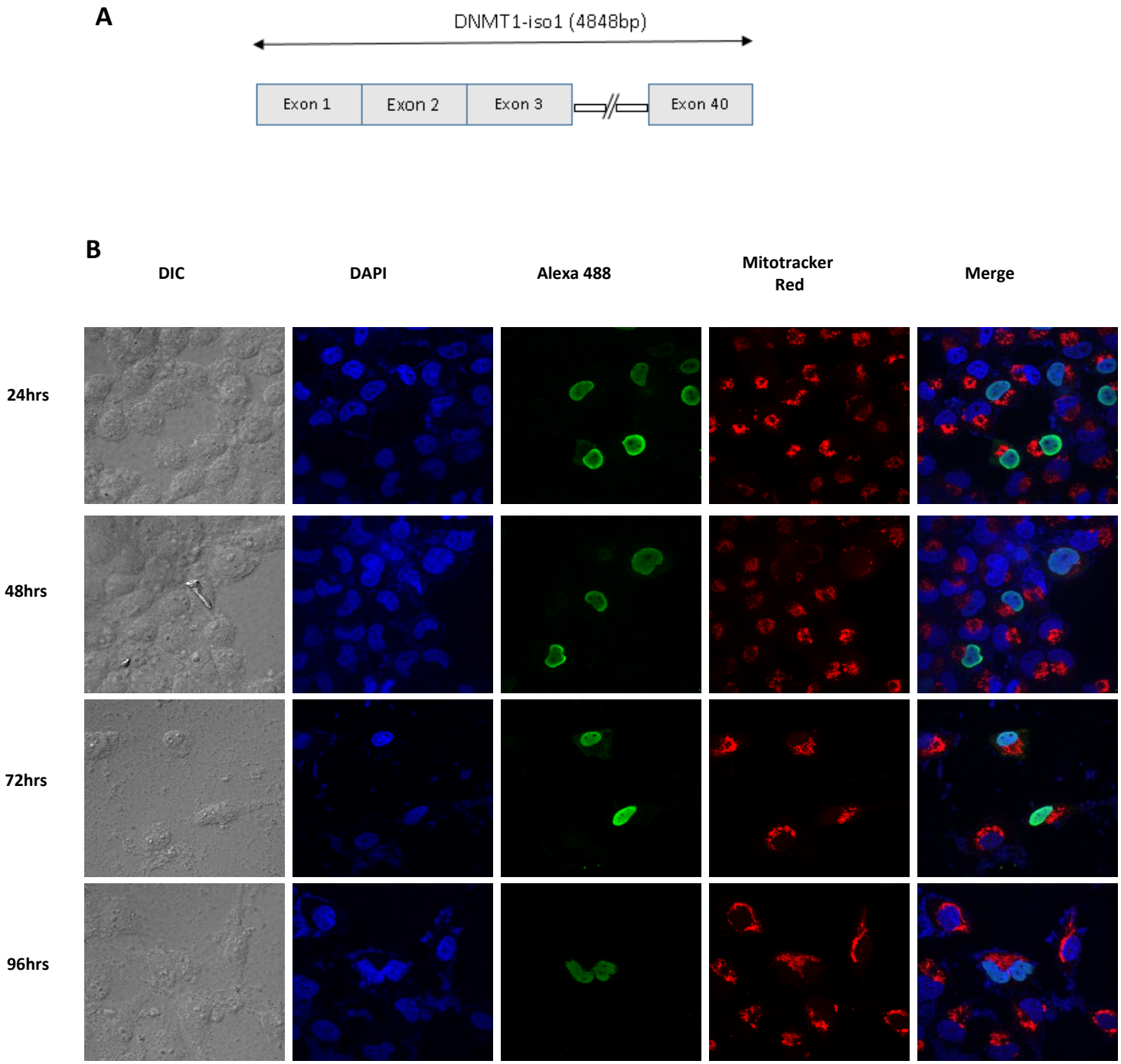

Figure 5.8: (A) Schematic diagram depicting DNMT1-iso1 structure. (B) Representative confocal images of H1299 cells showing localization pattern of exogenously overexpressed DNMT1-isoform1 at different time intervals (24 to 96 hrs).

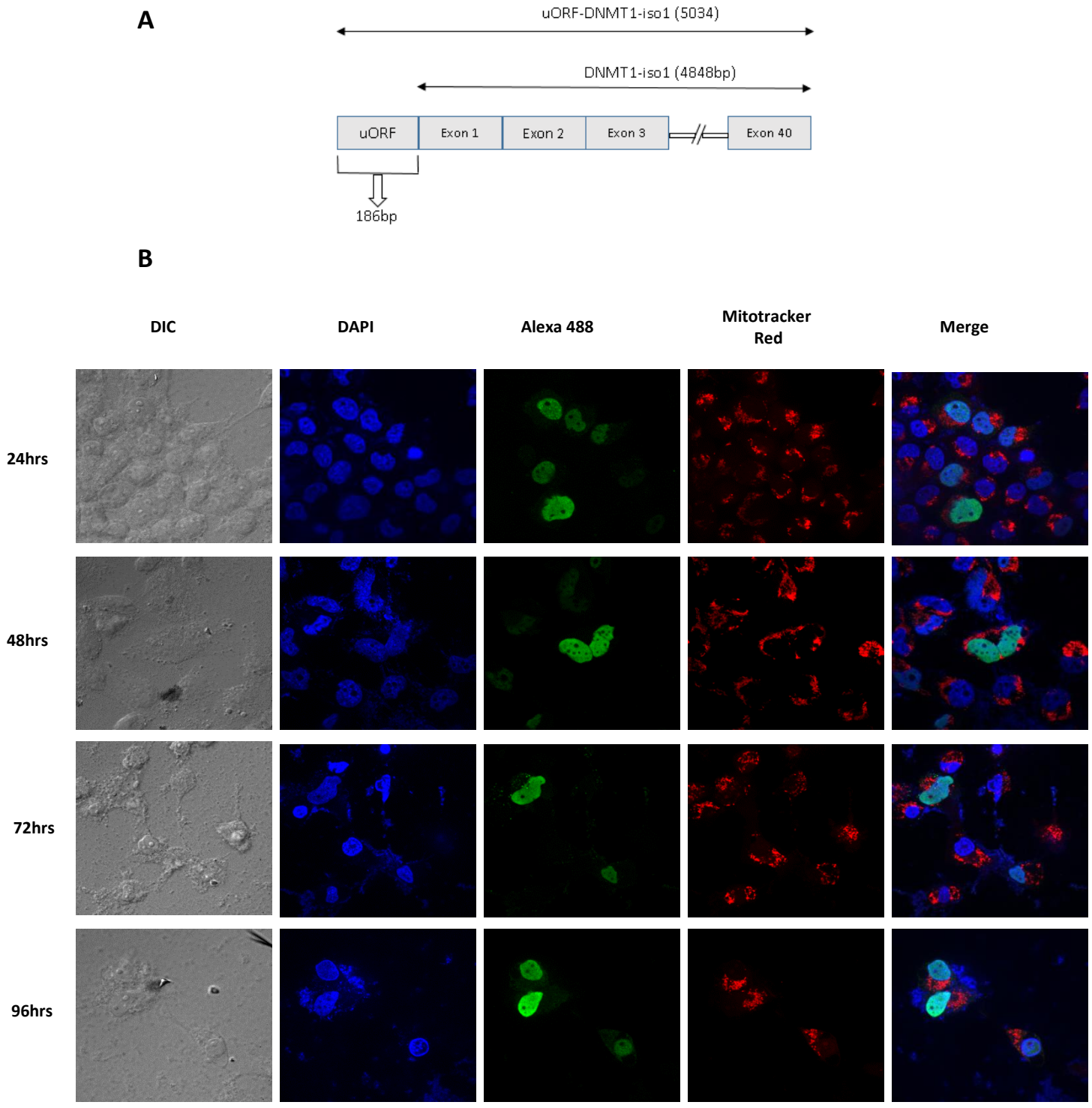

Figure 5.9: (A) Schematic diagram depicting uORF-DNMT1-iso1 structure. (B) Representative confocal images of H1299 cells showing localization pattern of exogenously overexpressed uORF-DNMT1-iso1 at different time intervals (24 to 96 hrs).

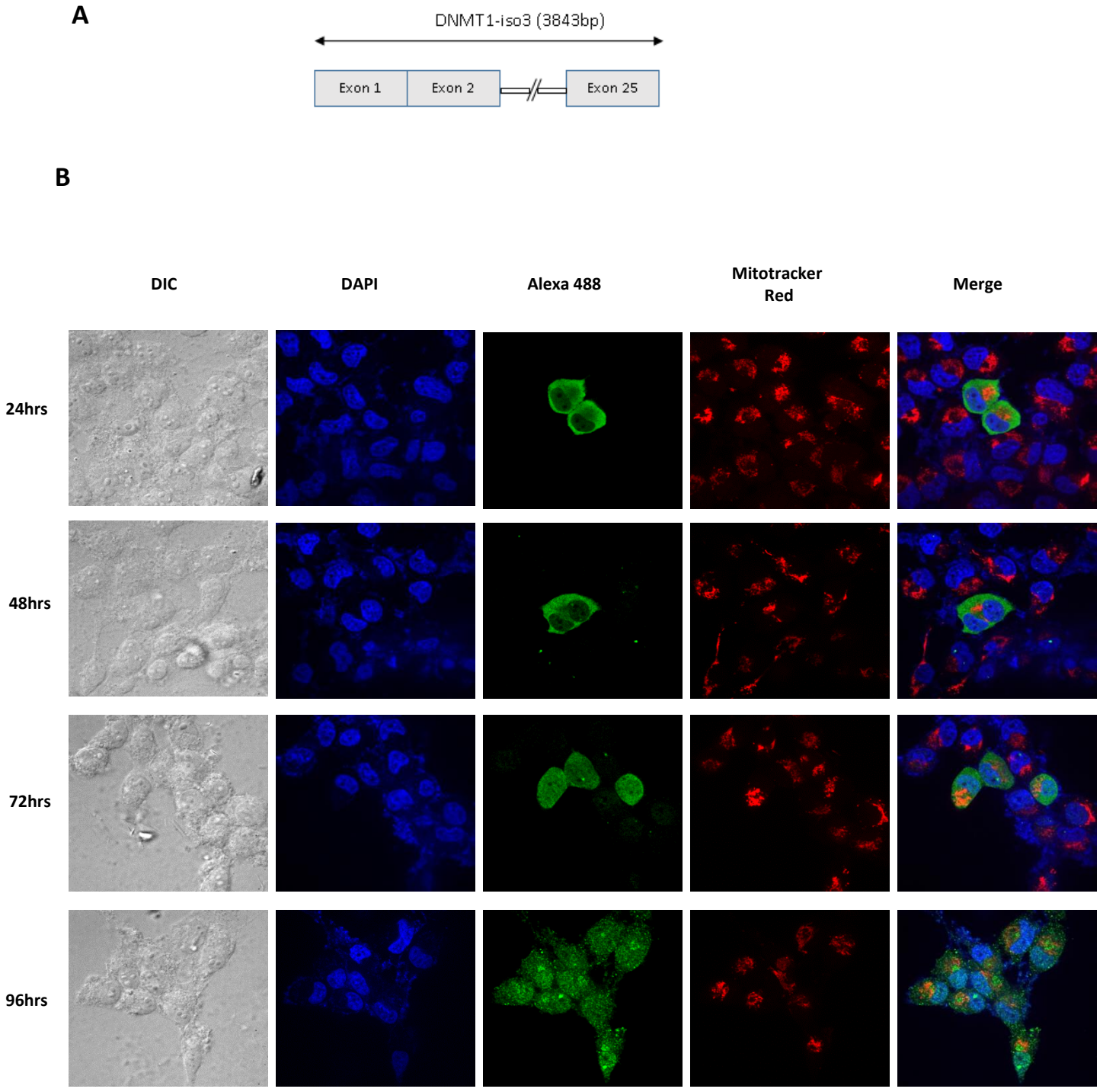

Figure 5.10: (A) Schematic diagram depicting DNMT1-iso3 structure. (B) Representative confocal images of H1299 cells showing localization pattern of exogenously overexpressed DNMT1-iso3 at different time intervals (24 to 96 hrs).

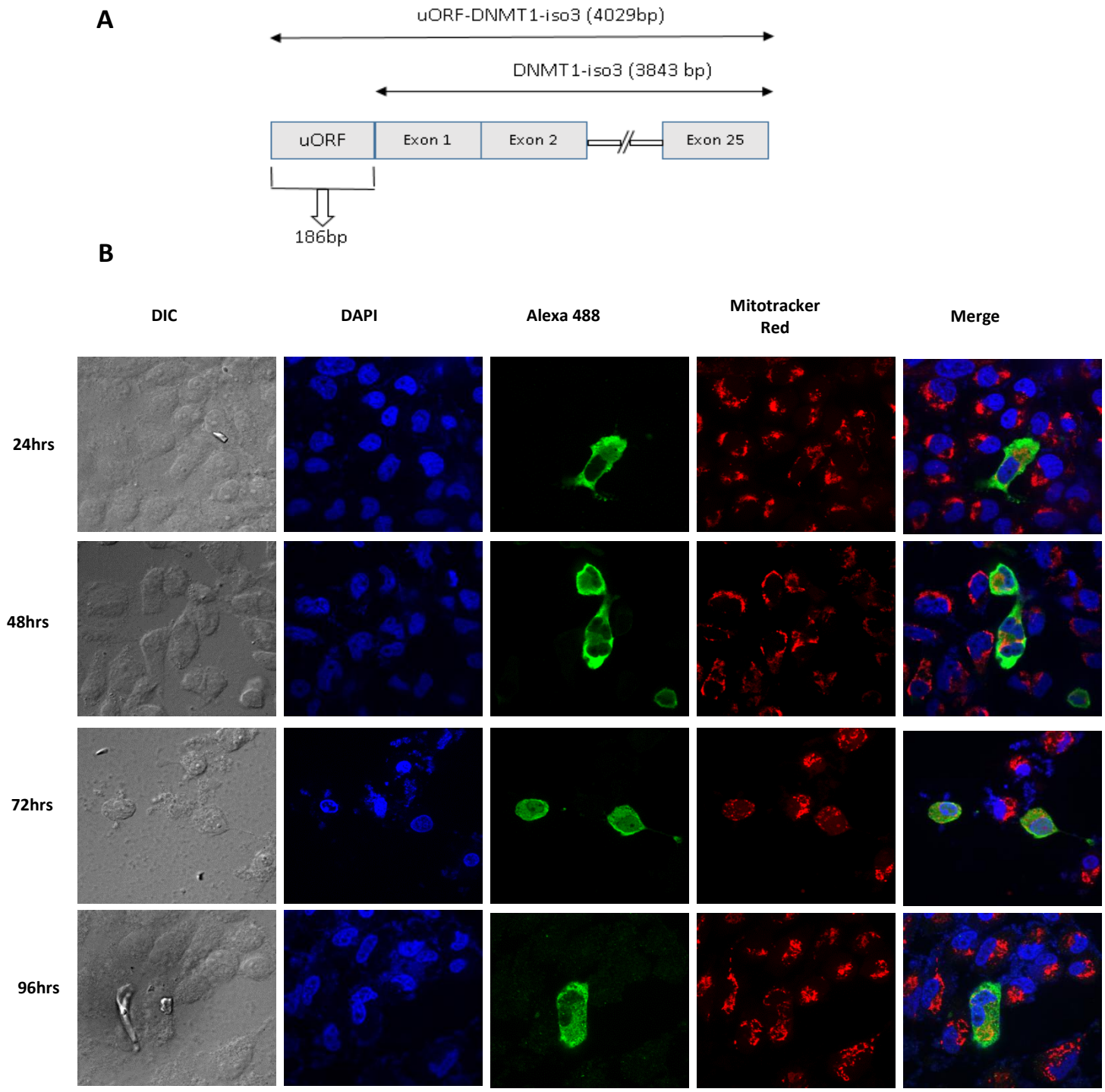

Figure 5.11: (A) Schematic diagram depicting uORF-DNMT1-iso3 structure. (B) Representative confocal images of H1299 cells showing localization pattern of exogenously overexpressed uORF-DNMT1-iso3 at different time intervals (24 to 96 hrs).

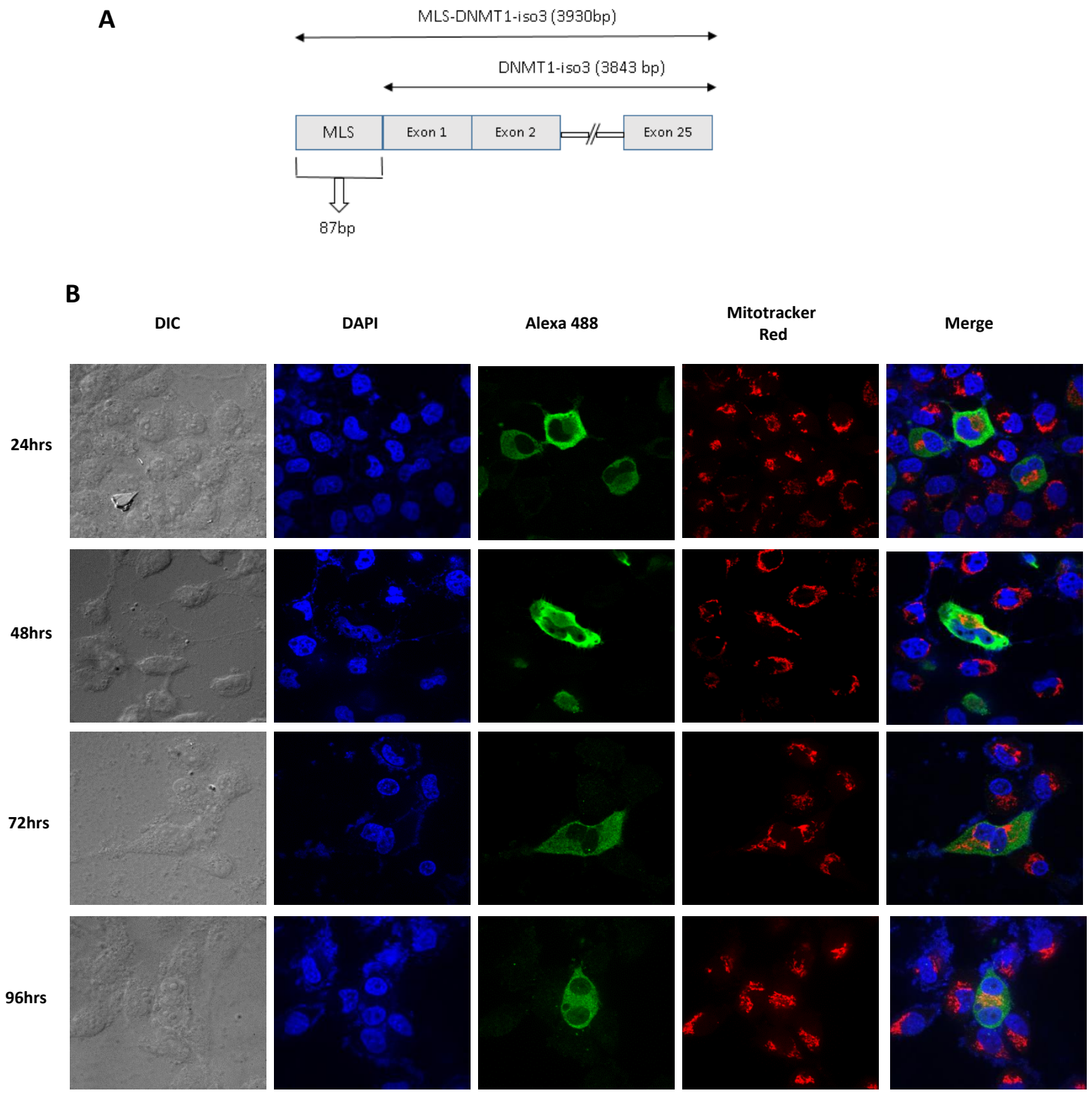

Figure 5. 12: Schematic diagram depicting MLS-DNMT1-iso3 structure. (B) Representative confocal images of H1299 cells showing localization pattern of exogenously overexpressed MLS-DNMT1-iso3 at different time intervals (24 to 96 hrs).

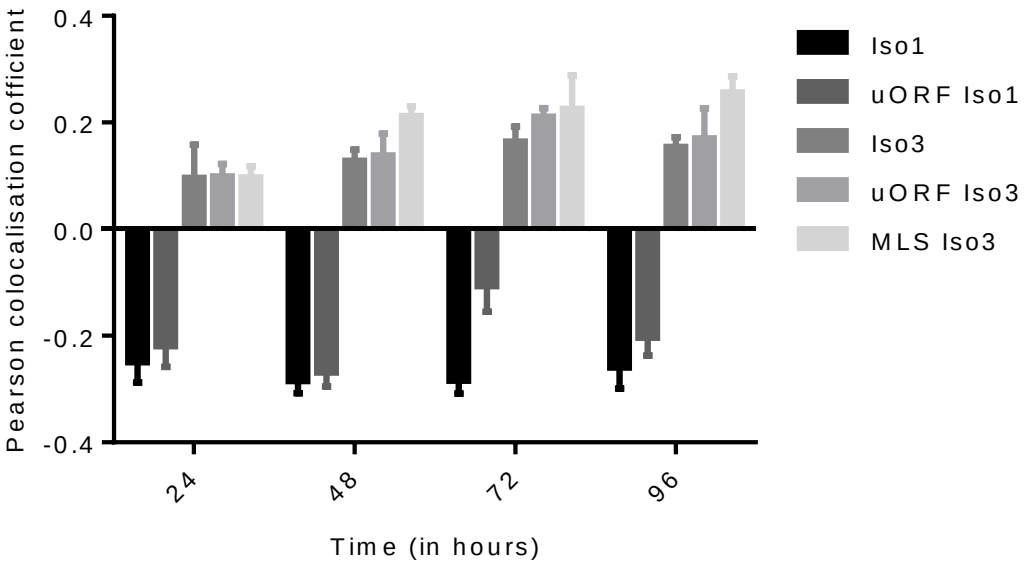

Figure 5.13: Subcellular localization of DNMT1-isoforms varies with advancing time period of expression. Pearson co-localisation coefficient for mitochondrial localization of DNMT1-iso1 and iso3 with additional upstream localization signal sequences.

5.5. Ectopic expression of DNMT1-isoform3 and validation of mitochondrial genome methylation

Next, we expedited if the ectopically expressed isoform3 present in mitochondria methylated its genome. DNMT1-isoform3 was stably overexpressed in H1299 cells and its localization was traced by staining with DNMT1 antibody (Figure. 5.14A); along with global mtDNA methylation analysis carried out by 5 methyl cytosine (5mC) antibody. In comparison to mock cells, the mitochondria of DNMT1-isoform3 overexpressing cells showed an increase in staining with 5mC (Figure. 5.14B).

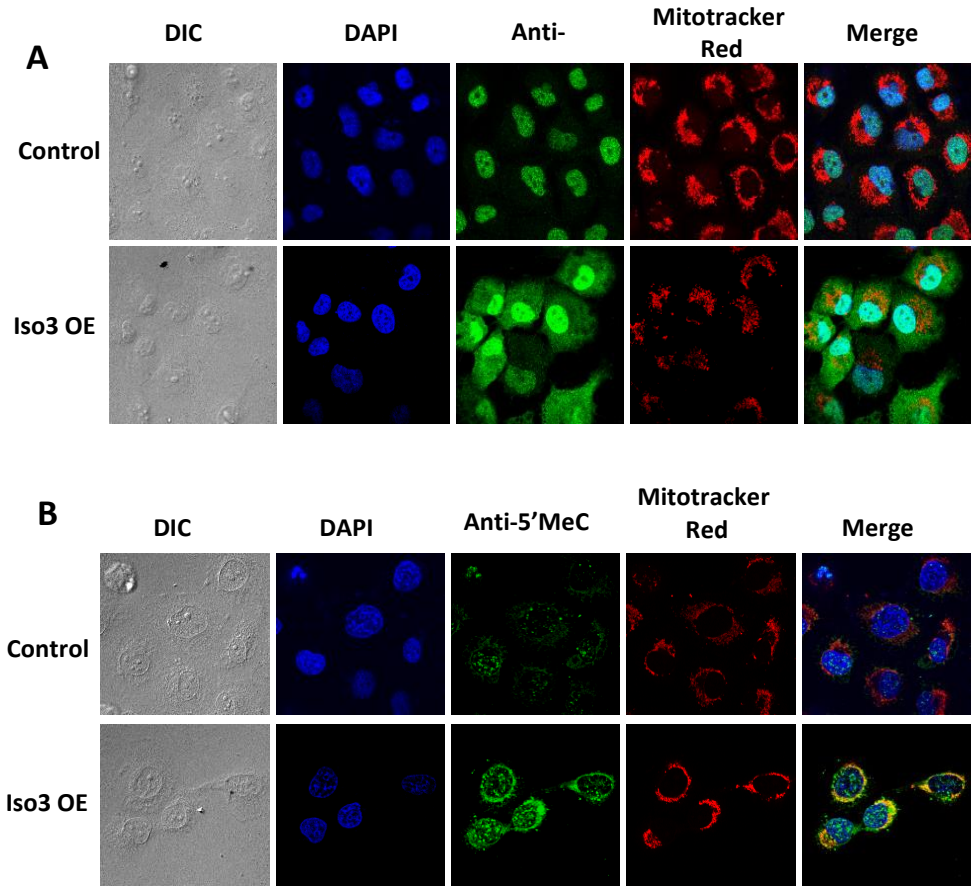

Figure 5.14: Overexpression of DNMT1-isoform3 causes hypermethylation of mitochondrial DNA. Representative confocal images of H1299 cells stably overexpressing DNMT1-iso3; (A) DNMT1 localisation pattern; (B) 5mC staining. Nucleus and mitochondria were stained with DAPI and Mitotracker red dyes respectively. Cells were stained with; DNMT1 antibody for localization, 5mC antibody for methylation analysis.

Once it was evident from the results that the DNMT1-isoform3 and not the isoform1, was localized to mitochondria and methylated mtDNA. For further confirmation and validation, six different CpG positions within the regulatory regions (TTF, LSO, MAS, HVR2, 12s, and 16s rRNA) of mitochondrial genome were screened and assessed for their methylation status on overexpression of both the isoforms in H1299 (Figure. 5.15A) and HCT116 (Figure. 5.15B) cells. All the studied positions, showed an increase in methylation levels only on overexpression of DNMT1-isoform3. There was no change observed in

methylation on the overexpression of DNMT1-isoform1 with uORF, in comparison to mock transfected. Among all these sites the maximum percentage of methylation was found on transcription termination factor (TTF) binding site. These results together suggested that it is the isoform3 and not the isoform1 that methylated CpG positions in mtDNA.

A. H1299

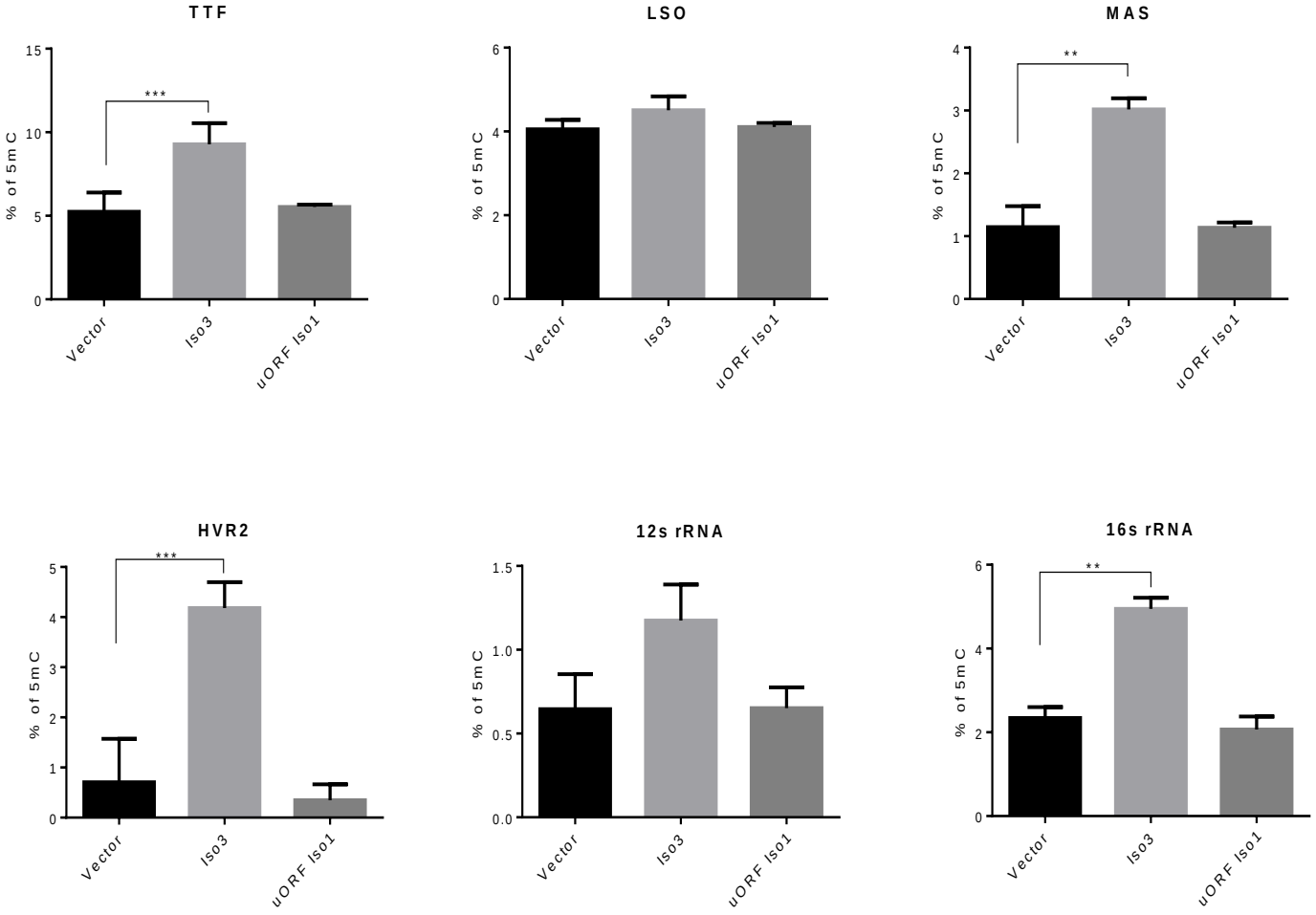

B. HCT116

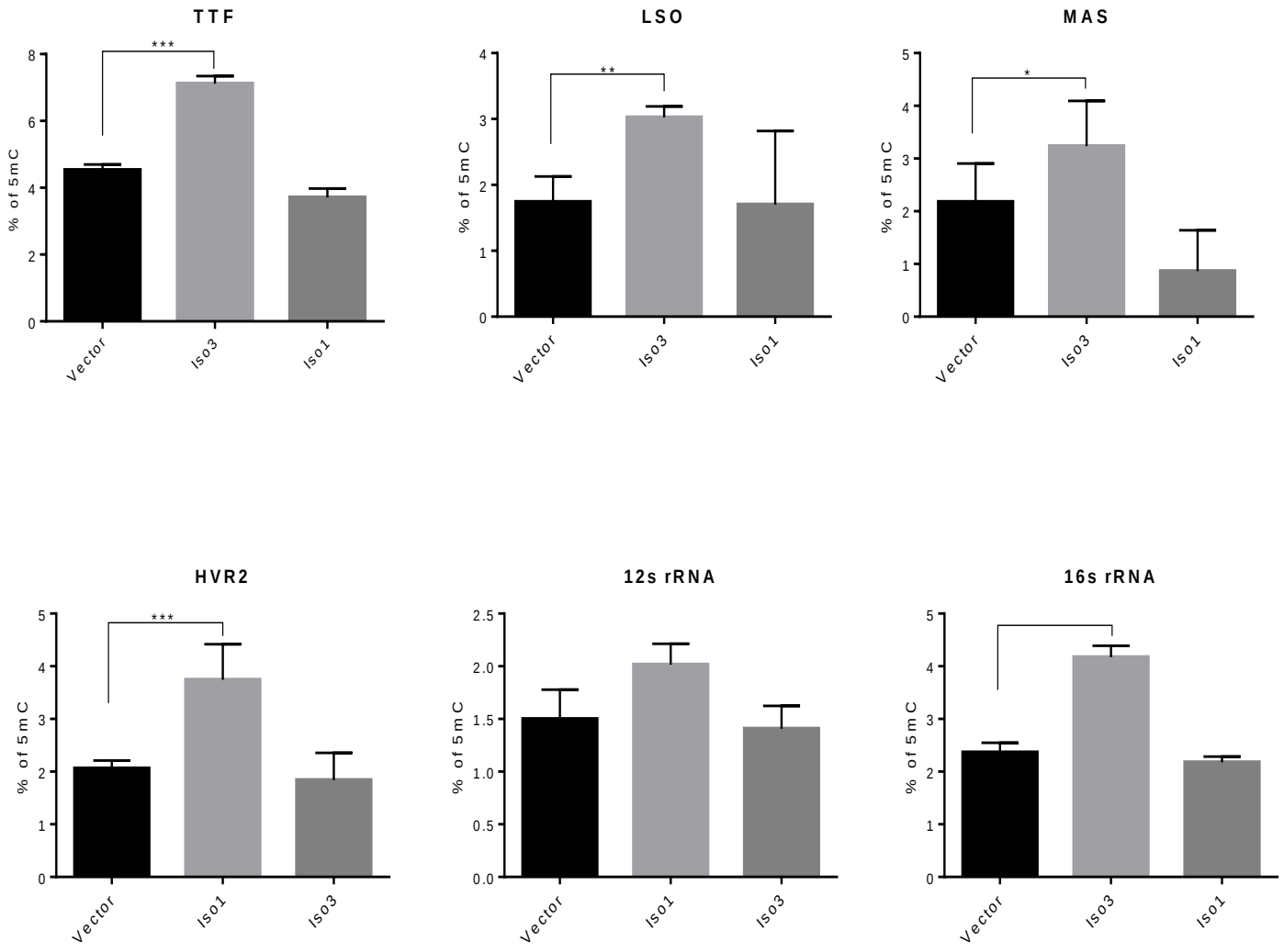

Figure 5.15: Overexpression of DNMT1-isoform3 causes methylation of mitochondrial DNA at CpG positions. % of 5mC at defined (TTF, LSO, MAS, HVR2, 12s rRNA & 16s rRNA) CpG sites of mitochondrial genome resulting from overexpression of DNMT1-iso3/ DNMT1-iso1 with uORF in (A) H1299 and (B) HCT116 cells.

For final confirmation and validation, the binding of DNMT1-isoform3 on mitochondrial DNA was checked by CHIP assay. All the regions screened (TTF, LSO, MAS, HVR2, 12s rRNA, 16s rRNA, CO1, ND3, ND6 and ATP6) within the mitochondrial genome, which included the 6 hypermethylated sites (shown in previous figure 5.15) as well, showed a significant increase in the enrichment of mtDNA fragments on overexpression of DNMT1-isoform3 (Figure. 5.16). It was observed that among all the analyzed region on mtDNA, the DNMT1 binding was more prominent at the regulatory regions such as: TTF, LSO, HVR2, 12s rRNA and 16s rRNA; while, at the gene regions such as: CO1, ND3, ND6 and ATP6, it was comparatively found to be less associated. The CHIP assay confirmed that DNMT1-isoform3 binds to mtDNA.

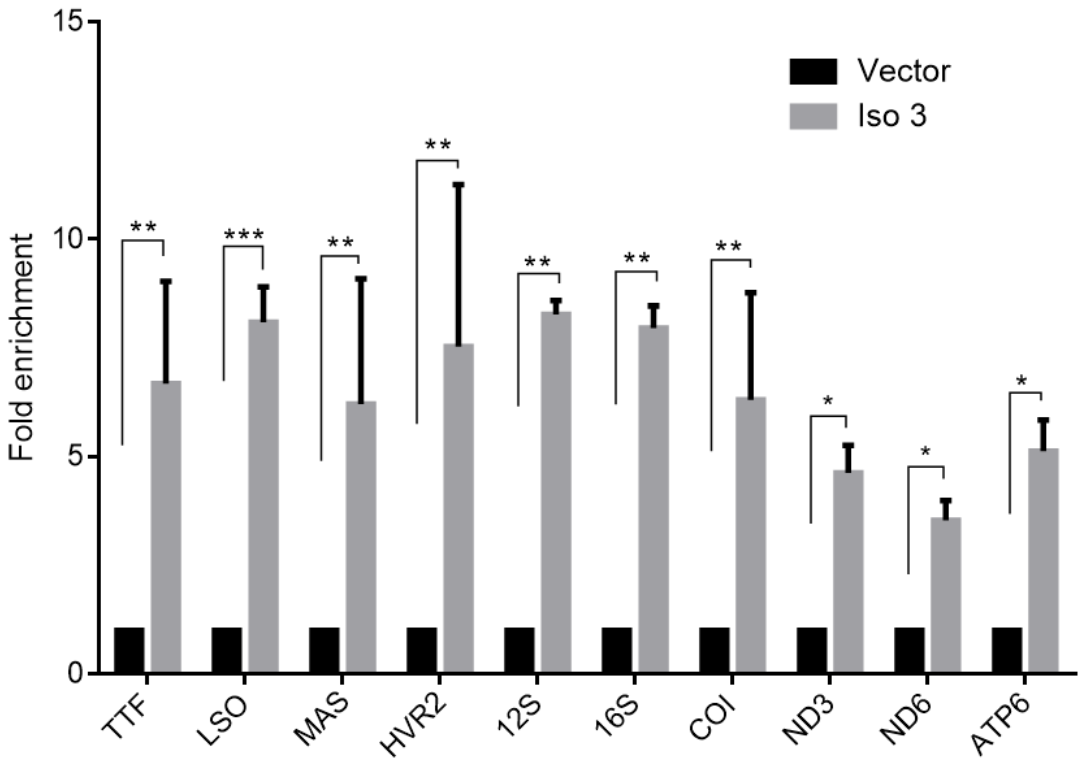

Figure 5.16: DNMT1-iso3 binds to mitochondrial DNA. Relative fold enrichment of selected (TTF, LSO, MAS, HVR2, 12s, 16s, COI, ND3, ND6 and ATP6) mitochondrial regions for DNMT1-isoform3 binding by CHIP analysis on overexpression of DNMT1-iso3 in H1299 cells.

5.6. Ectopic overexpression of DNMT1-isoform3 and its role in mitochondrial biology

As it became clear that it was only the isoform3 of DNMT1 that localized to mitochondria and methylated its genome; we sought to determine the role of this epigenetic process in the mitochondrial biology. The expression profile of mitochondrial genome encoded mitochondrial genes (ND3, ND6, CO1, ATP6, tRNAleu) and a set of nuclear genes involved in mitochondrial biogenesis (PGC1A, NRF1, NRF2, TFAM, TFB2M) was assessed, using real time qPCR analysis. A different pattern of expression was observed for these genes in H1299 and HCT116 cells. Isoform3 overexpressed H1299 cells exhibited more or less, a decrease in expression of mitochondrial genome encoded oxidative phosphorylation genes (Figure. 5.17A), whereas, the nuclear genome encoded mitochondrial biogenesis genes were found to be upregulated. However, in HCT116 cells (Figure. 5.17B), the tRNA leu and ATP6 genes were upregulated accompanied with nuclear genome encoded mitochondrial biogenesis genes. These results together suggested that the overexpression of DNMT1-isoform3 affects mitochondrial biology by modulating the expression of nuclear and mitochondrial genome encoded genes.

Since DNMT1-isoform3 overexpression differentially modulated the expression of nuclear and mitochondrial genome encoded biogenesis and structural genes. We performed flow cytometry experiments to assess mitochondrial membrane potential and mitochondrial mass by staining the cells with Mitotracker Red and Mitotracker Green dye respectively. There was a decrease in mitochondrial membrane potential (Figure. 5.18A) but a significant increase in mitochondrial mass (Figure. 5.18B) when DNMT1-isoform3 was overexpressed in both H1299 and HCT116 cells in comparison to the mock transfected.

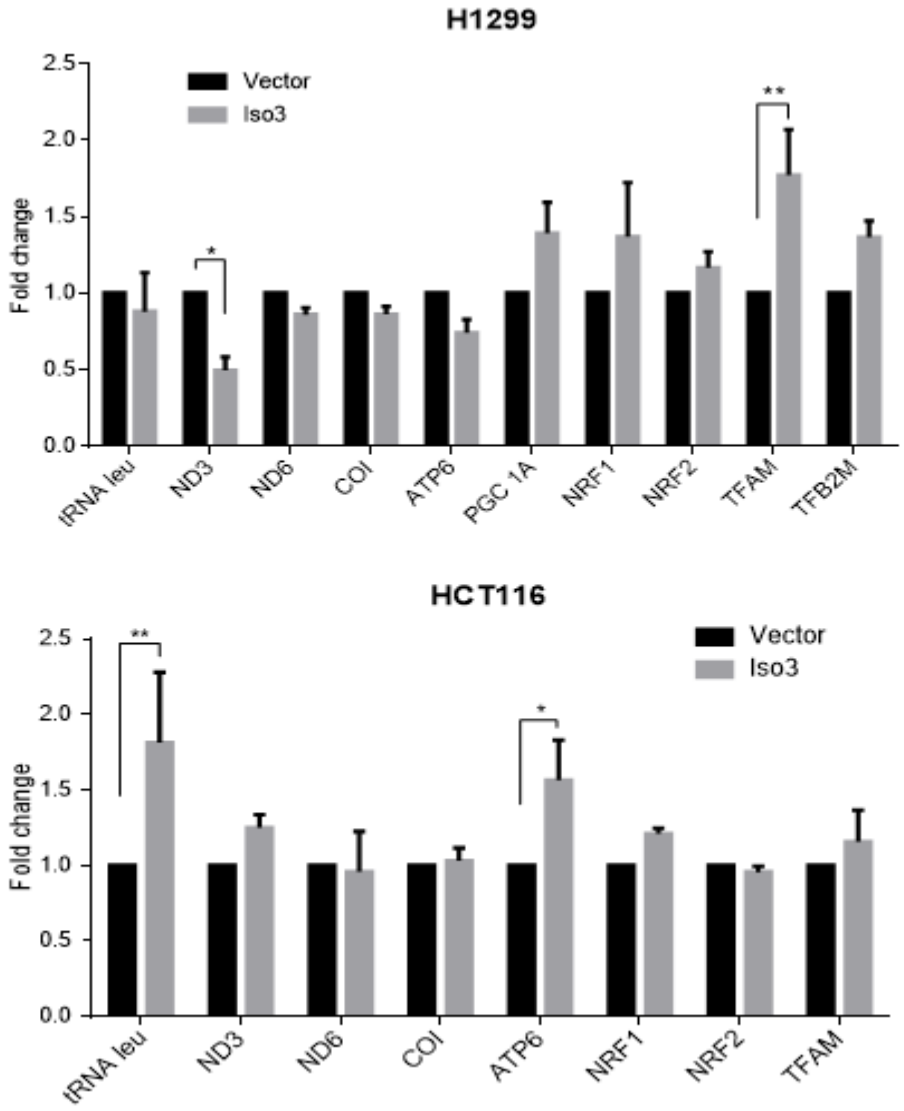

Figure 5.17: Exogenous overexpression of DNMT1-isoform3 modulates gene expression of mitochondrial genes.Semi quantitative gene expression profile of mitochondrial genome encoded OxPhos genes (ND3, ND6, COI and ATP6) and nuclear genome encoded mitochondrial biogenesis genes (PGC-1A, NRF1, NRF2, TFAM & TFB2M) on overexpression of DNMT1-Iso3 in (A) H1299 and (B) HCT116 cells.

Ai

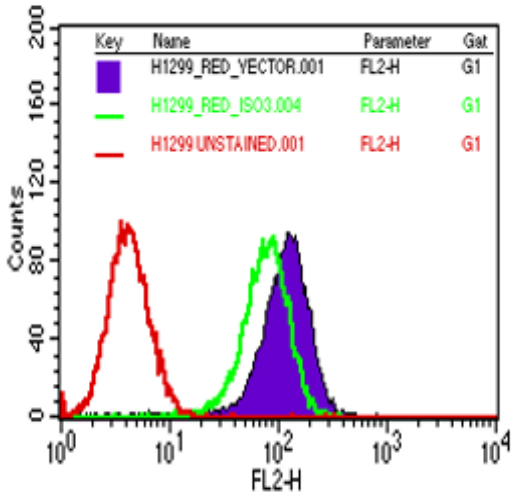
Key
Name
Parameter
Gat
H1299_RED_VECTOR.001
FL2-H
G1
H1299_RED_ISO3.004
FL2-H
G1
H1299 UNSTAINED.001
FL2-H
G1
Counts
FL2-H

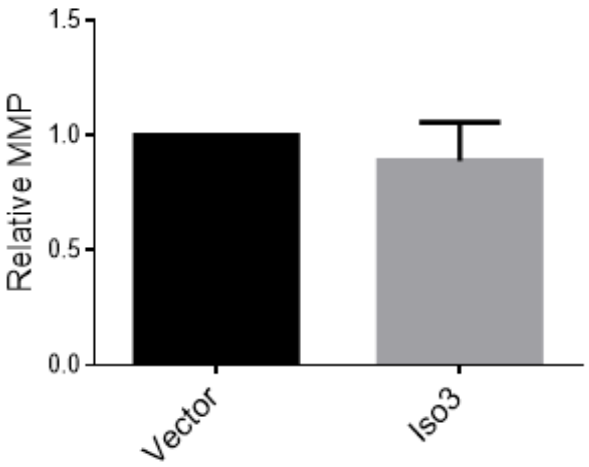
Relative MMP
1.5
1.0
0.5
0.0
Vector
Iso3

Aii

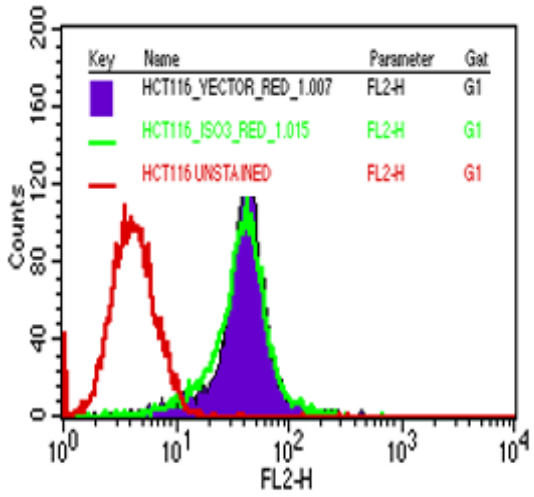
Key
Name
Parameter
Gat
HCT116_VECTOR_RED_1.007
FL2-H
G1
HCT116_ISO3_RED_1.015
FL2-H
G1
HCT116 UNSTAINED
FL2-H
G1
Counts
FL2-H

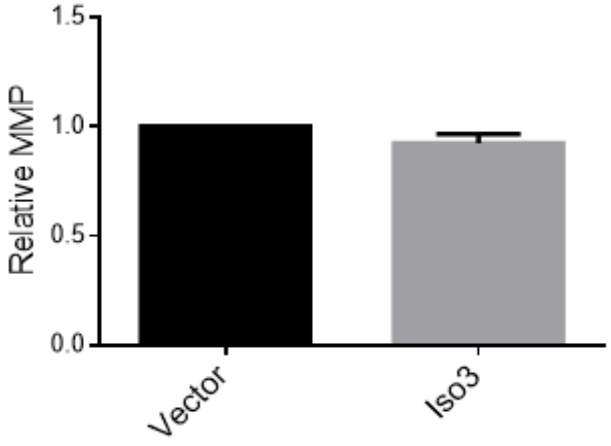
Relative MMP
1.5
1.0
0.5
0.0
Vector
Iso3

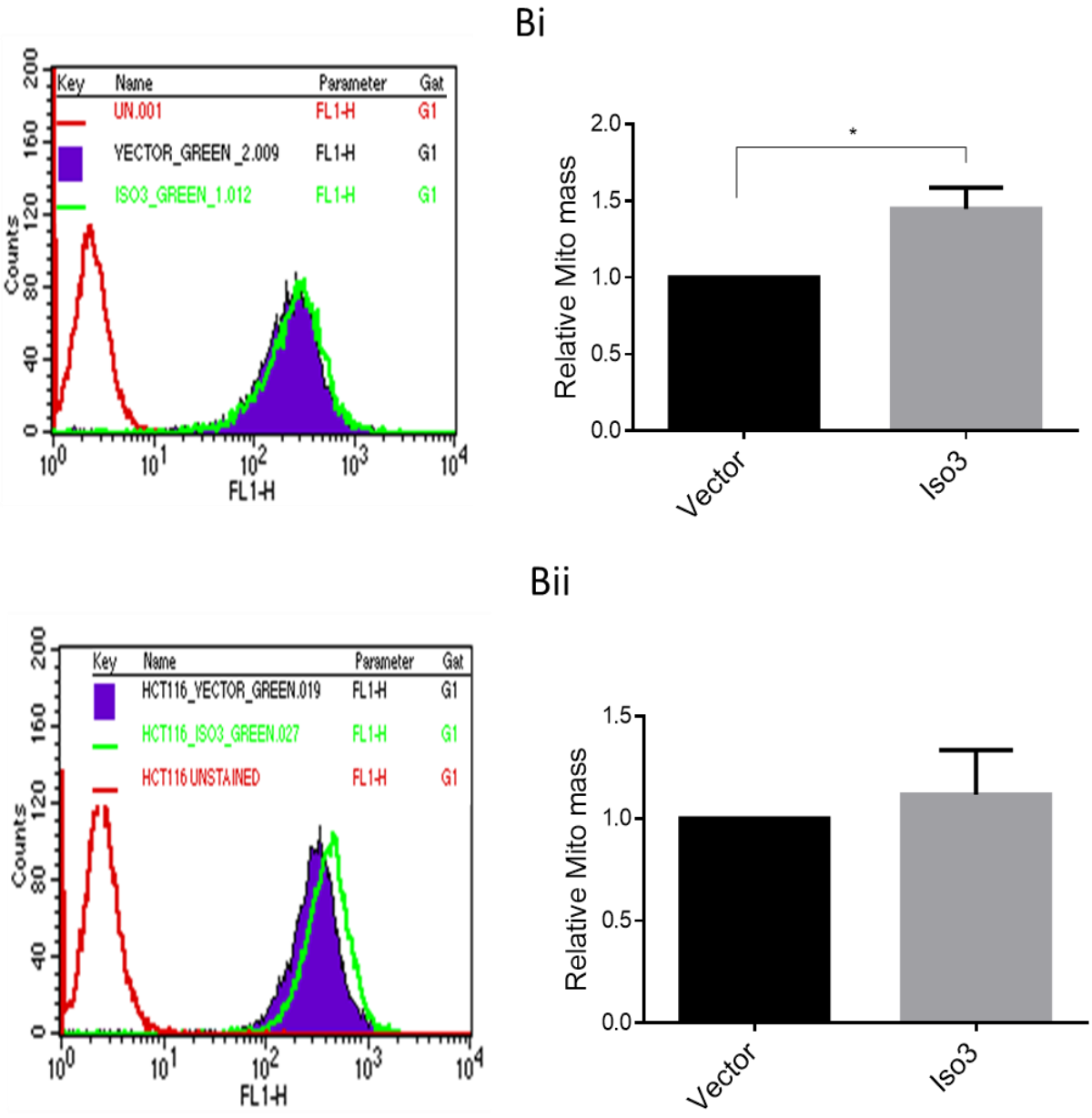

Figure 5.18: Exogenous overexpression of DNMT1-isoform3 affects mitochondrial membrane potential and mitochondrial mass. Representative screen shots and bar diagram of: (Ai) relative mitochondrial membrane potential in H1299 and (Aii) HCT116 cells; (Bi) relative mitochondrial mass in H1299 and (Bii) HCT116 cells on exogenous overexpression of DNMT1-isoform3 in H1299 cells.

5.7. MicroRNA targets key mitochondrial biogenesis genes-a bioinformatics analysis

The key mitochondrial biogenesis genes (PGC1A, NRF1, NRF2, TFAM and TFB2M) that were epigenetically upregulated on exogenous expression of DNMT1-isoform3, were explored bioinformatically for another mode of epigenetic regulation, i.e. microRNA mediated post-transcriptional gene silencing. The microRNA targeting these genes were predicted using four different target prediction programs (PICTAR, miRanda, PITA and TargetScan). These microRNAs were further refined for the potential candidate microRNAs targeting all of these genes, finding only one such candidate microRNA (hsa-miR-19b-2-5p) (Figure 5.19)

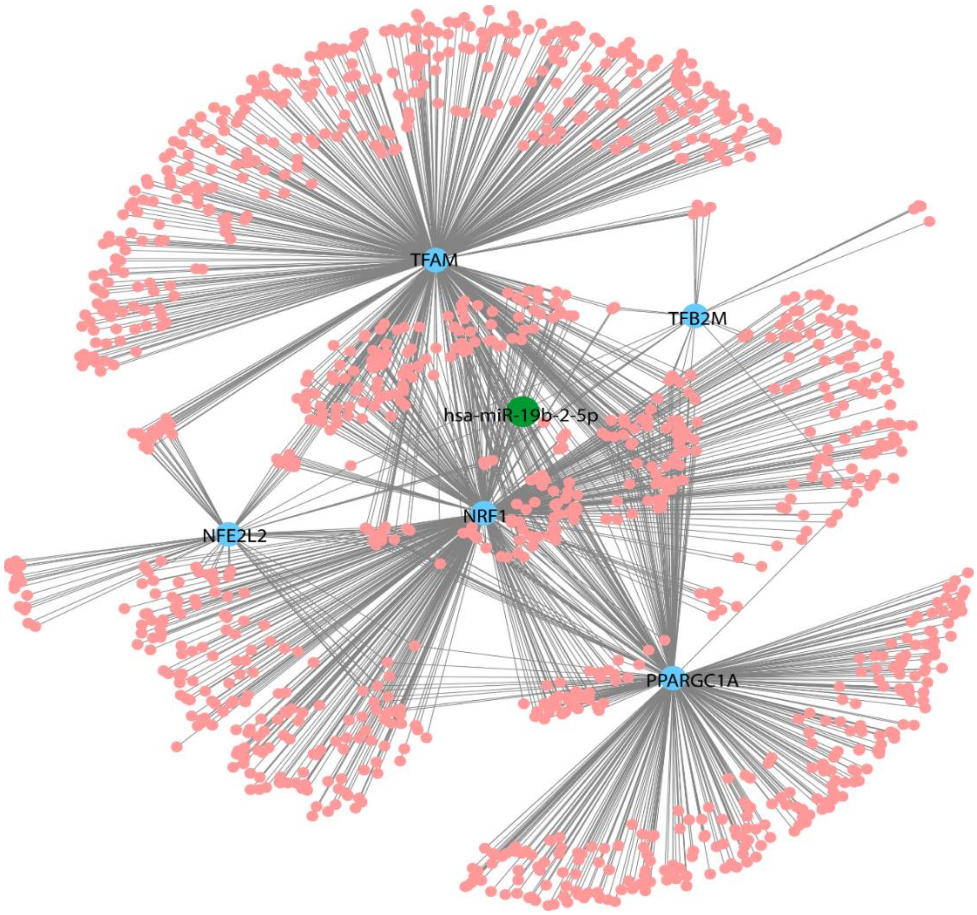

Figure 5.19: Gene-microRNA network interaction depicting the microRNA (hsa-miR-19b-2-5p) as a hub in the network, targeting all the 5 (PPARGC1A, NRF1, NFE2L2, TFAM and TFB2M) key genes involved in mitochondrial biogenesis.

The microRNA (hsa-miR-19b-2-5p) was assessed for its possible involvement in biological processes, molecular function and the regulation of cellular components. These were found to play a crucial physiological role in regulating the cellular and primary metabolic processes (Figure 5.20A). The molecular function analysis revealed their primary role in nucleic acid and organic/hetero cyclic compound binding properties (Figure 5.20B). The microRNA pathway enrichment analysis showed its involvement in folate-alcohol-cancer pathway, TSH signaling pathway, TGF beta signaling pathway, glioblastoma signaling pathway, mitochondrial gene expression, EGF-EGFR signaling pathway, SREBF and miR33 in cholesterol and lipid homeostasis (Figure 5.21A). Similarly, the disease association analysis revealed their involvement in synostosis, disturbance of amino acid transport, mesoblastic nephroma, genetic translocation, precocious puberty, nervous system diseases and learning disorders (Figure 5.21B).

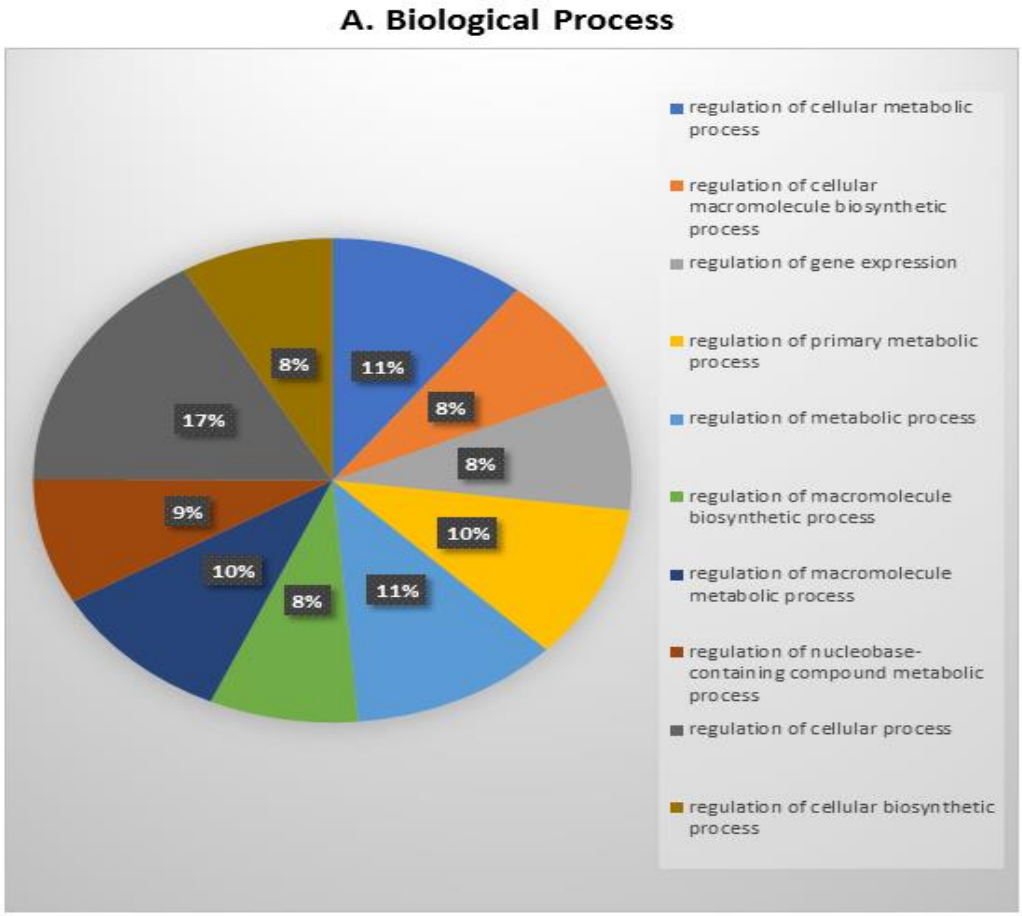

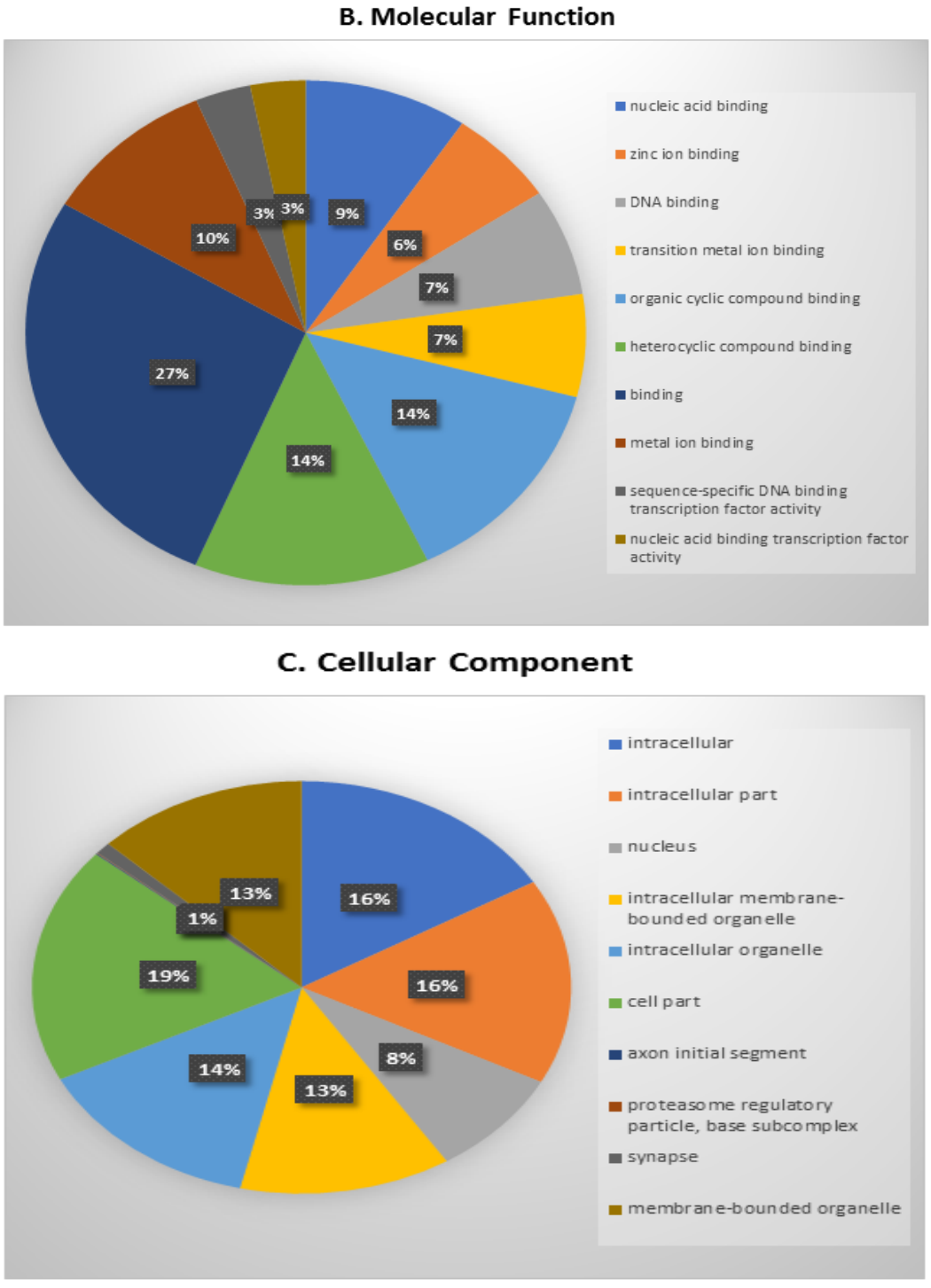

Figure 5.20: Functional annotation of miR-19b-2-5p targeted genes. The GO functional annotation is classified into three categories (A) Biological process, (B) molecular function (C) and the cellular components.

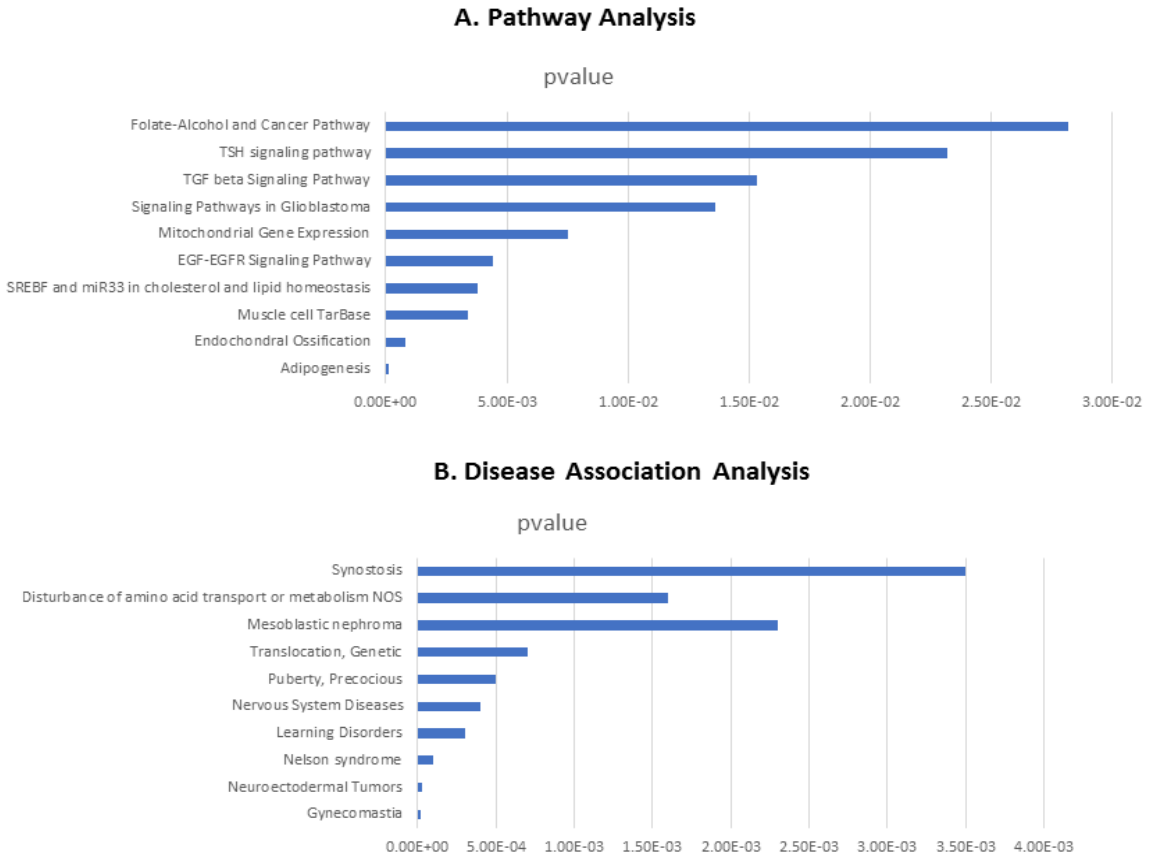

Figure 5.21: Representation of the possible predicted pathway involvement and the disease association analysis of hsa-miR-19b-2-5p, carried out using WEB-based GEne SeT AnaLysis Toolkit software (WebGestalt).

The microRNA was further investigated for its potential role in regulation of mitochondrial biology by targeting the entire set (1705) of nuclear coded mitochondrial proteins. All of these mitochondrial genes were assessed for their possible target prediction by mir-19b-2-5p, and a total of 112 genes were found to be targeted by this microRNA (Figure 5.22).

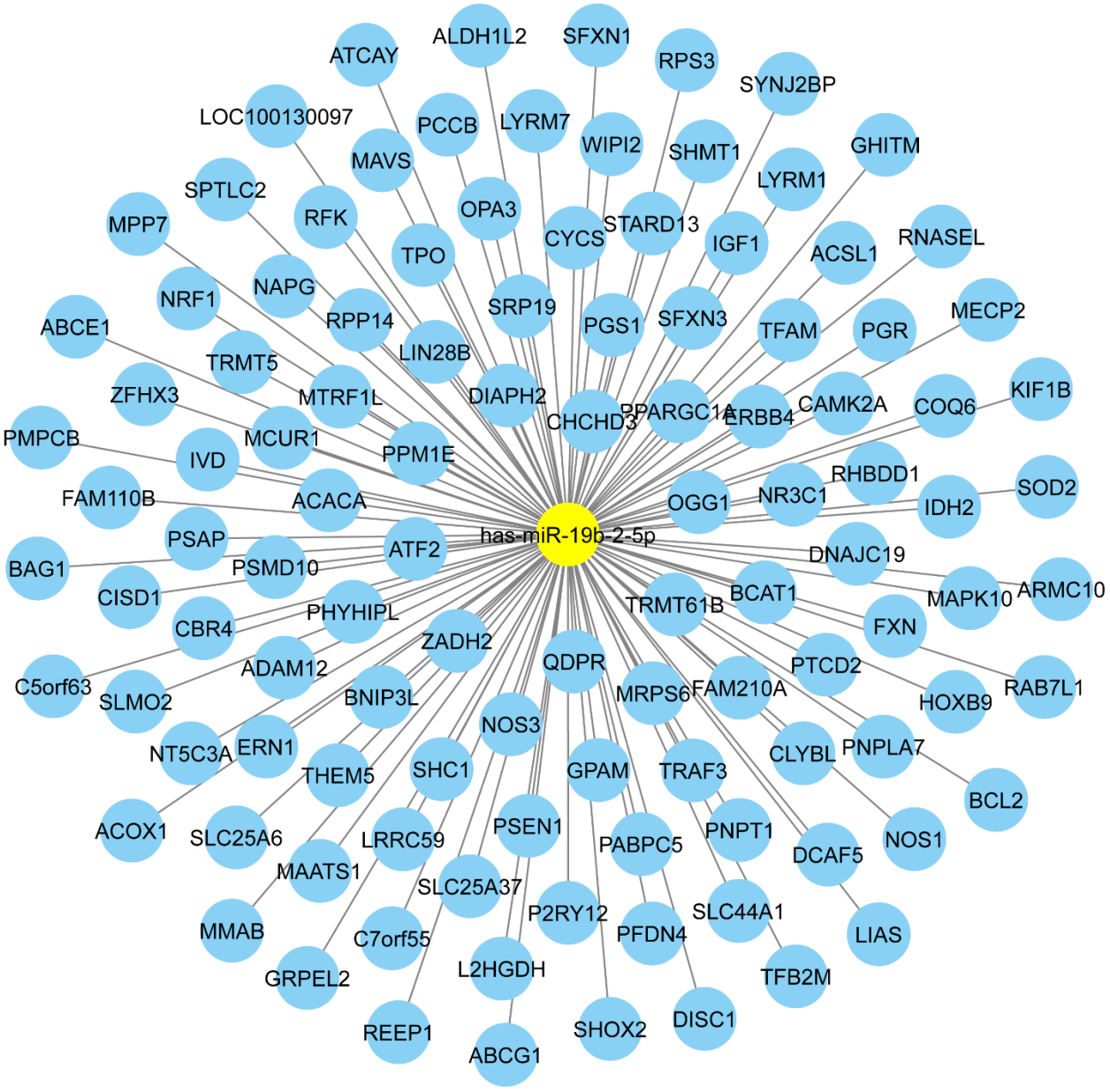

Figure 5.22: The schematic representation of hsa-miR-19b-2-5p sub-network. The network shows the miRNA target prediction results of hsa-miR-19b-2-5p. The targets, nuclear encoded mitochondrial genes show high interaction with hsa-miR-19b-2-5p, getting designated as a hub.

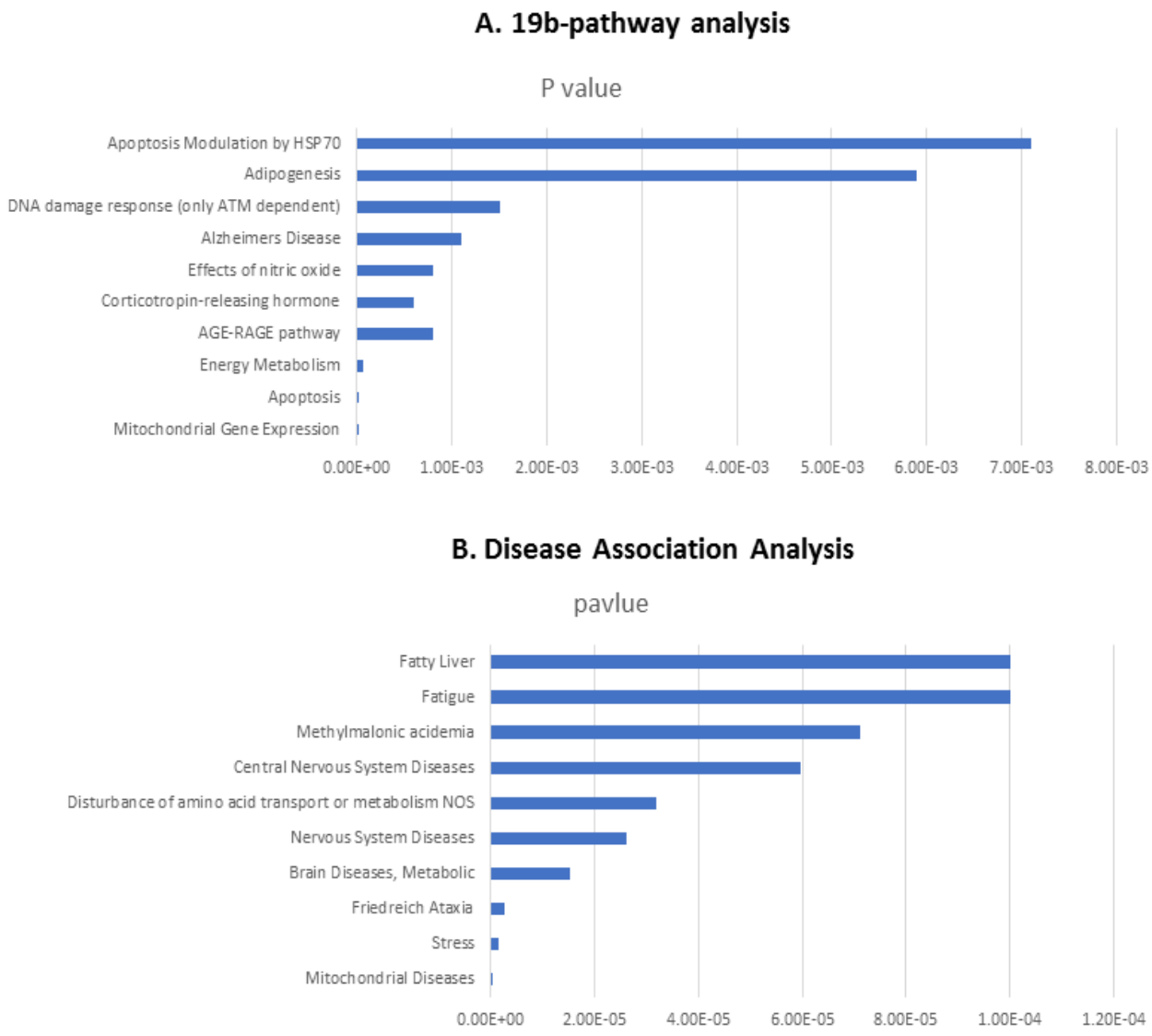

Figure 5.23: Representation of the predicted pathway involvement and the disease association analysis of hsa-miR-19b-2-5p, carried out using GEne SeT AnaLysis Toolkit software (WebGestalt).

These genes together were predicted for their possible involvement in different biological processes, molecular function and the cellular components (Appendix Figure. 1). The prediction program had suggested their involvement in the cellular component organization or biogenesis, cofactor metabolic process, small molecule metabolic process, generation of precursor metabolites/energy, and response to oxidative stress. The molecular function analysis revealed 55 of these genes to possess a catalytic activity and the remaining to act

as a cofactor or coenzymes, metal cluster, or with organic and heterocyclic compound binding properties. The pathway enrichment suggested their possible function in apoptotic modulation by HSP70, adipogenesis, DNA damage response, alzheimer's disease, effects of nitic oxide, corticotropin-releasing hormone and AGE-RAGE pathway (Figure 5.23A). Similarly, the disease association prediction program revealed their involvement in fatty liver disease, fatigue, methylmalonic acidemia, central nervous system disease, disturbance of amino acid transport, nervous system and brain metabolic diseases (Figure 5.23B).

6. DISCUSSION

DISCUSSION

Epigenetics generates phenotypic differences among different cell types even with same genotype. One of the ubiquitous epigenetic modification that takes place is the methylation of cytosines in DNA. However, the presence of this epigenetic modification in mitochondria has remained elusive and debatable for several years.

The present study provides a direct experimental proof of an isoform of DNMT1 methylating mitochondrial genome and influencing mitochondrial biology. An earlier report had suggested that DNMT-isoform1, with upstream 186bp (uORF) sequence as a part of the transcript, had the potential to localize in mitochondria (Shock et al., 2011). The localization to the mitochondria was proposed to be possible due to the uORF shown to code for the region that acted as a mitochondrial localization signal sequence, enabling the reporter construct with GFP to translocate in mitochondria. Although, this upstream sequence was found to be a part of the transcript, however, after fusing this uORF to the main ORF of DNMT1 followed by its (N terminal extended DNMT1) exogenous expression, it failed to localize DNMT-isoform1 to mitochondria. Even DNMT1 cloned downstream to the strong mitochondrial localization signal (MLS) sequence, failed again to localize in mitochondria and translocated exclusively to the nucleus. Finding the N terminal region of DNMT1-isoform1 rich in arginine and lysine amino acid residues, known for their strong nuclear localization potential (Fagerlund et al., 2002), in all probability, prevented the localization of DNMT1-isoform1 to mitochondria. The obvious question as to how this basic epigenetic modification was happening in mitochondria, remained to be addressed.

Incidentally, we found another isoform of DNMT1, the DNMT1-isoform3 which localized to the mitochondria. Structural analysis revealed the absence of the nuclear localization signal sequences, because of the deleted portion of N-terminal region within this shortest isoform of DNMT1. In-silico localization prediction by psortII program found 8.7% of the isoform3 to localize in human mitochondria. Exogenously overexpressed DNMT1-isoform3 confirmed the localization of the same fraction within the mitochondria. However, with advancing time of its exogenous expression, a change in the pattern of

localization was observed for DNMT1 isoform3 between mitochondria and the nucleus. This isoform exclusively localized to mitochondria and cytosol during 24 to 48 hours of expression. However, towards later hours of expression, it localized in the nucleus and gradually established throughout the cell. After the addition of uORF sequence, the potential of localization of the isoform3 in mitochondria increased and at the same time its presence in the nucleus showed a decrease. Further addition of strong MLS sequence to isoform3 prevented its localization in the nucleus completely. DNMT1-isoform3, when exogenously overexpressed, showed a concomitant increase in methylation of the cytosine residues in the mitochondrial genome, which was evident from 5 methyl cytosine immunostaining within mitochondria.

With the emerging insights of methylation of mitochondrial genome, it was pertinent to identify the CpG positions within the mitochondrial genome that differed in its methylation status. For this to begin with, ten different human cancer cell lines (HeLa, MCF-7, MDAMB-231, A549, H1299, SiHa, LNCAP, PC3, HT29 and HCT116) representing five most prominent cancer types worldwide, were chosen and sequenced for whole mitochondrial genome to identify CpG positions. These cell lines are globally used as in-vitro experimental models for understanding cancer cell biology. Mitochondrial rCRS sequence (provided in appendix section) when compared, showed a total of 432 CpG sites overlapping with the profile observed in the lung carcinoma cell lines, H1299 and A549. Whereas, in both the breast cancer cell lines (MCF-7 and MDAMB-231), there was a common disruption of CpG position at 709 position. This variation incidentally along with the variation at 4833, 5108 in mtDNA is the deciding mutation for defining Haplogroup G (van Oven and Kayser, 2009); and the computational analysis has revealed that the variation (G709A) changes the eighth and ninth stem-loop structure of the 12s rRNA, showing an association with a non-syndromic inherited hearing loss (Wei et al., 2009). A study from the Iranian population found this polymorphism to provide a risk to the Behçet's disease (Xavier et al., 2011). A disruption of the CpG site at 3010 position with the variation of G>A in HCT 116 cell line was located within 16s rRNA gene and had been found to be more frequent in patients with diabetes than in controls in Finnish population (Soini et al., 2012). The polymorphism was also shown to be associated with migraine, childhood cyclic vomiting syndrome, irritable bowel syndrome (IBS) and gastrointestinal

(GI) disorder. The disruption of the CpG site at 16129 position within the D-loop segment in mtDNA of LNCAP cell line, known for the replication-termination-associated 15 bp nucleotide sequence, was suggested to arrest D-loop strand elongation during replication (Doda et al., 1981). The variation has recently been reported to show a higher expression level of tRNA glycine in individuals sharing this SNP (Cohen et al., 2016).

The identification of the CpG sites in the whole mitochondrial genome of the studied cell lines set a foundation to study which of these was methylated. Mitochondrial whole genome sequence carrying a total of 432 CpG positions were screened for the sequence "CCGG" (a recognition sequence for the pair of methyl sensitive restriction enzyme- MspI and HpaII) to target methylated sites and amplify using methyl sensitive restriction qPCR (MSRP). These CpG sites when analyzed in silico turned out to be 23 in number in whole mitochondrial genome (details provided in Table 4.3). Of these, 6 sites (TTF: transcription termination factor, LSO: L-stand origin of replication, MAS: membrane attachment site, HVR2: hypervariable region2, 12s rRNA, 16s rRNA) located in important regulatory regions involved in transcription and replication of mtDNA with a possible role in mitochondrial function, were chosen to assess their methylation status. Further confirmation for mitochondrial methylation initiated by overexpressed DNMT1-isoform3 was obtained by the binding of DNMT1-isoform3 with mtDNA through CHIP assay. DNMT1-isoform3 was found to bind to different regions within mtDNA, which included the chosen 6 important regulatory regions involved in transcription and replication of mtDNA (TTF, LSO, MAS, HVR2, 12s rRNA, 16s rRNA, CO1, ND3, ND6 and ATP6), showing hypermethylation at these sites.

The resultant effect of overexpression of DNMT1-isoform3 on the mitochondrial biology showed acute mitochondrial dysfunction, evident from the decrease in mitochondrial membrane potential and a decrease in the expression profile of mitochondrial genome encoded OXPHOS related genes (ND3, ND6, COI and ATP6). At the same time, an increase in the expression of nuclear genome encoded mitochondrial biogenesis genes (PGC-1α, NRF1 NFE2L2, TFAM and TFB2M) with a concomitant increase in mitochondrial mass was observed. Such a decrease in mitochondrial membrane potential and an increase in the mitochondrial mass has been proposed as a characteristic feature of

a mild stress condition of acute mitochondrial dysfunction, which is tolerated by cells and is believed to invoke an adaptive response to maintain cellular homeostasis (Chandel, 2014). An increase in the expression of nuclear genome encoded mitochondrial biogenesis genes (PGC-1α, NRF1, NRF2, TFAM and TFB2M) apparently indicated an adaptive response. However, the retrograde signaling that probably was responsible for signaling the resultant effect within the nucleus remains to be addressed. It is conjectured that Ca^{+2} signaling could be a potential candidate to look for, since mitochondrial dysfunction due to a decrease in mitochondrial membrane potential (dΨ) is known to prevent Ca^{+2} uptake, generating elevated Ca^{+2} levels, which in turn activate calcineurin. Activated calcineurin governs diverse cellular outcomes, resulting from transcription activation / repression of a large set of genes involved in mitochondrial biogenesis, cellular metabolism, cell survival, apoptosis and cytoskeletal organization (Solesio et al., 2016).

Further, under the conditions of nutritional and oxidative stress, the methylation at TTF site in mitochondrial genome was the highest amongst other analyzed sites. The TTF site located immediately downstream of the 3′ end of the 16s rRNA within the tRNALeu (UUR) gene is known to act as a binding site for mTERF, and shown to arrest in vitro mitochondrial RNA polymerase (mtRNAP) progression from Heavy Strand Promoter I (Rambold et al., 2011). Similarly, CpG site within the LSO region, a part of the template sequence 5'- GCCGG -3'located immediately adjacent to the stem loop structure and known to be essential for efficient replication (Kruse et al., 1989), was also hypomethylated, though not to the same extent as was observed for TTF site. Whereas, CpG position in MAS, the region of mitochondrial genome associated with the inner mitochondrial membrane (Welter et al., 1989), showed hypermethylation on glucose starvation; without showing a change under serum deprivation condition, unlike other studied sites which were hypomethylated. Reports of differential methylation of a few CpG positions have been reported earlier. Hypomethylation at two of the CpG sites of 12s rRNA gene were shown to correlate with ageing in humans (Mawlood et al., 2016a). The environmental conditions of a long term exposure to air borne pollutants was shown to be associated with mtDNA methylation at 12s rRNA and Phe-tRNA genes and the D-loop area (Byun et al., 2013b). Similarly, the CpG region in the D-loop area of mitochondrial genome was indicated with the existence of methylated cytosine (Bellizzi et al., 2013). An

attempt in the present work to understand the status of methylation prevailing under the conditions of nutritional and oxidative stress, known to influence the biology of mitochondria and resulting in a change in its structure and function, the cells in culture were treated with H2O2 and CoCl2 to study the influence of oxidative stress on mitochondrial genome methylation. While for nutritional stress, cells were starved for serum and glucose. Oxidative stress conditions have been shown in the past to persist both in normal and disease conditions (Baran and Konopleva, 2017; Corbet and Feron, 2017) (Swinson and O'Byrne, 2006) with a manifestation of imbalance between the systemic levels of reactive oxygen species and the biological system's ability to neutralize the reactive intermediates through antioxidant machinery. The levels of H2O2 have been shown to be increased under various pathophysiological conditions (Kumar et al., 2017; Nindl et al., 2004; Rovira-Llopis et al., 2017). CoCl2 is a chemical inducer that stabilizes HIF1α and mimics the responses generated due to hypoxic conditions (van Laarhoven et al., 2006). Similarly, nutrition is vital for survival and proliferation of cells; and starving the cells in culture for serum, results in a roadblock of growth factor mediated signaling pathways, eliciting the cellular outcomes of protein degradation, cellular stress response, autophagy, mitophagy and apoptosis (Bhutia et al., 2010; Jung et al., 2015; Li et al., 2015; Mukhopadhyay et al., 2016). The state of hypoglycemia also persists under several conditions including: the core of tumor such as insulinoma, kidney failure, liver disease, hypothyroidism, starvation, inborn error of metabolism, severe infections, reactive hypoglycemia, and in response to a number of drugs including alcohol (Li et al., 2015). In the present study, the mitochondrial genome was hypomethylated under the studied conditions of oxidative stress and nutritional stress; and it is suggested that the assessment of mtDNA methylation could be an important tool for the prognosis of diseases which involve mitochondria.

The key mitochondrial biogenesis genes (PGC1A, NRF1, NRF2, TFAM and TFB2M) that were epigenetically upregulated on exogenous expression of DNMT1-isoform3 were further explored bioinformatically for another mode of epigenetic regulation, i.e. microRNA mediated post-transcriptional gene silencing. It was interesting to observe that a microRNA (hsa-miR-19b-2-5p), which targeted 112 nuclear coded mitochondrial genes, regulated all the five genes involved in mitochondrial biogenesis. PGC1A is a

transcriptional coactivator that is a central regulator of metabolism and known as a primary inducer of mitochondrial biogenesis (Austin and St-Pierre, 2012). NRF1, along with NRF2, is responsible for the coordination between nuclear and mitochondrial genomes by directly regulating the expression of a number of nuclear genome encoded ETC subunits, and indirectly regulating the three mitochondrial genome encoded COX subunit genes by transcriptional activation of TFAM, TFB1M, and TFB2M (Biswas and Chan, 2010). TFAM and TFB2M are the two transcriptional initiation factor helping in the recruitment of the POLRMT (mitochondrial RNA polymerase) and the melting of the promoter (Ramachandran et al., 2017). The other important genes targeted by this microRNA included: SOD2, BCL2, IGF1, OPA3, NOS1 and NOS3. As expected, the microRNA (hsa-miR-19b-2-5p) was predicted to play a crucial physiological role in regulating different biological processes including the cellular and primary metabolic process. The molecular function analysis revealed their possible involvement in binding with nucleic acid and organic/hetero cyclic compounds. The pathway enrichment analysis showed this microRNA to participate in several important metabolic pathway suggesting that this microRNA could be a key regulator of the cellular metabolism by regulating mitochondrial gene expression and biogenesis. Further, it would be interesting to study the expression of hsa-miR-19b-2-5p in metabolic disorders including cancer, diabetes; cardiovascular diseases and neurodegenerative disorders.

In summary, it was interesting to observe 13 positions in the mitochondrial genome of 10 different cancer cell lines showing variation at CpG positions, indicating that some of the disrupted CpG sites would not be methylated in some populations or disease conditions containing these variations in the mitochondrial genome. The implications of downregulated DNMT1-isoform3 resulting in hypomethylation of mitochondrial CpG sites in general under various nutritional and oxidative stress conditions, need to be studied in the context of mitochondrial and cellular homeostasis. Interestingly, in this study it was established clearly that the isoform3 of DNMT1 instead of isoform1 localized in mitochondria; the overexpression of which resulted in mitochondrial methylation and mitochondrial dysfunction, evident from decreased mitochondrial membrane potential and expression profile of mitochondrial genome encoded oxidative phosphorylation genes (Figure 6.1). A simultaneous increase in the expression of nuclear genome encoded

mitochondrial biogenesis genes as well as an increase in mitochondrial mass, is proposed to be an epigenetically modulated adaptive response to the acute mitochondrial dysfunction via upregulation of mitochondrial biogenesis genes to maintain homeostasis, which requires a detailed study in future in this direction.

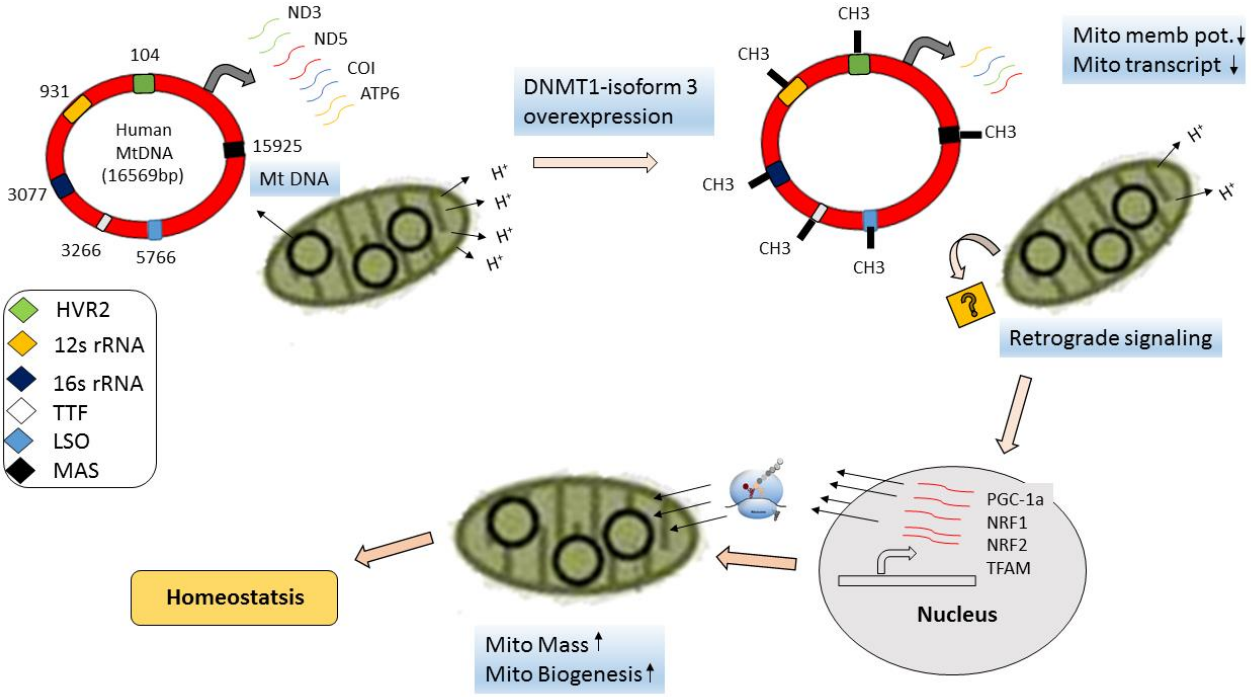

Figure 6.1: The proposed model depicting DNMT1-isoform3 function in mitochondrial biology.

7. REFERENCES

REFERENCES

1. Aloni, Y., and Attardi, G. (1971). Symmetrical in vivo transcription of mitochondrial DNA in HeLa cells. Proceedings of the National Academy of Sciences *68*, 1757-1761.
2. Anders, G., Mackowiak, S.D., Jens, M., Maaskola, J., Kuntzagk, A., Rajewsky, N., Landthaler, M., and Dieterich, C. (2012). doRiNA: a database of RNA interactions in post-transcriptional regulation. Nucleic acids research *40*, D180-186.
3. Anderson, S., Bankier, A.T., Barrell, B.G., De Bruijn, M., Coulson, A.R., Drouin, J., Eperon, I., Nierlich, D., Roe, B.A., and Sanger, F. (1981a). Sequence and organization of the human mitochondrial genome.
4. Anderson, S., Bankier, A.T., Barrell, B.G., de Bruijn, M.H., Coulson, A.R., Drouin, J., Eperon, I.C., Nierlich, D.P., Roe, B.A., Sanger, F., *et al.* (1981b). Sequence and organization of the human mitochondrial genome. Nature *290*, 457-465.
5. Anderson, S., De Bruijn, M., Coulson, A., Eperon, I., Sanger, F., and Young, I. (1982). Complete sequence of bovine mitochondrial DNA conserved features of the mammalian mitochondrial genome. Journal of molecular biology *156*, 683-717.
6. Attardi, G., and Schatz, G. (1988). Biogenesis of mitochondria. Annual review of cell biology *4*, 289-331.
7. Austin, S., and St-Pierre, J. (2012). PGC1α and mitochondrial metabolism–emerging concepts and relevance in ageing and neurodegenerative disorders. J Cell Sci *125*, 4963-4971.
8. Baccarelli, A.A., and Byun, H.M. (2015). Platelet mitochondrial DNA methylation: a potential new marker of cardiovascular disease. Clinical epigenetics *7*, 44.
9. Bandiera, S., Mategot, R., Girard, M., Demongeot, J., and Henrion-Caude, A. (2013). MitomiRs delineating the intracellular localization of microRNAs at mitochondria. Free radical biology & medicine *64*, 12-19.
10. Baran, N., and Konopleva, M. (2017). Molecular Pathways: Hypoxia-activated prodrugs in cancer therapy. Clinical cancer research : an official journal of the American Association for Cancer Research.
11. Barrey, E., Saint-Auret, G., Bonnamy, B., Damas, D., Boyer, O., and Gidrol, X. (2011). Pre-microRNA and mature microRNA in human mitochondria. PloS one *6*, e20220.
12. Bartley, W., and Davies, R.E. (1954). Active transport of ions by sub-cellular particles. Biochem J *57*, 37-49.
13. Battelli, F., and Stern, L. (1912). Frgeb Physiol *15*, 96-268.
14. Belitser, V.A., and Tsybakova, E.T. (1939). Biokhimiya *4*, 516-535.
15. Bellizzi, D., D'Aquila, P., Scafone, T., Giordano, M., Riso, V., Riccio, A., and Passarino, G. (2013). The control region of mitochondrial DNA shows an unusual CpG and non-CpG methylation pattern. DNA research : an international journal for rapid publication of reports on genes and genomes *20*, 537-547.
16. Bensley, R.R., and Hoerr, N.L. (1934). Studies on cell structure by the freezing-drying method VI. The preparation and properties of mitochondria. The Anatomical Record *60*, 449-455.
17. Bestwick, M.L., and Shadel, G.S. (2013). Accessorizing the human mitochondrial transcription machinery. Trends in biochemical sciences *38*, 283-291.

18. Betel, D., Koppal, A., Agius, P., Sander, C., and Leslie, C. (2010). Comprehensive modeling of microRNA targets predicts functional non-conserved and non-canonical sites. Genome biology *11*, R90.
19. Bhutia, S.K., Kegelman, T.P., Das, S.K., Azab, B., Su, Z.-z., Lee, S.-G., Sarkar, D., and Fisher, P.B. (2010). Astrocyte elevated gene-1 induces protective autophagy. Proceedings of the National Academy of Sciences *107*, 22243-22248.
20. Biswas, G., Adebanjo, O.A., Freedman, B.D., Anandatheerthavarada, H.K., Vijayasarathy, C., Zaidi, M., Kotlikoff, M., and Avadhani, N.G. (1999). Retrograde Ca2+ signaling in C2C12 skeletal myocytes in response to mitochondrial genetic and metabolic stress: a novel mode of inter-organelle crosstalk. The EMBO journal *18*, 522-533.
21. Biswas, M., and Chan, J.Y. (2010). Role of Nrf1 in antioxidant response element-mediated gene expression and beyond. Toxicology and applied pharmacology *244*, 16-20.
22. Bogdanovic, O., and Veenstra, G.J. (2009). DNA methylation and methyl-CpG binding proteins: developmental requirements and function. Chromosoma *118*, 549-565.
23. Bonfini, L., and Karlovich, C.A. (1992). The Son of sevenless gene product: a putative activator of Ras. Science *255*, 603.
24. Booker, L.M., Habermacher, G.M., Jessie, B.C., Sun, Q.C., Baumann, A.K., Amin, M., Lim, S.D., Fernandez-Golarz, C., Lyles, R.H., Brown, M.D., *et al.* (2006). North American white mitochondrial haplogroups in prostate and renal cancer. J Urol *175*, 468-472; discussion 472-463.
25. Booton, R., and Lindsay, M.A. (2014). Emerging role of MicroRNAs and long noncoding RNAs in respiratory disease. Chest *146*, 193-204.
26. Brand, M.D. (2010). The sites and topology of mitochondrial superoxide production. Experimental gerontology *45*, 466-472.
27. Byun, H.-M., Panni, T., Motta, V., Hou, L., Nordio, F., Apostoli, P., Bertazzi, P.A., and Baccarelli, A.A. (2013a). Effects of airborne pollutants on mitochondrial DNA methylation. Particle and fibre toxicology *10*, 18.
28. Byun, H.M., Panni, T., Motta, V., Hou, L., Nordio, F., Apostoli, P., Bertazzi, P.A., and Baccarelli, A.A. (2013b). Effects of airborne pollutants on mitochondrial DNA methylation. Particle and fibre toxicology *10*, 18.
29. Calvo, S.E., Clauser, K.R., and Mootha, V.K. (2015). MitoCarta2. 0: an updated inventory of mammalian mitochondrial proteins. Nucleic acids research, gkv1003.
30. Carrer, M., Liu, N., Grueter, C.E., Williams, A.H., Frisard, M.I., Hulver, M.W., Bassel-Duby, R., and Olson, E.N. (2012). Control of mitochondrial metabolism and systemic energy homeostasis by microRNAs 378 and 378. Proceedings of the National Academy of Sciences *109*, 15330-15335.
31. Chan, D.C. (2012). Fusion and fission: interlinked processes critical for mitochondrial health. Annual review of genetics *46*, 265-287.
32. Chandel, N., Maltepe, E., Goldwasser, E., Mathieu, C., Simon, M., and Schumacker, P. (1998). Mitochondrial reactive oxygen species trigger hypoxia-induced transcription. Proceedings of the National Academy of Sciences *95*, 11715-11720.
33. Chandel, N.S. (2014). Mitochondria as signaling organelles. BMC biology *12*, 34.
34. Chandel, N.S., McClintock, D.S., Feliciano, C.E., Wood, T.M., Melendez, J.A., Rodriguez, A.M., and Schumacker, P.T. (2000a). Reactive oxygen species generated

at mitochondrial complex III stabilize hypoxia-inducible factor-1α during hypoxia A MECHANISM OF O2 SENSING. Journal of Biological Chemistry *275*, 25130-25138.
35. Chandel, N.S., Schumacker, P.T., and Arch, R.H. (2001). Reactive oxygen species are downstream products of TRAF-mediated signal transduction. The Journal of biological chemistry *276*, 42728-42736.
36. Chandel, N.S., Trzyna, W.C., McClintock, D.S., and Schumacker, P.T. (2000b). Role of oxidants in NF-kappa B activation and TNF-alpha gene transcription induced by hypoxia and endotoxin. Journal of immunology *165*, 1013-1021.
37. Chen, Q., Lin, R.-Y., and Rubin, C.S. (1997). Organelle-specific Targeting of Protein Kinase AII (PKAII) MOLECULAR AND IN SITU CHARACTERIZATION OF MURINE A KINASE ANCHOR PROTEINS THAT RECRUIT REGULATORY SUBUNITS OF PKAII TO THE CYTOPLASMIC SURFACE OF MITOCHONDRIA. Journal of Biological Chemistry *272*, 15247-15257.
38. Clary, D.O., and Wolstenholme, D.R. (1985). The mitochondrial DNA molecule ofDrosophila yakuba: nucleotide sequence, gene organization, and genetic code. Journal of Molecular Evolution *22*, 252-271.
39. Cohen, T., Levin, L., and Mishmar, D. (2016). Ancient Out-of-Africa Mitochondrial DNA Variants Associate with Distinct Mitochondrial Gene Expression Patterns. PLoS genetics *12*, e1006407.
40. Collins, Y., Chouchani, E.T., James, A.M., Menger, K.E., Cochemé, H.M., and Murphy, M.P. (2012). Mitochondrial redox signaling at a glance. J Cell Sci *125*, 801-806.
41. Corbet, C., and Feron, O. (2017). Cancer cell metabolism and mitochondria: Nutrient plasticity for TCA cycle fueling. Biochimica et biophysica acta *1868*, 7-15.
42. Corneo, G., Moore, C., Sanadi, D.R., Grossman, L.I., and Marmur, J. (1966). Mitochondrial DNA in Yeast and Some Mammalian Species. Science *151*, 687-689.
43. Crane, R.K., and Sols, A. (1953). THE ASSOCIATION OF HEXOKINASE WITH PARTICULATE FRACTIONS OF BRAIN AND OTHER TISSUE HOMOGENATES. Journal of Biological Chemistry *203*, 273-292.
44. Cummings, D.J., McNally, K.L., Domenico, J.M., and Matsuura, E.T. (1990). The complete DNA sequence of the mitochondrial genome of Podospora anserina. Current genetics *17*, 375-402.
45. Dancy, B.M., Sedensky, M.M., and Morgan, P.G. (2014). Effects of the mitochondrial respiratory chain on longevity in C. elegans. Experimental gerontology *56*, 245-255.
46. Darvishi, K., Sharma, S., Bhat, A.K., Rai, E., and Bamezai, R.N. (2007). Mitochondrial DNA G10398A polymorphism imparts maternal Haplogroup N a risk for breast and esophageal cancer. Cancer letters *249*, 249-255.
47. Das, S., Bedja, D., Campbell, N., Dunkerly, B., and Chenna, V. (2014). miR-181c Regulates the Mitochondrial Genome. Bioenergetics, and Propensity for Heart.
48. Dasgupta, N., Peng, Y., Tan, Z., Ciraolo, G., Wang, D., and Li, R. (2015). miRNAs in mtDNA-less cell mitochondria. Cell death discovery *1*, 15004.
49. Dasgupta, S., Hoque, M.O., Upadhyay, S., and Sidransky, D. (2008). Mitochondrial cytochrome B gene mutation promotes tumor growth in bladder cancer. Cancer Res *68*, 700-706.
50. Davidson, S.M., Yellon, D.M., Murphy, M.P., and Duchen, M.R. (2012). Slow calcium waves and redox changes precede mitochondrial permeability transition pore opening

in the intact heart during hypoxia and reoxygenation. Cardiovascular research *93*, 445-453.
51. Dawid, I.B. (1974). 5-methylcytidylic acid: absence from mitochondrial DNA of frogs and HeLa cells. Science *184*, 80-81.
52. Dhillon, V.S., and Fenech, M. (2014). Mutations that affect mitochondrial functions and their association with neurodegenerative diseases. Mutat Res *759*, 1-13.
53. Doda, J.N., Wright, C.T., and Clayton, D.A. (1981). Elongation of displacement-loop strands in human and mouse mitochondrial DNA is arrested near specific template sequences. Proceedings of the National Academy of Sciences of the United States of America *78*, 6116-6120.
54. Durhuus, J.A., Desler, C., and Rasmussen, L.J. (2015). Mitochondria in health and disease - 3rd annual conference of society for mitochondrial research and medicine - 19-20 December 2013 - Bengaluru, India. Mitochondrion *20*, 7-12.
55. Elliott, H.R., Samuels, D.C., Eden, J.A., Relton, C.L., and Chinnery, P.F. (2008). Pathogenic mitochondrial DNA mutations are common in the general population. Am J Hum Genet *83*, 254-260.
56. Fagerlund, R., Melen, K., Kinnunen, L., and Julkunen, I. (2002). Arginine/lysine-rich nuclear localization signals mediate interactions between dimeric STATs and importin alpha 5. The Journal of biological chemistry *277*, 30072-30078.
57. Fan, X., Zhou, S., Zheng, M., Deng, X., Yi, Y., and Huang, T. (2017). MiR-199a-3p enhances breast cancer cell sensitivity to cisplatin by downregulating TFAM (TFAM). Biomedicine & Pharmacotherapy *88*, 507-514.
58. Feng, S., Jacobsen, S.E., and Reik, W. (2010). Epigenetic reprogramming in plant and animal development. Science *330*, 622-627.
59. Finnila, S., Hassinen, I.E., Ala-Kokko, L., and Majamaa, K. (2000). Phylogenetic network of the mtDNA haplogroup U in Northern Finland based on sequence analysis of the complete coding region by conformation-sensitive gel electrophoresis. American journal of human genetics *66*, 1017-1026.
60. Fogel, G.B., Kai, Z.S., Zargar, S., Hinton, A., Jones, G.A., Wong, A.S., Ficici, S.G., Lopez, A.D., and King, C.C. (2015). MicroRNA dynamics during human embryonic stem cell differentiation to pancreatic endoderm. Gene *574*, 359-370.
61. Friedkin, M., and Lehninger, A.L. (1948). PHOSPHORYLATION COUPLED TO ELECTRON TRANSPORT BETWEEN DIHYDRODIPHOSPHOPYRIDINE NUCLEOTIDE AND OXYGEN. Journal of Biological Chemistry *174*, 757-758.
62. Friedkin, M., and Lehninger, A.L. (1949). Esterification of inorganic phosphate coupled to electron transport between dihydrodiphosphopyridine nucleotide and oxygen. J Biol Chem *178*, 611-644.
63. Gao, J., Wen, S., Zhou, H., and Feng, S. (2015). De-methylation of displacement loop of mitochondrial DNA is associated with increased mitochondrial copy number and nicotinamide adenine dinucleotide subunit 2 expression in colorectal cancer. Molecular medicine reports *12*, 7033-7038.
64. Garcia, D.M., Baek, D., Shin, C., Bell, G.W., Grimson, A., and Bartel, D.P. (2011). Weak seed-pairing stability and high target-site abundance decrease the proficiency of lsy-6 and other microRNAs. Nature structural & molecular biology *18*, 1139-1146.

65. Gaudet, F., Hodgson, J.G., Eden, A., Jackson-Grusby, L., Dausman, J., Gray, J.W., Leonhardt, H., and Jaenisch, R. (2003). Induction of tumors in mice by genomic hypomethylation. Science *300*, 489-492.
66. Ghosh, S., Sengupta, S., and Scaria, V. (2014). Comparative analysis of human mitochondrial methylomes shows distinct patterns of epigenetic regulation in mitochondria. Mitochondrion *18*, 58-62.
67. Giampazolias, E., and Tait, S.W. (2016). Mitochondria and the hallmarks of cancer. FEBS J *283*, 803-814.
68. Gochhait, S., Bhatt, A., Sharma, S., Singh, Y.P., Gupta, P., and Bamezai, R.N. (2008). Concomitant presence of mutations in mitochondrial genome and p53 in cancer development - a study in north Indian sporadic breast and esophageal cancer patients. Int J Cancer *123*, 2580-2586.
69. Gomes, L.C., Di Benedetto, G., and Scorrano, L. (2011). During autophagy mitochondria elongate, are spared from degradation and sustain cell viability. Nature cell biology *13*, 589-598.
70. Gonzalo, S., Jaco, I., Fraga, M.F., Chen, T., Li, E., Esteller, M., and Blasco, M.A. (2006). DNA methyltransferases control telomere length and telomere recombination in mammalian cells. Nature cell biology *8*, 416-424.
71. Goyal, R., Reinhardt, R., and Jeltsch, A. (2006). Accuracy of DNA methylation pattern preservation by the Dnmt1 methyltransferase. Nucleic acids research *34*, 1182-1188.
72. Gray, M.W. (1982). Mitochondrial genome diversity and the evolution of mitochondrial DNA. Canadian journal of biochemistry *60*, 157-171.
73. Gray, M.W. (2015). Mosaic nature of the mitochondrial proteome: Implications for the origin and evolution of mitochondria. Proceedings of the National Academy of Sciences of the United States of America *112*, 10133-10138.
74. Gray, M.W., Burger, G., and Lang, B.F. (1999). Mitochondrial evolution. Science *283*, 1476-1481.
75. Groot, G.S., and Kroon, A.M. (1979). Mitochondrial DNA from various organisms does not contain internally methylated cytosine in -CCGG- sequences. Biochimica et biophysica acta *564*, 355-357.
76. Guay, C., and Regazzi, R. (2015). Role of islet microRNAs in diabetes: which model for which question? Diabetologia *58*, 456-463.
77. Guo, B., Zhai, D., Cabezas, E., Welsh, K., Nouraini, S., Satterthwait, A.C., and Reed, J.C. (2003). Humanin peptide suppresses apoptosis by interfering with Bax activation. Nature *423*, 456-461.
78. Han, J., and Sun, P. (2007). The pathways to tumor suppression via route p38. Trends in biochemical sciences *32*, 364-371.
79. Hansford, R.G. (1994). Physiological role of mitochondrial Ca2+ transport. Journal of bioenergetics and biomembranes *26*, 495-508.
80. Harada, H., Becknell, B., Wilm, M., Mann, M., Huang, L.J.-s., Taylor, S.S., Scott, J.D., and Korsmeyer, S.J. (1999). Phosphorylation and inactivation of BAD by mitochondria-anchored protein kinase A. Molecular cell *3*, 413-422.
81. Harman, D. (1956). Aging: a theory based on free radical and radiation chemistry. Journal of gerontology *11*, 298-300.
82. Hashimoto, Y., Niikura, T., Tajima, H., Yasukawa, T., Sudo, H., Ito, Y., Kita, Y., Kawasumi, M., Kouyama, K., Doyu, M., *et al.* (2001). A rescue factor abolishing

neuronal cell death by a wide spectrum of familial Alzheimer's disease genes and Abeta. Proceedings of the National Academy of Sciences of the United States of America *98*, 6336-6341.
83. Hayes, C.N., and Chayama, K. (2016). MicroRNAs as Biomarkers for Liver Disease and Hepatocellular Carcinoma. International journal of molecular sciences *17*, 280.
84. He, Y., and Ecker, J.R. (2015). Non-CG Methylation in the Human Genome. Annual review of genomics and human genetics *16*, 55-77.
85. Hekimi, S., Lapointe, J., and Wen, Y. (2011). Taking a "good" look at free radicals in the aging process. Trends in cell biology *21*, 569-576.
86. Herbert, E., and Potter, V.R. (1956). NUCLEOTIDE METABOLISM: VI. THE PHOSPHORYLATION OF 5'-CYTOSINE AND GUANINE NUCLEOTIDES BY CELL FRACTIONS FROM RAT LIVER. Journal of Biological Chemistry *222*, 453-467.
87. Hernandez-Toro, J., Prieto, C., and De las Rivas, J. (2007). APID2NET: unified interactome graphic analyzer. Bioinformatics *23*, 2495-2497.
88. Hong, E.E., Okitsu, C.Y., Smith, A.D., and Hsieh, C.L. (2013). Regionally specific and genome-wide analyses conclusively demonstrate the absence of CpG methylation in human mitochondrial DNA. Molecular and cellular biology *33*, 2683-2690.
89. Hoyer-Hansen, M., Bastholm, L., Szyniarowski, P., Campanella, M., Szabadkai, G., Farkas, T., Bianchi, K., Fehrenbacher, N., Elling, F., Rizzuto, R., *et al.* (2007). Control of macroautophagy by calcium, calmodulin-dependent kinase kinase-beta, and Bcl-2. Mol Cell *25*, 193-205.
90. Hsu, S.D., Tseng, Y.T., Shrestha, S., Lin, Y.L., Khaleel, A., Chou, C.H., Chu, C.F., Huang, H.Y., Lin, C.M., Ho, S.Y., *et al.* (2014). miRTarBase update 2014: an information resource for experimentally validated miRNA-target interactions. Nucleic acids research *42*, D78-85.
91. Hunter, F.E., and Hixon, W.S. (1949). ANAEROBIC PHOSPHORYLATION DUE TO THE DISMUTATION OF α-KETOGLUTARIC ACID IN THE PRESENCE OF AMMONIA. Journal of Biological Chemistry *181*, 67-71.
92. Illingworth, R.S., Gruenewald-Schneider, U., Webb, S., Kerr, A.R., James, K.D., Turner, D.J., Smith, C., Harrison, D.J., Andrews, R., and Bird, A.P. (2010). Orphan CpG islands identify numerous conserved promoters in the mammalian genome. PLoS genetics *6*, e1001134.
93. Infantino, V., Castegna, A., Iacobazzi, F., Spera, I., Scala, I., Andria, G., and Iacobazzi, V. (2011). Impairment of methyl cycle affects mitochondrial methyl availability and glutathione level in Down's syndrome. Molecular genetics and metabolism *102*, 378-382.
94. Janssen, B.G., Byun, H.M., Gyselaers, W., Lefebvre, W., Baccarelli, A.A., and Nawrot, T.S. (2015). Placental mitochondrial methylation and exposure to airborne particulate matter in the early life environment: An ENVIRONAGE birth cohort study. Epigenetics *10*, 536-544.
95. Jiangpan, P., Qingsheng, M., Zhiwen, Y., and Tao, Z. (2016). Emerging Role of microRNA in Neuropathic Pain. Current drug metabolism *17*, 336-344.
96. Jin, S.M., Lazarou, M., Wang, C., Kane, L.A., Narendra, D.P., and Youle, R.J. (2010). Mitochondrial membrane potential regulates PINK1 import and proteolytic destabilization by PARL. The Journal of cell biology *191*, 933-942.

97. Jones, P.A., and Liang, G. (2009). Rethinking how DNA methylation patterns are maintained. Nature Reviews Genetics *10*, 805-811.
98. Jung, E.H., Lee, J.H., Kim, S.C., and Kim, Y.W. (2015). AMPK activation by liquiritigenin inhibited oxidative hepatic injury and mitochondrial dysfunction induced by nutrition deprivation as mediated with induction of farnesoid X receptor. European journal of nutrition.
99. Jurkowska, R.Z., Jurkowski, T.P., and Jeltsch, A. (2011). Structure and function of mammalian DNA methyltransferases. Chembiochem *12*, 206-222.
100. Kairo, A., Fairlamb, A., Gobright, E., and Nene, V. (1994). A 7.1 kb linear DNA molecule of Theileria parva has scrambled rDNA sequences and open reading frames for mitochondrially encoded proteins. The EMBO journal *13*, 898.
101. Kalckar, H. (1937). Biochem J *2*, 47-52.
102. Kalckar, H. (1939). The nature of phosphoric esters formed in kidney extracts. Biochem J *33*, 631-641.
103. Karolchik, D., Hinrichs, A.S., Furey, T.S., Roskin, K.M., Sugnet, C.W., Haussler, D., and Kent, W.J. (2004). The UCSC Table Browser data retrieval tool. Nucleic acids research *32*, D493-496.
104. Kazuno, A.A., Munakata, K., Nagai, T., Shimozono, S., Tanaka, M., Yoneda, M., Kato, N., Miyawaki, A., and Kato, T. (2006). Identification of mitochondrial DNA polymorphisms that alter mitochondrial matrix pH and intracellular calcium dynamics. PLoS Genet *2*, e128.
105. Keilin, D. (1925). On Cytochrome, a Respiratory Pigment, Common to Animals, Yeast, and Higher Plants. Proceedings of the Royal Society of London Series B, Containing Papers of a Biological Character *98*, 312-339.
106. Kennedy, E.P., and Weiss, S.B. (1956). THE FUNCTION OF CYTIDINE COENZYMES IN THE BIOSYNTHESIS OF PHOSPHOLIPIDES. Journal of Biological Chemistry *222*, 193-214.
107. Kertesz, M., Iovino, N., Unnerstall, U., Gaul, U., and Segal, E. (2007). The role of site accessibility in microRNA target recognition. Nature genetics *39*, 1278-1284.
108. Kielley, W.W., and Kielley, R.K. (1951). MYOKINASE AND ADENOSINETRIPHOSPHATASE IN OXIDATIVE PHOSPHORYLATION. Journal of Biological Chemistry *191*, 485-500.
109. Kim, J., Villarroel, J.P., Zhang, W., Yin, T., Shinozaki, K., Hong, A., Lampe, J.W., and Becker, L.B. (2016). The Responses of Tissues from the Brain, Heart, Kidney, and Liver to Resuscitation following Prolonged Cardiac Arrest by Examining Mitochondrial Respiration in Rats. Oxidative medicine and cellular longevity *2016*, 7463407.
110. Klose, R.J., and Bird, A.P. (2006). Genomic DNA methylation: the mark and its mediators. Trends in biochemical sciences *31*, 89-97.
111. Kluck, R.M., Bossy-Wetzel, E., Green, D.R., and Newmeyer, D.D. (1997). The release of cytochrome c from mitochondria: a primary site for Bcl-2 regulation of apoptosis. Science *275*, 1132-1136.
112. Koch, L. (2016). Genetic variation: Nuclear and mitochondrial genome interplay. Nature reviews Genetics *17*, 502.

113. Kozomara, A., and Griffiths-Jones, S. (2014). miRBase: annotating high confidence microRNAs using deep sequencing data. Nucleic acids research *42*, D68-73.
114. Krebs, H.A., and Johnson, W.A. (1937). Metabolism of ketonic acids in animal tissues. Biochem J *31*, 645-660.
115. Kruse, B., Narasimhan, N., and Attardi, G. (1989). Termination of transcription in human mitochondria: identification and purification of a DNA binding protein factor that promotes termination. Cell *58*, 391-397.
116. Kumar, S., Kim, Y.R., Vikram, A., Naqvi, A., Li, Q., Kassan, M., Kumar, V., Bachschmid, M.M., Jacobs, J.S., Kumar, A., *et al.* (2017). Sirtuin1-regulated lysine acetylation of p66Shc governs diabetes-induced vascular oxidative stress and endothelial dysfunction. Proceedings of the National Academy of Sciences of the United States of America.
117. Lam, E.T., Bracci, P.M., Holly, E.A., Chu, C., Poon, A., Wan, E., White, K., Kwok, P.Y., Pawlikowska, L., and Tranah, G.J. (2012). Mitochondrial DNA sequence variation and risk of pancreatic cancer. Cancer Res *72*, 686-695.
118. Lardy, H.A., and Adler, J. (1956). SYNTHESIS OF SUCCINATE FROM PROPIONATE AND BICARBONATE BY SOLUBLE ENZYMES FROM LIVER MITOCHONDRIA. Journal of Biological Chemistry *219*, 933-942.
119. Latronico, M.V., and Condorelli, G. (2012). The might of microRNA in mitochondria (Am Heart Assoc).
120. Lee, H., Tak, H., Park, S., Jo, Y., Cho, D., and Lee, E. (2017). microRNA-200a-3p enhances mitochondrial elongation by targeting mitochondrial fission factor. BMB reports.
121. Leung, A.K. (2015). The whereabouts of microRNA actions: cytoplasm and beyond. Trends in cell biology *25*, 601-610.
122. Li, G.L., Xu, Y.J., Huang, X.M., Xiao, J., Nong, S., and Li, C.G. (2017). MeDIP-seq reveals the features of mitochondrial genomic methylation in immature testis of Chinese mitten crab Eriocheir sinensis. Mitochondrial DNA Part A, DNA mapping, sequencing, and analysis, 1-8.
123. Li, L., Gao, G., Shankar, J., Joshi, B., Foster, L.J., and Nabi, I.R. (2015). p38 MAP kinase-dependent phosphorylation of the Gp78 E3 ubiquitin ligase controls ER-mitochondria association and mitochondria motility. Molecular biology of the cell *26*, 3828-3840.
124. Li, X.Y., Guo, Y.B., Su, M., Cheng, L., Lu, Z.H., and Tian, D.P. (2011). Association of mitochondrial haplogroup D and risk of esophageal cancer in Taihang Mountain and Chaoshan areas in China. Mitochondrion *11*, 27-32.
125. Liesa, M., Palacín, M., and Zorzano, A. (2009). Mitochondrial dynamics in mammalian health and disease. Physiological reviews *89*, 799-845.
126. Lightowlers, R.N., Chinnery, P.F., Turnbull, D.M., and Howell, N. (1997). Mammalian mitochondrial genetics: heredity, heteroplasmy and disease. Trends in Genetics *13*, 450-455.
127. Lipmann, F.A. (1941). Metabolic generation and utilization of phosphate bond energy. Adv Enzymol *1*, 99.

128. Liu, V.W., Wang, Y., Yang, H.J., Tsang, P.C., Ng, T.Y., Wong, L.C., Nagley, P., and Ngan, H.Y. (2003). Mitochondrial DNA variant 16189T>C is associated with susceptibility to endometrial cancer. Hum Mutat *22*, 173-174.
129. Liu, X., Jiang, N., Hughes, B., Bigras, E., Shoubridge, E., and Hekimi, S. (2005). Evolutionary conservation of the clk-1-dependent mechanism of longevity: loss of mclk1 increases cellular fitness and lifespan in mice. Genes & development *19*, 2424-2434.
130. Liu, X., Kim, C.N., Yang, J., Jemmerson, R., and Wang, X. (1996a). Induction of apoptotic program in cell-free extracts: requirement for dATP and cytochrome c. Cell *86*, 147-157.
131. Liu, X., Kim, C.N., Yang, J., Jemmerson, R., and Wang, X. (1996b). Induction of apoptotic program in cell-free extracts: requirement for dATP and cytochrome c. Cell *86*, 147-157.
132. Luck, D.J., and Reich, E. (1964). DNA in Mitochondria of Neurospora Crassa. Proc Natl Acad Sci U S A *52*, 931-938.
133. Madeddu, G., Ortu, S., Garrucciu, G., Maida, I., Melis, M., Muredda, A.A., Mura, M.S., and Babudieri, S. (2016). DNMT1 modulation in Chronic Hepatitis B patients and hypothetic influence on Mitochondrial DNA methylation status during long-term Nucleo(t)side Analogues Therapy. Journal of medical virology.
134. Maegdefessel, L. (2014). The emerging role of microRNAs in cardiovascular disease. Journal of internal medicine *276*, 633-644.
135. Martinus, R.D., Garth, G.P., Webster, T.L., Cartwright, P., Naylor, D.J., Høj, P.B., and Hoogenraad, N.J. (1996). Selective induction of mitochondrial chaperones in response to loss of the mitochondrial genome. European Journal of Biochemistry *240*, 98-103.
136. Maunakea, A.K., Nagarajan, R.P., Bilenky, M., Ballinger, T.J., D'Souza, C., Fouse, S.D., Johnson, B.E., Hong, C., Nielsen, C., Zhao, Y., *et al.* (2010). Conserved role of intragenic DNA methylation in regulating alternative promoters. Nature *466*, 253-257.
137. Mawlood, S.K., Dennany, L., Watson, N., Dempster, J., and Pickard, B.S. (2016a). Quantification of global mitochondrial DNA methylation levels and inverse correlation with age at two CpG sites. Aging *8*, 636.
138. Mawlood, S.K., Dennany, L., Watson, N., Dempster, J., and Pickard, B.S. (2016b). Quantification of global mitochondrial DNA methylation levels and inverse correlation with age at two CpG sites. Aging *8*, 636-641.
139. Maynard, L.S., and Cotzias, G.C. (1955). THE PARTITION OF MANGANESE AMONG ORGANS AND INTRACELLULAR ORGANELLES OF THE RAT. Journal of Biological Chemistry *214*, 489-495.
140. McCormack, J.G., Halestrap, A.P., and Denton, R.M. (1990). Role of calcium ions in regulation of mammalian intramitochondrial metabolism. Physiol Rev *70*, 391-425.
141. Menga, A., Palmieri, E.M., Cianciulli, A., Infantino, V., Mazzone, M., Scilimati, A., Palmieri, F., Castegna, A., and Iacobazzi, V. (2017). SLC25A26 overexpression impairs cell function via mtDNA hypermethylation and rewiring of methyl metabolism. The FEBS Journal.
142. Meves, F. (1908). Die Chondriosomen als Träger erblicher Anlagen. Cytologische Studien am Hühnerembryo. Archiv für mikroskopische Anatomie *72*, 816-867.

143. Montoya, J., Gaines, G.L., and Attardi, G. (1983). The pattern of transcription of the human mitochondrial rRNA genes reveals two overlapping transcription units. Cell *34*, 151-159.
144. Mukhopadhyay, S., Naik, P.P., Panda, P.K., Sinha, N., Das, D.N., and Bhutia, S.K. (2016). Serum starvation induces anti-apoptotic cIAP1 to promote mitophagy through ubiquitination. Biochemical and biophysical research communications *479*, 940-946.
145. Murphy, M.P. (2009). How mitochondria produce reactive oxygen species. The Biochemical journal *417*, 1-13.
146. Nass, M.M. (1973). Differential methylation of mitochondrial and nuclear DNA in cultured mouse, hamster and virus-transformed hamster cells. In vivo and in vitro methylation. Journal of molecular biology *80*, 155-175.
147. Nass, M.M., and Nass, S. (1963a). Intramitochondrial Fibers with DNA Characteristics. I. Fixation and Electron Staining Reactions. J Cell Biol *19*, 593-611.
148. Nass, S., and Nass, M.M. (1963b). Intramitochondrial Fibers with DNA Characteristics. Ii. Enzymatic and Other Hydrolytic Treatments. J Cell Biol *19*, 613-629.
149. Nemoto, S., Takeda, K., Yu, Z.X., Ferrans, V.J., and Finkel, T. (2000). Role for mitochondrial oxidants as regulators of cellular metabolism. Molecular and cellular biology *20*, 7311-7318.
150. Nie, Y., Sato, Y., Wang, C., Yue, F., Kuang, S., and Gavin, T.P. (2016). Impaired exercise tolerance, mitochondrial biogenesis, and muscle fiber maintenance in miR-133a–deficient mice. The FASEB Journal *30*, 3745-3758.
151. Nindl, G., Peterson, N.R., Hughes, E.F., Waite, L.R., and Johnson, M.T. (2004). Effect of hydrogen peroxide on proliferation, apoptosis and interleukin-2 production of Jurkat T cells. Biomedical sciences instrumentation *40*, 123-128.
152. Nunnari, J., and Suomalainen, A. (2012a). Mitochondria: in sickness and in health. Cell *148*, 1145-1159.
153. Nunnari, J., and Suomalainen, A. (2012b). Mitochondria: in sickness and in health. Cell *148*, 1145-1159.
154. Ochoa, S. (1943). EFFICIENCY OF AEROBIC PHOSPHORYLATION IN CELL-FREE HEART EXTRACTS. Journal of Biological Chemistry *151*, 493-505.
155. Oda, K., Yamato, K., Ohta, E., Nakamura, Y., Takemura, M., Nozato, N., Akashi, K., Kanegae, T., Ogura, Y., and Kohchi, T. (1992). Gene organization deduced from the complete sequence of liverwort Marchantia polymorpha mitochondrial DNA: a primitive form of plant mitochondrial genome. Journal of molecular biology *223*, 1-7.
156. Paul, P., Chakraborty, A., Sarkar, D., Langthasa, M., Rahman, M., Bari, M., Singha, R.S., Malakar, A.K., and Chakraborty, S. (2017). Interplay between miRNAs and Human Diseases: A Review. Journal of cellular physiology.
157. Pellegrini, L., and Scorrano, L. (2007). A cut short to death: Parl and Opa1 in the regulation of mitochondrial morphology and apoptosis. Cell death and differentiation *14*, 1275-1284.
158. Petros, J.A., Baumann, A.K., Ruiz-Pesini, E., Amin, M.B., Sun, C.Q., Hall, J., Lim, S., Issa, M.M., Flanders, W.D., Hosseini, S.H., *et al.* (2005). mtDNA mutations increase tumorigenicity in prostate cancer. Proc Natl Acad Sci U S A *102*, 719-724.
159. Pirola, C.J., Gianotti, T.F., Burgueno, A.L., Rey-Funes, M., Loidl, C.F., Mallardi, P., Martino, J.S., Castano, G.O., and Sookoian, S. (2013). Epigenetic modification of

liver mitochondrial DNA is associated with histological severity of nonalcoholic fatty liver disease. Gut *62*, 1356-1363.

160. Pollack, Y., Kasir, J., Shemer, R., Metzger, S., and Szyf, M. (1984). Methylation pattern of mouse mitochondrial DNA. Nucleic acids research *12*, 4811-4824.
161. Qian, W., Choi, S., Gibson, G.A., Watkins, S.C., Bakkenist, C.J., and Van Houten, B. (2012). Mitochondrial hyperfusion induced by loss of the fission protein Drp1 causes ATM-dependent G2/M arrest and aneuploidy through DNA replication stress. J Cell Sci *125*, 5745-5757.
162. Rabinowitz, M., Sinclair, J., DeSalle, L., Haselkorn, R., and Swift, H.H. (1965). Isolation of deoxyribonucleic acid from mitochondria of chick embryo heart and liver. Proc Natl Acad Sci U S A *53*, 1126-1133.
163. Ragaud, C. (1909).
164. Ramachandran, A., Basu, U., Sultana, S., Nandakumar, D., and Patel, S.S. (2017). Human mitochondrial transcription factors TFAM and TFB2M work synergistically in promoter melting during transcription initiation. Nucleic acids research *45*, 861-874.
165. Rambold, A.S., Kostelecky, B., Elia, N., and Lippincott-Schwartz, J. (2011). Tubular network formation protects mitochondria from autophagosomal degradation during nutrient starvation. Proceedings of the National Academy of Sciences *108*, 10190-10195.
166. Ramirez-Carrozzi, V.R., Braas, D., Bhatt, D.M., Cheng, C.S., Hong, C., Doty, K.R., Black, J.C., Hoffmann, A., Carey, M., and Smale, S.T. (2009). A unifying model for the selective regulation of inducible transcription by CpG islands and nucleosome remodeling. Cell *138*, 114-128.
167. Ramsahoye, B.H., Biniszkiewicz, D., Lyko, F., Clark, V., Bird, A.P., and Jaenisch, R. (2000). Non-CpG methylation is prevalent in embryonic stem cells and may be mediated by DNA methyltransferase 3a. Proceedings of the National Academy of Sciences of the United States of America *97*, 5237-5242.
168. Raza, H., John, A., and Howarth, F.C. (2015). Increased oxidative stress and mitochondrial dysfunction in zucker diabetic rat liver and brain. Cellular physiology and biochemistry : international journal of experimental cellular physiology, biochemistry, and pharmacology *35*, 1241-1251.
169. Regaud, C. (1908).
170. Ricci, J.-E., Muñoz-Pinedo, C., Fitzgerald, P., Bailly-Maitre, B., Perkins, G.A., Yadava, N., Scheffler, I.E., Ellisman, M.H., and Green, D.R. (2004). Disruption of mitochondrial function during apoptosis is mediated by caspase cleavage of the p75 subunit of complex I of the electron transport chain. Cell *117*, 773-786.
171. Rizzuto, R., Brini, M., Murgia, M., and Pozzan, T. (1993). Microdomains with high Ca2+ close to IP3-sensitive channels that are sensed by neighboring mitochondria. Science *262*, 744-747.
172. Rovira-Llopis, S., Banuls, C., Diaz-Morales, N., Hernandez-Mijares, A., Rocha, M., and Victor, V.M. (2017). Mitochondrial dynamics in type 2 diabetes: Pathophysiological implications. Redox biology *11*, 637-645.
173. Sanger, F., Nicklen, S., and Coulson, A.R. (1977). DNA sequencing with chain-terminating inhibitors. Proc Natl Acad Sci U S A *74*, 5463-5467.
174. Sano, S., Inoue, S., Tanabe, Y., Sumiya, C., and Koike, S. (1959). Significance of mitochondria for porphyrin and heme biosynthesis. Science *129*, 275-276.

175. Sano, S., Inoue, S., Tanabe, Y., Sumiya, C., and Koike, S. (1960). Significance of mitochondria for porphyrin and haem biosynthesis. Acta Sch Med Univ Kioto *36*, 191-200.
176. Schulz, T.J., Zarse, K., Voigt, A., Urban, N., Birringer, M., and Ristow, M. (2007). Glucose restriction extends Caenorhabditis elegans life span by inducing mitochondrial respiration and increasing oxidative stress. Cell metabolism *6*, 280-293.
177. Sena, L.A., and Chandel, N.S. (2012). Physiological roles of mitochondrial reactive oxygen species. Molecular cell *48*, 158-167.
178. Shigenaga, M.K., Hagen, T.M., and Ames, B.N. (1994). Oxidative damage and mitochondrial decay in aging. Proceedings of the National Academy of Sciences of the United States of America *91*, 10771-10778.
179. Shinde, S., and Bhadra, U. (2015). A complex genome-microRNA interplay in human mitochondria. BioMed research international *2015*.
180. Shmookler Reis, R.J., and Goldstein, S. (1983). Mitochondrial DNA in mortal and immortal human cells. Genome number, integrity, and methylation. The Journal of biological chemistry *258*, 9078-9085.
181. Shock, L.S., Thakkar, P.V., Peterson, E.J., Moran, R.G., and Taylor, S.M. (2011). DNA methyltransferase 1, cytosine methylation, and cytosine hydroxymethylation in mammalian mitochondria. Proceedings of the National Academy of Sciences of the United States of America *108*, 3630-3635.
182. Siekevitz, P., and Potter, V.R. (1953). INTRAMITOCHONDRIAL REGULATION OF OXIDATIVE RATE. Journal of Biological Chemistry *201*, 1-13.
183. Siekevitz, P., and Potter, V.R. (1955). BIOCHEMICAL STRUCTURE OF MITOCHONDRIA: I. INTRAMITOCHONDRIAL COMPONENTS AND OXIDATIVE PHOSPHORYLATION. Journal of Biological Chemistry *215*, 221-235.
184. Singh, R.K., Srivastava, A., Kalaiarasan, P., Manvati, S., Chopra, R., and Bamezai, R.N. (2014). mtDNA germ line variation mediated ROS generates retrograde signaling and induces pro-cancerous metabolic features. Scientific reports *4*, 6571.
185. Sioud, M., and Cekaite, L. (2010). Profiling of miRNA expression and prediction of target genes. Methods in molecular biology *629*, 257-271.
186. Slater, E.C., and Cleland, K.W. (1953). The effect of calcium on the respiratory and phosphorylative activities of heart-muscle sarcosomes. Biochem J *55*, 566-590.
187. Soini, H.K., Moilanen, J.S., Finnila, S., and Majamaa, K. (2012). Mitochondrial DNA sequence variation in Finnish patients with matrilineal diabetes mellitus. BMC research notes *5*, 350.
188. Solesio, M.E., Elustondo, P.A., Zakharian, E., and Pavlov, E.V. (2016). Inorganic polyphosphate (polyP) as an activator and structural component of the mitochondrial permeability transition pore. Biochemical Society Transactions *44*, 7-12.
189. Sripada, L., Tomar, D., Prajapati, P., Singh, R., Singh, A.K., and Singh, R. (2012). Systematic analysis of small RNAs associated with human mitochondria by deep sequencing: detailed analysis of mitochondrial associated miRNA. PloS one *7*, e44873.
190. Swinson, D.E., and O'Byrne, K.J. (2006). Interactions between hypoxia and epidermal growth factor receptor in non-small-cell lung cancer. Clinical lung cancer *7*, 250-256.
191. Taylor, R., and Gilleard, C.J. (1990). Encoding preferences in memory in dementia. The British journal of clinical psychology *29 (Pt 2)*, 243-244.

192. Torroni, A., and Wallace, D.C. (1994). Mitochondrial DNA variation in human populations and implications for detection of mitochondrial DNA mutations of pathological significance. J Bioenerg Biomembr *26*, 261-271.
193. Vahrenholz, C., Riemen, G., Pratje, E., Dujon, B., and Michaelis, G. (1993). Mitochondrial DNA of Chlamydomonas reinhardtii: the structure of the ends of the linear 15.8-kb genome suggests mechanisms for DNA replication. Current genetics *24*, 241-247.
194. van Laarhoven, H.W., Kaanders, J.H., Lok, J., Peeters, W.J., Rijken, P.F., Wiering, B., Ruers, T.J., Punt, C.J., Heerschap, A., and van der Kogel, A.J. (2006). Hypoxia in relation to vasculature and proliferation in liver metastases in patients with colorectal cancer. International journal of radiation oncology, biology, physics *64*, 473-482.
195. van Oven, M., and Kayser, M. (2009). Updated comprehensive phylogenetic tree of global human mitochondrial DNA variation. Human mutation *30*, E386-394.
196. Wallace, D.C. (2013). A mitochondrial bioenergetic etiology of disease. J Clin Invest *123*, 1405-1412.
197. Wallace, D.C., Shoffner, J.M., Trounce, I., Brown, M.D., Ballinger, S.W., Corral-Debrinski, M., Horton, T., Jun, A.S., and Lott, M.T. (1995). Mitochondrial DNA mutations in human degenerative diseases and aging. Biochim Biophys Acta *1271*, 141-151.
198. Wallace, D.C., and Torroni, A. (1992). American Indian prehistory as written in the mitochondrial DNA: a review. Hum Biol *64*, 403-416.
199. Wang, J., Duncan, D., Shi, Z., and Zhang, B. (2013). WEB-based GEne SeT AnaLysis Toolkit (WebGestalt): update 2013. Nucleic acids research *41*, W77-83.
200. Wang, W.-X., and Springer, J.E. (2015). Role of mitochondria in regulating microRNA activity and its relevance to the central nervous system. Neural regeneration research *10*, 1026.
201. Warburg, H.O. (1913). Arch GesamtePhysiol *154*, 599-617.
202. Watson, E., Forster, P., Richards, M., and Bandelt, H.J. (1997). Mitochondrial footprints of human expansions in Africa. American journal of human genetics *61*, 691-704.
203. Weber, M., Hellmann, I., Stadler, M.B., Ramos, L., Pääbo, S., Rebhan, M., and Schübeler, D. (2007). Distribution, silencing potential and evolutionary impact of promoter DNA methylation in the human genome. Nature genetics *39*, 457-466.
204. Wei, Q., Lu, Y., Zhang, Y., Chen, Z., Xing, G., and Cao, X. (2009). [Mutation analysis of mitochondrial 12S rRNA gene G709A in a maternally inherited pedigree with non-syndromic deafness]. Zhonghua yi xue yi chuan xue za zhi = Zhonghua yixue yichuanxue zazhi = Chinese journal of medical genetics *26*, 610-614.
205. Weimer, S., Priebs, J., Kuhlow, D., Groth, M., Priebe, S., Mansfeld, J., Merry, T.L., Dubuis, S., Laube, B., and Pfeiffer, A.F. (2014). D-Glucosamine supplementation extends life span of nematodes and of ageing mice. Nature communications *5*.
206. Welter, C., Dooley, S., Zang, K.D., and Blin, N. (1989). DNA curvature in front of the human mitochondrial L-strand replication origin with specific protein binding. Nucleic acids research *17*, 6077-6086.
207. West, A.P., Shadel, G.S., and Ghosh, S. (2011). Mitochondria in innate immune responses. Nature Reviews Immunology *11*, 389-402.

208. Wu, C., Zhu, J., and Zhang, X. (2012). Integrating gene expression and protein-protein interaction network to prioritize cancer-associated genes. BMC bioinformatics *13*, 182.
209. Xavier, J.M., Shafiee, N.M., Ghaderi, F., Rosa, A., Abdollahi, B.S., Nadji, A., Shahram, F., Davatchi, F., and Oliveira, S.A. (2011). Association of mitochondrial polymorphism m. 709G> A with Behçet's disease. Annals of the rheumatic diseases, annrheumdis143537.
210. Xiao, F., Zuo, Z., Cai, G., Kang, S., Gao, X., and Li, T. (2009). miRecords: an integrated resource for microRNA-target interactions. Nucleic acids research *37*, D105-110.
211. Yamada, Y., Jackson-Grusby, L., Linhart, H., Meissner, A., Eden, A., Lin, H., and Jaenisch, R. (2005). Opposing effects of DNA hypomethylation on intestinal and liver carcinogenesis. Proceedings of the National Academy of Sciences of the United States of America *102*, 13580-13585.
212. Yamamoto, H., Morino, K., Nishio, Y., Ugi, S., Yoshizaki, T., Kashiwagi, A., and Maegawa, H. (2012). MicroRNA-494 regulates mitochondrial biogenesis in skeletal muscle through mitochondrial transcription factor A and Forkhead box j3. American Journal of Physiology-Endocrinology and Metabolism *303*, E1419-E1427.
213. Yang, J., Liu, X., Bhalla, K., Kim, C.N., Ibrado, A.M., Cai, J., Peng, T.I., Jones, D.P., and Wang, X. (1997). Prevention of apoptosis by Bcl-2: release of cytochrome c from mitochondria blocked. Science *275*, 1129-1132.
214. Yee, C., Yang, W., and Hekimi, S. (2014). The intrinsic apoptosis pathway mediates the pro-longevity response to mitochondrial ROS in C. elegans. Cell *157*, 897-909.
215. Youle, R.J., and Van Der Bliek, A.M. (2012). Mitochondrial fission, fusion, and stress. Science *337*, 1062-1065.
216. Zarse, K., Schmeisser, S., Groth, M., Priebe, S., Beuster, G., Kuhlow, D., Guthke, R., Platzer, M., Kahn, C.R., and Ristow, M. (2012). Impaired insulin/IGF1 signaling extends life span by promoting mitochondrial L-proline catabolism to induce a transient ROS signal. Cell metabolism *15*, 451-465.
217. Zhang, X., Zuo, X., Yang, B., Li, Z., Xue, Y., Zhou, Y., Huang, J., Zhao, X., Zhou, J., and Yan, Y. (2014). MicroRNA directly enhances mitochondrial translation during muscle differentiation. Cell *158*, 607-619.
218. Zhou, S., Kachhap, S., Sun, W., Wu, G., Chuang, A., Poeta, L., Grumbine, L., Mithani, S.K., Chatterjee, A., Koch, W., *et al.* (2007). Frequency and phenotypic implications of mitochondrial DNA mutations in human squamous cell cancers of the head and neck. Proc Natl Acad Sci U S A *104*, 7540-7545.

8. APPENDIX

APPENDIX

Table A1: Primers used in the study

Name of Primers	Primer Sequence	Reference
mitochondrial DNA sequencing primers		
1aF	CGCCTCAACCGCCTTTTCATCA	In this study
1aR	GCGATAAATAATAGGATGAGGC	In this study
1bF	TACACAATCAAAGACGCCCTC	In this study
1bR	GTTGGTATCCTAGTGGGTGAG	In this study
1cF	AGTCTTTAACTCCACCATTAG	In this study
1cR	GTGAAGTATAGTACGGATGCT	In this study
2aF	CTGTATCCGACATCTGGTTCCT	In this study
2aR	GTTTAGCTCAGAGCGGTCAAGT	In this study
2bF	CGGTATGCACTTTTAACAGTC	In this study
2bR	TAAGCTGTGGCTCGTAGTGT	In this study
2cF	GATTAACCCAAGTCAATAGAA	In this study
2cR	GGTGATGTGAGCCCGTCTAAA	In this study
3aF	CTTAAGGGTCGAAGGTGGATTT	In this study
3aR	GGGGTTCGGTTGGTCTCTGCTA	In this study
3bF	GATAGAATCTTAGTTCAACTT	In this study
3bR	TTCGTTCGGTAAGCATTAGGA	In this study
3cF	GGTTCAGCTGTCTCTTACTTT	In this study
3cR	TAATGCAGGTTTGGTAGTTTA	In this study
3dF	GCAGAGCCCGGTAATCGCATA	In this study
3dR	GGGTGTGAGGAGTTCAGTTAT	In this study
4aF	CCATCATTCTACTATCAACATT	In this study
4aR	ACAGAAATTAAGTATTGCAACT	In this study
4bF	GAACCCATCCCTGAGAATCCA	In this study
4bR	GAGGAGTATGCTAAGATTTTG	In this study
4cF	TACCAAATCTCTCCCTCACTA	In this study
4cR	CTTATTTAGCTGACCTTACTT	In this study
5aF	CTACTCCTACCTATCTCCCCTT	In this study
5aR	TTATTCCGAAGCCTGGTAGGATA	In this study
5bF	CAGCTCTAAGCCTCCTTATTC	In this study
5bR	GGAACTAGTCAGTTGCCAAAG	In this study
6aF	CCCTCTCTCCTACTCCTGCTC	In this study
6aR	GTGAAGATGATAAGTGTAGAG	In this study
6bF	CCGGAAAAAAAGAACCATTTGGAT	In this study
6bR	AGAATGATCAGTACTGCGGCG	In this study
6cF	ACACCCTAGACCAAACCTACG	In this study
6cR	CAACGTCAAGGAGTCGCAGGT	In this study
6dF	TCCTAACACTCACAACAAAAC	In this study
6dR	CTACTATTAGGACTTTTCGCT	In this study
6eF	TAGCATTAACCTTTTAAGTTA	In this study
7aF	CTTACCACAAGGCACACCTACA	In this study
7aR	GGCACAATATTGGCTAAGAGGG	In this study
7bF	CGAGAAAGCACATACCAAGGC	In this study

7bR	TTCTATGTAGCCGTTGAGTTG	In this study
7cF	TAATATTTCACTTTACATCCA	In this study
7cR	AGCTCAGGTGATTGATACTCC	In this study
8aF	GTCTGGCCTATGAGTGACTACA	In this study
8aR	CAGTTCTTGTGAGCTTTCTCGG	In this study
8bF	ATCAACAACAACCTATTTAGC	In this study
8br	GTTTGGATGAGAATGGCTGTT	In this study
8cF	ACTCTTAAAACTAGGCGGCTA	In this study
8cR	CGGGTGATGATAGCCAAGGTG	In this study
9aF	CTCCCTCTACATATTTACCACAAC	In this study
9aR	AAGTCCTAGGAAAGTGACAGCGA	In this study
9bF	TGTGCCTAGACCAAGAAGTTA	In this study
9bR	GGTTGATGCCGATTGTAACTA	In this study
9cF	CTAGCAGCAGCAGGCAAATCA	In this study
9cR	CGATGAACAGTTGGAATAGGT	In this study
10aF	GCAGGAATACCTTTCCTCACAG	In this study
10aR	GTGCAAGAATAGGAGGTGGAGT	In this study
10bF	CTATCTAGGCCTTCTTACGAG	In this study
10bR	CATCATGCGGAGATGTTGGAT	In this study
10cF	ATACTCCTCAATAGCCATCGC	In this study
10cR	AACTTTAATAGTGTAGGAAGC	In this study
DNMT1 Cloning primers		
uORF NheI F	TTTGCTAGCATGGCCGGCTCCGTT	In this study
uORF EcoRI R	TTTGAATTCCTCGGAGGCTTCAGCAGACG	In this study
DNMT1 Iso1 EcoRI F	TTTGAATTCATGCCGGCGCGTACCGCCCCA	In this study
DNMT1 Iso1 KpnI R	GGGCGGTACCGTCCTTAGCAGCTTCCTCCTCCTTTA	In this study
DNMT1 Iso3 EcoRI F	TTTGAATTCATGGCTCGCGCCAAAACAG	In this study
DNMT1 Iso3 KpnI R	GGGCGGTACCGTCCTTAGCAGCTTCCTCCTCCTTTA	In this study
DNMT1 Iso1 SalI F	TTAGTCGACATGCCGGCGCGTACC	In this study
DNMT1 Iso1 NotI R	TTTGCGGCCGCGTCCTTAGCAGCTTC	In this study
DNMT1 Iso3 SalI F	TTAGTCGACATGGCTCGCGCCAAAACAGTC	In this study
DNMT1 Iso3 NotI R	TTTGCGGCCGCGTCCTTAGCAGCTTC	In this study
DNMT1 XbaI R	TTAATCTAGAGAGGAAGCTGCTAAGGAC	In this study
Primers for SDM		
DNMT1 Iso1 EcoRI Deletion F	ATGCCGGCGCGTACCGCC	In this study
DNMT1 Iso3 EcoRI Deletion F	ATGGCTCGCGCCAAAACAGT	In this study
DNMT1 EcoRI Deletion R	CTCGGAGGCTTCAGCAGACGCG	In this study
Primers for 5' RACE		
5' CDS A F	Sequence not disclosed by manufacturer	
UPM Short	CTAATACGACTCACTATAGGGC	
DNMT1 internal R	CACACTGAAGCAGGTCAGTTTGTGCTGG	In this study
Primers for qPCR		
DNMT1 F	GGCTGAGATGAGGCAAAAAG	
DNMT1 R	ACCAACTCGGTACAGGATGC	In this study
HVR2 F	GCTCTCCATGCATTTGGTAT	In this study
HVR2 R	AGGATGAGGCAGGAATCAAAG	In this study

Transcription term. factor F	CACCCAAGAACAGGGTTTGT	In this study
Transcription term. factor R	TGGCCATGGGTATGTTGTTAAG	In this study
L- Strand origin F	CCCTAATCAACTGGCTTCAATCT	In this study
L- Strand origin R	TACCAGCTCCGAGGTGATTT	In this study
Membrane attach site F	ATGGGCCTGTCCTTGTAGTA	In this study
Membrane attach site R	GGGTGCTAATGGTGGAGTTAAA	In this study
COI F	TTCTGACTCTTACCTCCCTCTC	In this study
COI R	TGGGAGTAGTTCCCTGCTAA	In this study
ND3 F	CCACAACTCAACGGCTACATA	In this study
ND3 R	AGGAGGGCAATTTCTAGATCAAA	In this study
ND6 F	AGGATTGGTGCTGTGGGTGAAAGA	In this study
ND6 R	ATAGGATCCTCCCGAATCAACCCT	In this study
ATP6 F	TAGCCCACTTCTTACCACAAGGCA	In this study
ATP6 R	TGAGTAGGTGGCCTGCAGTAATGT	In this study
12s rRNA F	GGTCACACGATTAACCCAAGT	In this study
12s rRNA R	TGTTAAAGCCACTTTCGTAGTCTAT	In this study
16s rRNA F	GCCGCTATTAAAGGTTCGTTTG	In this study
16s rRNA R	CCTTTCGTACAGGGAGGAATTT	In this study
PPARGC1A F	TGTCACCACCCAAATCCTTATTT	In this study
PPARGC1A R	TGTGTCGAGAAAAGGACCTTGA	In this study
NRF1 F	CCATCTG GTGGCCTGAAG	In this study
NRF1 R	GTGCCTGGGTCCATGAAA	In this study
NFE2L2 F	ACACGGTCCACAGCTCATC	In this study
NFE2L2 R	TGTCAATCAAATCCATGTCCTG	In this study
TFAM F	GAACAACTACCCATATTTAAAGCTCA	In this study
TFAM R	GAATCAGGAAGTTCCCTCCA	In this study

Table A2: List of mitochondrial genomic variations of all 10 cell lines

Position	**A549**	**H1299**	**HCT116**	**HT29**	**MCF7**	**MDAMB231**	**HeLa**	**SiHa**	**LNCAP**	**PC3**
73	A>G			A>G	A>G	A>G	A>G	A>G		A>G
114				C>T						
146								T>C	T>C	
150								C>T		
152		T>C						T>C		
153						A>G				
195						T>C				T>C
225	G>T									
252								T>C		
263	A>G		A>G	A>G	A>G	A>G	A>G	A>G	A>G	A>G
310		T>C			T>C					
315	Ins-C		Ins-C	INS C					Ins-C	
375								C>A		

389		G>A								
489								T>C		
497				C>T						
523-524	Del-AC									
681								T>C		
683						G>A				
709					G>A	G>A				INS G
732										INS A
733								T>C		
750	A>G		A>G	A>G	A>G	A>G	A>G	A>G	A>G	A>G
796						G>T				
927						G>A				
975						A>T				
978	Ins-T									
980	T>A									
982	A>C									
1015	Ins-A									
1026					A>G					
1048								C>T		
1107								T>C		
1123	Ins-C									
1168								A>G		
1189				T>C						
1196								DEL A		
1413				T>C						
1431						G>A				
1438	A>G		A>G	A>G	A>G	A>G	A>G	A>G	A>G	A>G
1445						G>A				
1598								G>A		
1616	A>G									
1683	C>G									
1715					C>G					
1719						G>A				
1811				A>G						
2141							InsT			
2194									Del-T	
2252									C>T	
2276	C>T									
2291	Ins-A									

2316							T>A			
2359							C>T			
2511-12	Del-CA									
2545	T>C									
2580	T>C									
2699							C>T			
2706				A>G	A>G	A>G	A>G	A>G		A>G
2805									Ins-A	
2941					G>A					
3010			G>A							
3197										A>C
3313						A>G				
3450							C>T			
3480				A>G						
3604					C>T					
3759								A>G		
3796			A>G							
3859									T>G	
3992	C>T									
4024	A>G									
4115										
4136					A>G					
4137										
4153									G>A	
4168										
4172									T>A	
4264										G>C
4296	G>C									
4301	A>C									
4569					G>A					
4587	T>C									
4629					G>A					
4769	A>G		A>G	A>G	A>G	A>G	A>G	A>G		A>G
4844								INS G		
4856								T>A		
4883								C>T		
4957			Del-T							
5004	T>C		C>T							
5085										
5116										
5151										

5153				A>G				A>G		
5168										
5178								C>A		
5181										
5195										
5214										
5236										
5246										
5251									T>G	
5301								A>G		
5339					C>T					
5773							G>A			
5803					C>A					
5969										
6106	T>G									
6124				T>A						
6187	C>G									
6198	A>C									
6221						T>C	T>C			
6253								T>C		
6267				G>A						
6366							G>A			
6371						C>T				
6267	G>A									
7028				C>T	C>T	C>T	C>T	C>T		C>T
7714									C>G	
7946									T>A	
7746							A>G			
8018								C>A		
8269	G>A									
8312	A>G									
8328	G>C									
8476	Ins-C									
8484	A>T									
8506						T>C				
8611							C>G			
8701							A>G	A>G		
8860	A>G		A>G	A>G	A>G	A>G	A>G	A>G	A>G	A>G
8913	Ins-A									
9055				G>A						
9123	G>A									

9180								A>G		
9401									C>G	
9449							C>T			
9477					G>A					G>A
9510				T>C						
9540							T>C	T>C		
9698				T>C						
9912							G>C			
10044	A>G									
10086							A>G			
10182			G>A							
10373							G>A			
10385									Del-A	
10397								A>G		
10398				A>G			A>G	A>G		
10400								C>T		
10550				A>G						
10562									A>G	
10738								T>A		
10873								T>C		
10895							T>C			
10899		A>G								
10978				A>G						
11002		A>G								
11120										T>C
11152									T>C	
11299				T>C						
11347							A>G			
11467				A>G	A>G		A>G			A>G
11470				A>G						
11719				G>A	G>A	G>A	G>A	G>A		G>A
11800							A>G			
11914				G>A						
12084						C>T				
12258						C>A				
12270						T>A				
12273									A>T	
12308				A>G	A>G					
12372				G>A	G>A					
12595					A>C					
12705						C>T	C>T	C>T		

12801					C>T					
12895				G>A			G>A			
12946				C>T						
12954				T>C						
13042							G>A			
13105	A>G						A>G			
13306				C>G						
13397			A>G							
13413			A>C							
13543								DEL T		
13617					T>C					T>C
13802										C>T
13889					G>A					
13966						A>G				
13968							G>A			
14029	Ins-A									
14082								C>T		
14167				C>T						
14195		A>C								
14394	C>G									
14460		C>G								
14470						T>C				
14582	A>G									
14766				C>T	C>T		C>T	C>T		C>T
14783								T>C		
14793					A>G					A>G
14798				T>C						
15043								G>A		
15218					A>G					A>G
15301							G>A			
15310						T>C				
15326	A>G		A>G	A>G	A>G	A>G			A>G	A>G
15343										
15466					G>A					
15479		T>C								
15645								T>G		
15824							A>G			
15875										C>T
15883							G>A			
15924				A>G						
16059									A>G	

16093						T>C				
16129									G>A	
16172										T>C
16183								A>C		
16189			T>C					T>C		
16192					C>T					C>T
16223						C>T	C>T			
16224				T>C						
16234				C>T						
16256					C>T					C>T
16265						A>G				
16270					C>T					C>T
16274				DEL G						
16278						C>T	C>T			
16311				T>C						
16320										C>T
16322		A>C								
16326		A>T								
16356			T>C							
16358		C>T								
16362			T>C				T>C			
16399										A>G
16519			T>C			T>C	T>C		T>C	

Table A 3: Recipe for Phosphate-Buffer Saline (PBS)

Components	Amount
NaCl	137mM
KCl	2.7mM
Na_2HPO_4	10mM
KH_2PO_4	2mM

8g of NaCl, 0.2g of KCl, 1.44g of Na_2HPO_4 and 0.24g of KH_2PO_4 was dissolved in 800ml of distilled water. pH was adjusted to 7.4 with the help of HCl. The resulting solution was autoclaved for 20 minutes. Buffer was stored at room temperature.

Table A 4: Recipe for Tris Acetic Acid Electrophoresis (TAE) buffer

Components	Amount for 50X stock
Tris-base	242g
Glacial acetic acid	57.1 ml of glacial acetic acid
EDTA	100 ml of 0.5 M EDTA (pH 8.0)

The above components were mixed for 50X stock solution and autoclaved for 20 minutes. The autoclaved stock was stored at room temperature.

Table A 5: Ethidium Bromide stock (10 mg/ml)

0.1g of ethidium bromide was dissolved in 10 ml of water. The falcon was wrapped in aluminum foil and stored at room temperature.

Table A 6: Recipe for 30% Acrylamide solution

Components	Amount
Acrylamide	29.22g
N, N'-methylenebisacrylamide	0.78g
Water	to 100 ml

Solution was filtered through Whatman filter paper and stored in a dark bottle at 4℃.

Table A 7: Recipe for 10% (w/v) Ammomium Persulphate

1g of ammonium persulphate was dissolved in 10 ml of water and stored at 4℃ in a covered falcon.

Table A 8: Recipe for 1X SDS Running Buffer

Components	Amount
Tris-base	3.02g
Glycine	14.26g
SDS	1g
Water	Up to 1000 ml

The components were dissolved and autoclaved for 20 minutes at 15 psi (1.05 kg/cm^2). Fresh running buffer was used every time.

Table A 9: Recipe for 1X SDS Transfer Buffer

Components	Amount
Tris-base	3.02g
Glycine	14.26g
10% SDS	3.75ml
Water	800ml

Tris and glycine were dissolved in 800ml of water followed by addition to SDS and 20% ethanol. Buffer was stored at 4℃.

Table A 10: Recipe for 20X Tris Buffer Saline

Components	Amount

NaCl	160g
KCl	4g
Tris-base	60g
Water	1000ml

100 ml of distilled water was added to the above mixture and autoclaved for 20 minutes and stored at room temperature. Before use 50ml of 20X stock was diluted in water and 0.5ml Tween 20 was added to prepare 0.5% Tween-20-TBST.

Table A 11: Recipe to prepare 10% SDS

10g of SDS was added in 100 ml of double distilled water. The resulting mixture was kept at 37℃ for overnight to assist dissolution. Stored at room temperature.

Table A 12: Recipe for LB Medium (Luria-Bertani medium) preparation

Components	Amount
LB broth powder	2.5 g
Deionized water	100 ml

The dissolved medium was autoclave sterilized for 20 minutes and stored at 4℃. The medium was thawed at room temperature before use.

Table A 13: Recipe for Innoue Transformation Buffer preparation

Reagent	Amount (per litre)	Final concentration
MnCl2.4H2O	10.88g	55mM
CaCl2.2H2O	2.20g	15mM
KCl	18.65g	250mM
PIPES (0.5M, pH 6.7)	20ml	10mM
H2O	Made upto 1litre	

The buffer was sterilized by filtration and stored at 4℃.

Table A 14: Antibiotics stocks and working dilutions

Antibiotic	Stock solution	Working	Storage
Ampicillin	100 mg/ml	100 µg/ml	-20°C
Spectinomycin	100 mg/ml	50 µg/ml	-20°C
Penicillin/Streptomycin mix	100X	1X	-20℃

Table A 15: Recipe to prepare Dulbecco Modified Eagle's Medium (DMEM)

For 1 liter

Components	Amount
DMEM powder high glucose (4.5 g/l)	13.48 g
Sodium bicarbonate	3.7 g

Penicillin Streptomycin mix (100X)	1X
Fetal Bovine Serum (FBS)	10 % of volume

DMEM and sodium bicarbonate was mixed in autoclaved milli-Q water, filtered through 0.22µ nitrocellulose membrane filter and stored at 4℃. Antibiotic mix and fetal bovine serum were added at the time of use.

Table A 16: Recipe for Roswell Park Memorial Institute medium (RPMI) preparation

For 1 liter

Components	Amount
RPMI powder	13.48 g
Sodium bicarbonate	2.8 g
Penicillin Streptomycin mix (100X)	1X
Fetal Bovine Serum (FBS)	10 % of volume

RPMI and sodium bicarbonate was mixed in autoclaved milli-Q water, filtered through 0.22µ nitrocellulose membrane filter and stored at 4℃. Antibiotic mix and fetal bovine serum were added at the time of use.

Table A 17: Recipe to prepare 2.5% Trypsin-EDTA solution

For 100 ml,

Components	Amount
Trypsin	250 mg
EDTA	20 mg
Glucose	100 mg

Above mentioned components were mixed with 100ml of PBS and filter sterilized. The Trypsin-EDTA solution was stored at 4℃.

Mammalian Cell Lysate Preparation:

i. Spent media was decanted and cells were washed with ice-cold PBS followed by decanting the cell debris etc.
ii. Cells were trypsinised (0.2% solution of Trypsin-EDTA) and 1ml complete DMEM media was added after 5 minutes to inactivate trypsin. Further, the cells were collected in a 1.5ml microfuge tube and kept on ice.

iii. Cells were pelleted down at 3000 rpm for 3-5 minutes and supernatant was discard. Meanwhile, 1X lysis buffer was prepared consisted of protease inhibitors (Aprotinin, Pepstatin and Leupeptin), PMSF, DTT and water.

iv. Depending on the size of the cell pellet, volume of lysis buffer to be used for cell lysis was decided. Cell pellet was dissolved in the lysis buffer by pipetting and incubated on ice for 30 minutes.

v. Finally, the cells were subjected to high speed centrifugation at 13000 rpm for 30 minutes to separate cell debris from the lysate in a pre-chilled centrifuge machine. The supernatant was collected in fresh tubes and the protein was quantified by Bradford method.

SDS PAGE Electrophoresis:

i. The 1.5mm glass plates were arranged in the gel casting stands and then the assembly was placed on stand which was having sponge at its bottom and plates were kept on that form which was functioning as sealing the glass plates.

ii. 10ml of 8% resolving gel was prepared and it was poured in between the glass plates, sufficient space should be left for stacking. A layer of water saturated butanol was added over resolving gel.

iii. After polymerisation of resolving gel, butanol was removed and was washed with water, wipe with tissue paper.

iv. Then pour the 5% stacking gel, comb was placed into the stacking gel, then stacking gel was allowed to polymerise.

v. After polymerisation, clamps and comb were removed and the plates were kept in the apparatus in which 1x SDS running buffer was kept.

vi. Sample preparation: cell lysates which were prepared by using lysis buffer and whose protein Quantitation was done by using BCA method, according to the requirement the specific volume of sample is mixed with 4x loading dye and lysis buffer.

vii. The samples were then boiled in boiling water for 5 minutes. Samples were centrifuged at 13000rpm for 1 minute.

viii. Samples were loaded on gel along with prestained marker and gel was allowed to run at 60V till the samples were in stacking gel, as soon as samples entered in resolving gel voltage was increased to 80V.

Protein Transfer

i. Filter paper and nitrocellulose membrane of proper dimensions were 1st cut and they were allowed to be kept in chilled transfer buffer for some time before being used in transfer along with sponges.
ii. The gel between the glass plates was taken out and its stacking portion was removed.
iii. The sandwich on cassette was prepared from the negative side sponge-filter paper-gel-NC membrane-filter paper- sponge.
iv. The cassette was closed firmly; the cassette was placed in the tank for the transfer in the 1x transfer buffer.
v. Magnetic stirrer was also added inside the tank, to maintain the even distribution of ions in the buffer.
vi. Current of 120mA for 4hours at 4^{o} C was passed across the membrane.
vii. After transfer, the membrane was stained with Ponceau S to saw the transfer of protein on the membrane.
viii. After that the membrane was washed completely with 1x TBST so that no staining mark is left of Ponceau S.
ix. *Blocking*- The membrane was kept in Blocking buffer (5% BSA in 1xTBST) for 1 hour with gentle agitation on a shaker. After 1 hour blocking buffer was removed and membrane was cut.
x. The membrane was incubated in primary antibody (1:1000 dilutions) at 4^{0} C for overnight.
xi. Next day the membrane was washed 3 times with 1x TBST and then it was kept in secondary antibody which was HRP(Horseradish Peroxidase) labelled, for 1 hour with gentle agitation on shaker and then washed 3 times with 1xTBST.

Membrane Developing

i. The membrane was developed on X-ray film in dark room.
ii. 1st membrane was placed on polythene sheet and then chromogenic substrate named ECL was added to the membrane, the membrane was covered with polythene sheet.
iii. X-ray film was taken and then placed on membrane. Exposure time of X-ray films should vary so that we could get protein bands in a time dependent manner.
iv. X-ray film was removed and was sequentially placed in developer, water and fixer.

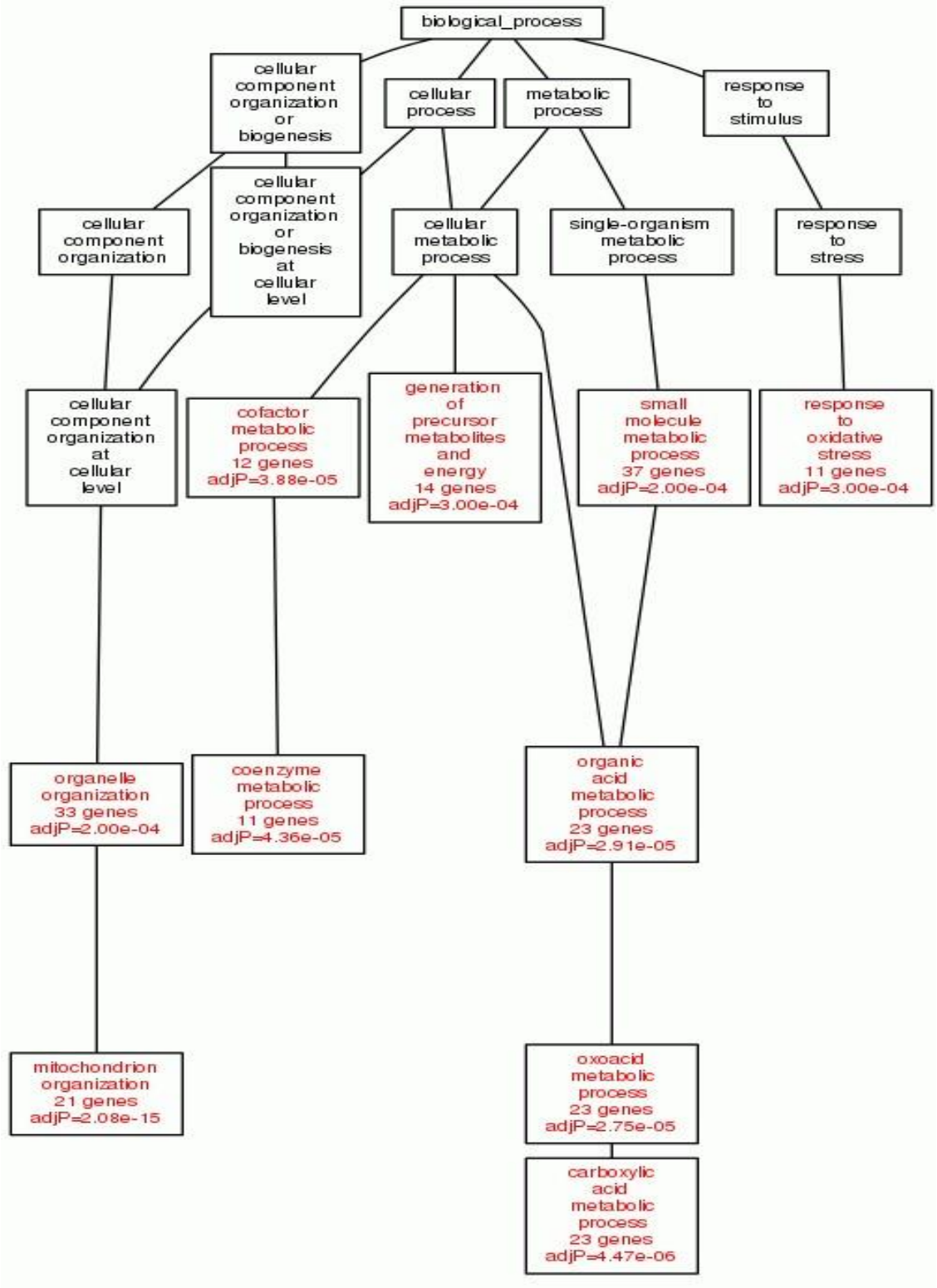

Figure 8.1: Functional annotation of miR-19b-2-5p targeting mitochondrial genes. The GO functional annotation revealing the predicted involvement in biological process.

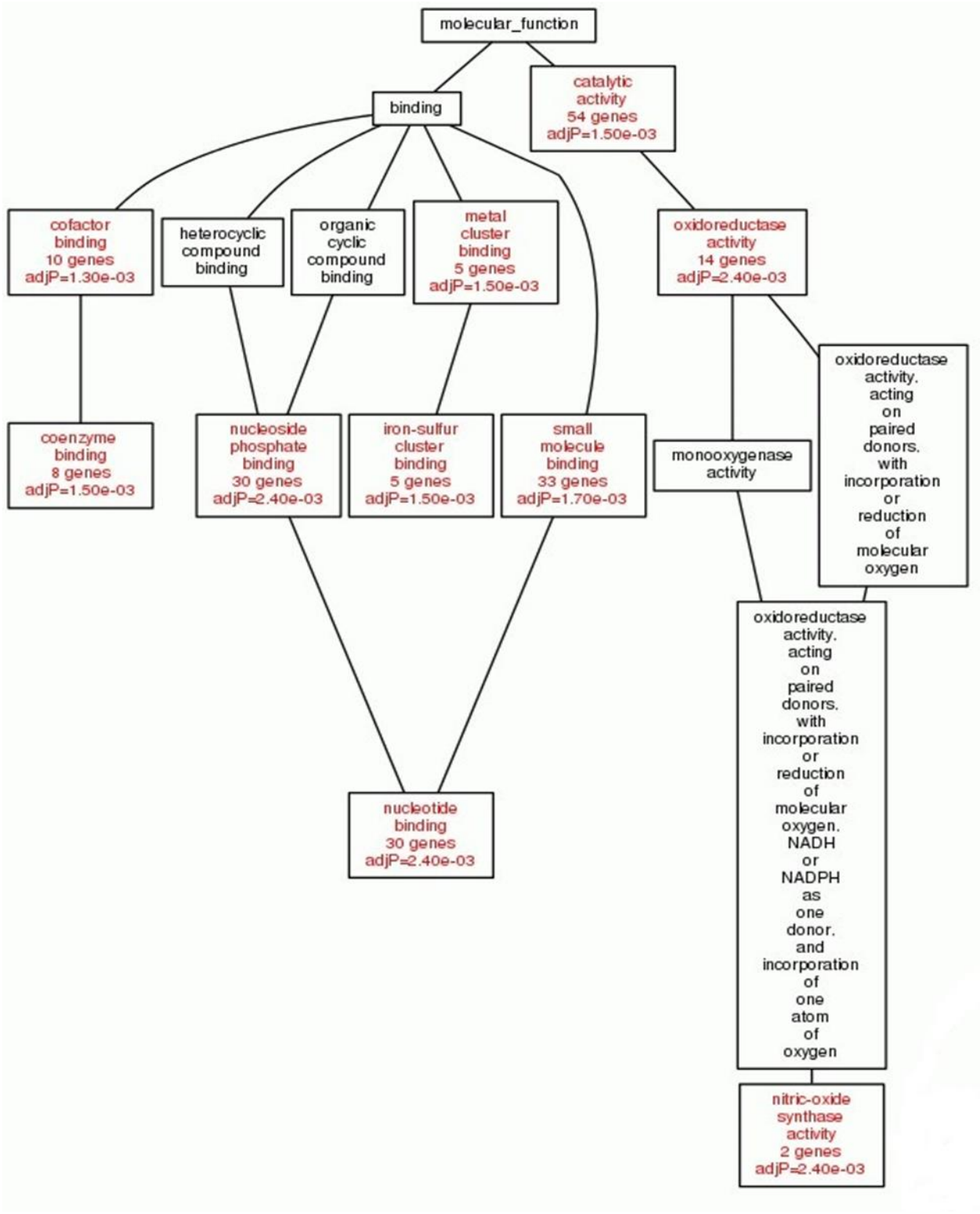

Figure 8.2: Functional annotation of miR-19b-2-5p targeting mitochondrial genes. The GO functional annotation revealing the predicted molecular functions of miR-19b-2-5p.

PUBLICATIONS AND CONFERENCES

Publications in process:

1. **SK Saini**, KC Mangalhara, G Prakasam, RNK Bamezai. DNA Methyltransferase1 (DNMT1) Isoform3 methylates mitochondrial genome and modulates its biology (Under Revision).
2. KC Mangalhara, S Manvati, **SK Saini**, K Ponnusamy, G Agarwal, SK Abraham, RNK Bamezai. ERK2-ZEB1-miR-101-1 axis contributes to epithelial-mesenchymal transition and cell migration in cancer. Cancer Letters 2017 Jan 18;391:59-73.
3. G Prakasam, RK Singh, MA Iqbal, **SK Saini**, AB Tiku, RNK Bamezai. Knockdown of PKM isoforms in cancer cells activates AMPK signaling to reprogram energy metabolism by stimulating mitochondrial biogenesis and autophagy for cell survival (Under Communication).

Awards and Conferences:

1. Awarded with A.R. Rao memorial Young Researcher Award 2017
2. Oral work presentation in International Conference on Mitochondria in Health and Disease-2017 organized by Society of Mitochondrial Research in Medicine at Jawaharlal Nehru University, New Delhi.